THESIS

# OPTIMIZING POWER CYLINDER LUBRICATION ON A LARGE BORE NATURAL GAS ENGINE

Submitted by

Matthew R. Luedeman

Department of Mechanical Engineering

In partial fulfillment of the requirements

For the Degree of Master of Science

Colorado State University

Fort Collins, Colorado

Summer 2013

Master's Committee:

Advisor: Daniel Olsen

Allan T. Kirkpatrick
Michael A. DeMiranda

# ABSTRACT

## OPTIMIZING POWER CYLINDER LUBRICATION ON A LARGE BORE NATURAL GAS ENGINE

More than 6000 integral compressors, located along America's natural gas pipelines, pump natural gas across the United States. These compressors are powered by 2-stroke, large bore natural gas burning engines. Lowering the operating costs, reducing the emissions, and ensuring that these engines remain compliant with future emission regulations are the drivers for this study. Substantial research has focused on optimizing efficiency and reducing the fuel derived emissions on this class of engine. However, significantly less research has focused on the effect and reduction of lubricating oil derived emissions. This study evaluates the impact of power cylinder lubricating oil on overall engine emissions with an emphasis on reducing oxidation catalyst poisoning. A traditional power cylinder lubricator was analyzed; power cylinder lubricating oil was found to significantly impact exhaust emissions. Lubricating oil was identified as the primary contributor of particulate matter production in a large bore natural gas engine. The particulate matter was determined to be primarily organic carbon, and most likely direct oil carryover of small oil droplets. The particulate matter production equated to 25% of the injected oil at a nominal power cylinder lubrication rate.

In addition, power cylinder friction is considered the primary contributor to friction loss in the internal combustion engine. This study investigates the potential for optimizing power cylinder lubrication by controlling power cylinder injection to occur at the optimal time in the piston cycle. By injecting oil directly into the ring pack, it is believed that emissions, catalyst poisoning, friction, and wear can all be reduced. This report outlines the design and theory of

two electronically controlled lubrication systems.  Experimental results and evaluation of one of the systems is included.

## ACKNOWLEDGMENTS

I dedicate the time spent on this work to my parents, whose support, tolerance, and sacrifice has often gone unacknowledged but never unnoticed.

Among my parents, I acknowledge my uncle for his role as one of my three greatest influences. I also recognize my brothers for their unspoken, yet understood love and support.

I extend special thanks to Dr. Daniel Olsen for providing me the opportunity to work at the EECL and attend Colorado State University. The atmosphere of the EECL and Fort Collins has proven beneficial to my own personal and professional growth. Dr. Olsen's ambition, guidance, and resources made this research possible. I thank the entire staff at the EECL, but I pay special acknowledgement to Kirk Evans and Philip Bacon. Without Kirk Evan's assistance, extensive practical knowledge, and programming skills this project would not have been possible. I thank Philip Bacon for his approachability and enthusiastic assistance throughout this research. I also show my gratitude to the following individuals whose knowledge and skills accomplished much more than I would have alone: Maddie Padhour, Cody Lanham, and Corey DeGroot.

Lastly, I acknowledge the Fort Collins friends that have played significant roles in my own personal growth and happiness over the last 16 months: Jake Doyle, Frank Sutley, Elaina Jennings, Wildcard Hockett, Jake DePierre, and Timo Holzfuß.

TABLE OF CONTENTS

LIST OF TABLES

LIST OF FIGURES

LIST OF ACRONYMS

| | |
|---|---|
| ATDC | Above Top Dead Center |
| BMEP | Brake Mean Effective Pressure |
| CCD | Charge Coupled Device |
| DAQ | Data Acquisition |
| EC | Elemental Carbon |
| ECL | Electronically Controlled Lubricator |
| EECL | Engines and Energy Conversion Laboratory |
| EPA | Environmental Protection Agency |
| FMEP | Friction Mean Effective Pressure |
| FTIR | Fourier Transform Infrared |
| HC | Hydrocarbon |
| IMEP | Indicated Mean Effective Pressure |
| LBNGE | Large Bore Natural Gas Engine |
| LIF | Laser Induced Fluorescence |
| OC | Organic Compound |
| OEM | Original Equipment Manufacturer |
| OIA | Optimal Injection Angle |
| OIT | Optimal Injection Time |
| PID | Proportional-Integral-Derivative |
| PM | Particulate Matter |
| TDC | Top Dead Center |
| UV | Ultraviolet |
| VOC | Volatile Organic Compound |

## 1 Introduction and Background

Many Americans depend on natural gas daily, to meet their energy needs. However, in order to utilize this vast resource, the gas must travel from the drilling sites to homes. Natural Gas in the United States is transported through a vast network of pipelines. Even with this large infrastructure, flow remains impossible in the pipelines without a pressure gradient. Natural gas compressors pressurize these pipelines. The more than 1200 natural gas compressor stations, located on the pipelines, have the throughput capability of approximately 743 billion cubic feet per day[1].

Many of the natural gas compressors are composed of integral compressors (about 3000[2]) where the engine pistons and compressor pistons are connected to a common crankshaft. The engine unit is a large bore natural gas engine (LBNGE). The engine unit operates by burning a portion of the compressible natural gas to drive the compressor unit.

One compressor model used on the pipeline is a Cooper Bessemer GMV. This compressor dates back to the 1940s, yet many are still in service. Though these compressors still accommodate for America's natural gas demand, many have poor efficiency and high emissions. These compressors have remained in service because of their robustness and the large capital investment required for replacement. Optimizing these compressors remains practical through the implementation of retrofit technologies, such as advanced controls, fuel injectors, exhaust after-treatment, and ignition systems.

Retrofit technologies for the GMV have been implemented to improve exhaust emissions of LBNGEs. The integration of lean combustion and exhaust after treatment are a couple ways that emissions have been reduced in LBNGEs[3]. Although extensive research has been conducted on fuel derived emissions, little research has looked into lubricant derived emissions.

Recent research has shown that lubricant derived emissions in LBNGEs are significant[4]. Reducing the lubricant based emissions in LBNGEs is a secondary driver for this research, yet this reduction is necessary to fulfill this research's primary objective. The primary objective of this research is to reduce oxidation catalyst poisoning in LBNGEs (see Section 1.3.1).

## 1.1 Power Cylinder Lubrication

Lubrication between the piston and power cylinder liner of a 2-stroke LBNGE is essential for engine operation. LBNGEs utilize lubrication ports, located midway up the cylinder, to provide oil to the piston. These ports are not present on small 2-stroke engines, which utilize an oil/fuel mix to lubricate the cylinder.

Lubrication of the cylinder/piston may be the most critical of all lubrication points on an engine. Many researchers credit the piston/cylinder interaction as the primary frictional loss in the internal combustion engine[5].

LBNGEs provide lubrication to the cylinder/piston through the use of lubricators. The lubricator's purpose is to regulate and deliver oil into the power cylinders via the lubrication ports on the engine.

### 1.1.1 Mechanically Operated Lubricators

Modern lubricators used in LBNGEs are of the force-feeding style. These lubricators operate entirely mechanically. The lubricator is primarily composed of two components: a positive displacement pump and a divider assembly.

The positive displacement pump drives off of the crank shaft. Therefore, the lubricator flow rate is rpm dependent. Many lubricator pumps also offer manual flow rate adjustment. This adjustment alters the oil output/shaft speed ratio of the pump.

The divider assembly, located downstream of the pump, distributes the pumped oil equally to each of the lubrication ports. A divider assembly is shown in Figure 1-1.

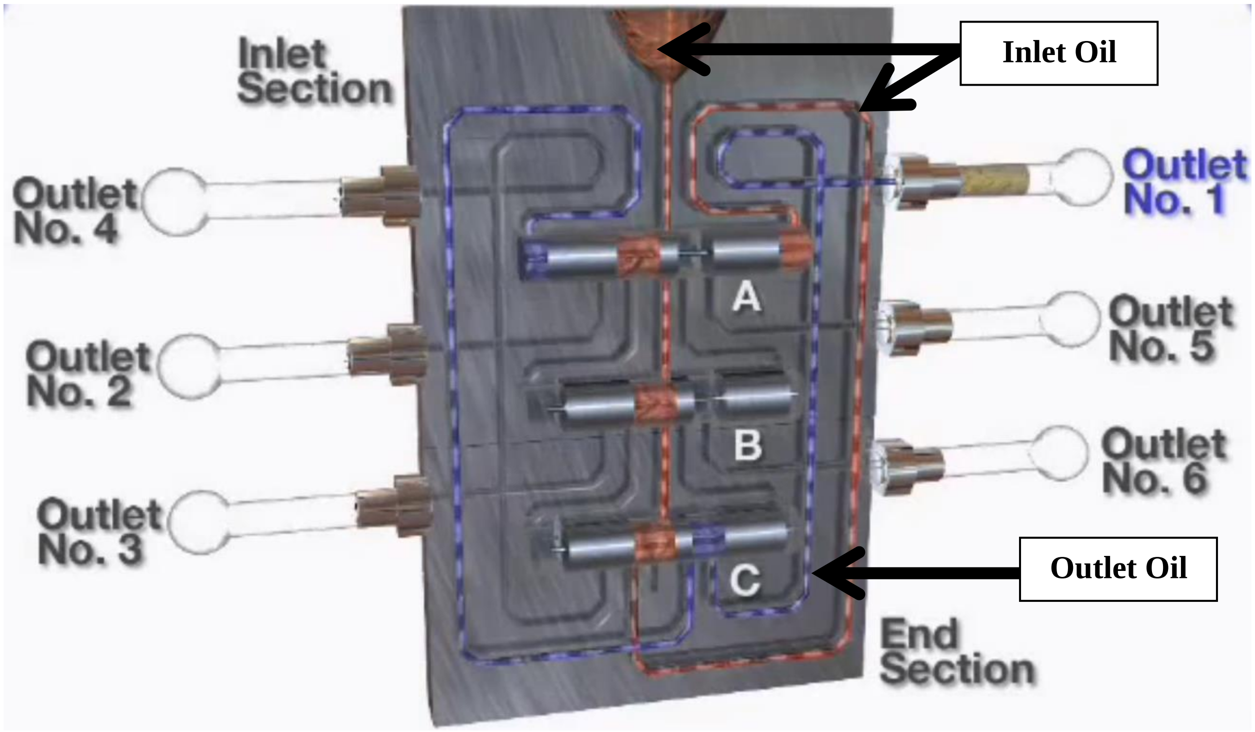


**Figure 1-1 Cutaway of divider block assembly[6].**

The divider assembly is composed of a series of stacked divider blocks. Each divider block houses a double acting piston, two outlet ports, and an intricate internal geometry of oil passages. The number of divider blocks in the assembly is determined by the number of lubrication ports on the engine; one divider block per every two lubrication ports. The divider block assembly shown in Figure 1-1 feeds six lube ports. The divider assembly delegates an equal supply of oil to each of the cylinder ports by utilizing the oil pressure to systematically translate one piston at a time. As a piston reaches the end of its stroke it blocks one oil passage and opens another, which hydraulically drives another piston. Figure 1-1 displays this process; oil passes through the inlet at the top of the divider block assembly and flows through the open passages (denoted as “inlet oil” in Figure 1-1). At this point in the cycle, the only open passage leads into the right side of Cylinder A, hydraulically pushing piston A leftward. Since the divider block is fully flooded, as the piston translates leftward, the once stagnant oil in the left side of Cylinder A (denoted as “outlet oil” in Figure 1-1) is pushed through outlet No. 1. After Piston A is pushed fully to the left, an inlet passage into the right side of Cylinder B opens, which drives Piston B leftward and injects oil into Outlet No. 2. This process continues in numerical order (1-6) and then repeats.

Secondary components of the force-feed system are a filter, pressure relief valves, and check valves. The 10 micron filter, installed downstream of the pump, removes heavy particulate that could clog the divider assembly. The pressure relief valves, located on the divider blocks, provide overpressure protection for each divider block outlet. These valves also serve a secondary function. The valves “pop” and remain open in overpressure situations. When a valve “pops” an engine kill switch is triggered. This “pop” also allows the engine operator to quickly identify where the overpressure situation occurred. Check valves are located at each lube port entrance to prevent backflow and protect the lubrication system from the combustion events occurring in the power cylinders.

Some of the benefits of the force-feeding power cylinder lubricator are as follows:

- Accurate and equal distribution of oil into the power cylinders.
- Reliable system.

- Protects the engine if loss of cylinder lubrication occurs.

Though the force-feed lubricator proves to be a reliable system for cylinder lubrication, the lubricator has detriments. The detriments of force-feed lubricator are as follows:

- Oil flow rate at constant engine speed is independent of the load on the engine. Several companies have shown that the lubrication requirements of power cylinders are dependent on engine load[7,8,9].
- Oil is injected into the lube ports independent of piston position in the cylinder. The injection event rarely occurs at optimal times in the piston cycle. If injection occurs after the piston has passed the lube port toward top dead center (TDC), oil may be scraped directly into the exhaust on the piston’s down stroke. If this scraping mechanism occurs it may drastically impact emissions.
- Injection delay of this system is thought to occur when cylinder pressures are relatively high. The delay likely takes place in the lubrication port, downstream of the check valve. Due to the lube port’s relatively large diameter (.2 inches), it is doubtful that the port is ever fully flooded with oil. The un-flooded volume of the port, referred to as the dead volume, allows for displacement of oil within the lube port. At relatively high backpressures (cylinder pressures at the lube port), oil in the port could flow back towards the check valve. When the backpressure subsides, flow would continue towards the cylinder wall. Therefore, oil likely spills into the cylinder when cylinder pressure at the port is low. The lowest lube port pressure occurs after the piston has passed the lube port towards TDC.

### 1.1.2 Electronically Controlled Lubricators

Electronically controlled lubricators (ECLs) for power cylinders can likely address the detriments of the force feed lubricators used in LBNGEs. Recent advances in fast response solenoid technology make it possible to control high speed injection. Precisely controlling power cylinder oil injection to occur only at the most optimal time in the piston cycle is believed to:

- Increase lubrication efficiency (decrease friction) between the cylinder and piston.
- Decrease lubricant derived emissions.
- Reduce operating costs. More efficient lubrication could lead to reduced lube oil consumption. Reduced lubricant derived emissions could lower operational costs associated with exhaust after treatment, see section 1.2.

In addition to precise injection, ECLs have the potential to be more diverse and operator friendly than force feed lubricators. ECLs could be designed to provide:

- Quick satellite adjustment of system parameters. These parameters could include: flow rate, injection volume, injection interval, injection timing, system pressure, etc.
- Engine load dependent flow rates.
- Increased lubrication during engine start-up.

### 1.1.3 Electronically Controlled Lubricators in Marine Engines

There are at least 3 manufacturers in the large bore, 2-stroke diesel industry that utilize electronic cylinder lubrication injection. Each markets a retrofit electronic oil injection system specifically for large marine shipping engines. All of these lubrication systems essentially operate the same.

The systems are composed of positive displacement pumps, solenoid controlled lubricators, and injection nozzles.  Figure 1-2 displays Wartsila's Pulse Lubrication System, the marketing equivalent to Doosan Engine's and MAN Diesel's Adaptive Cylinder Oil Control System[7,8,9].

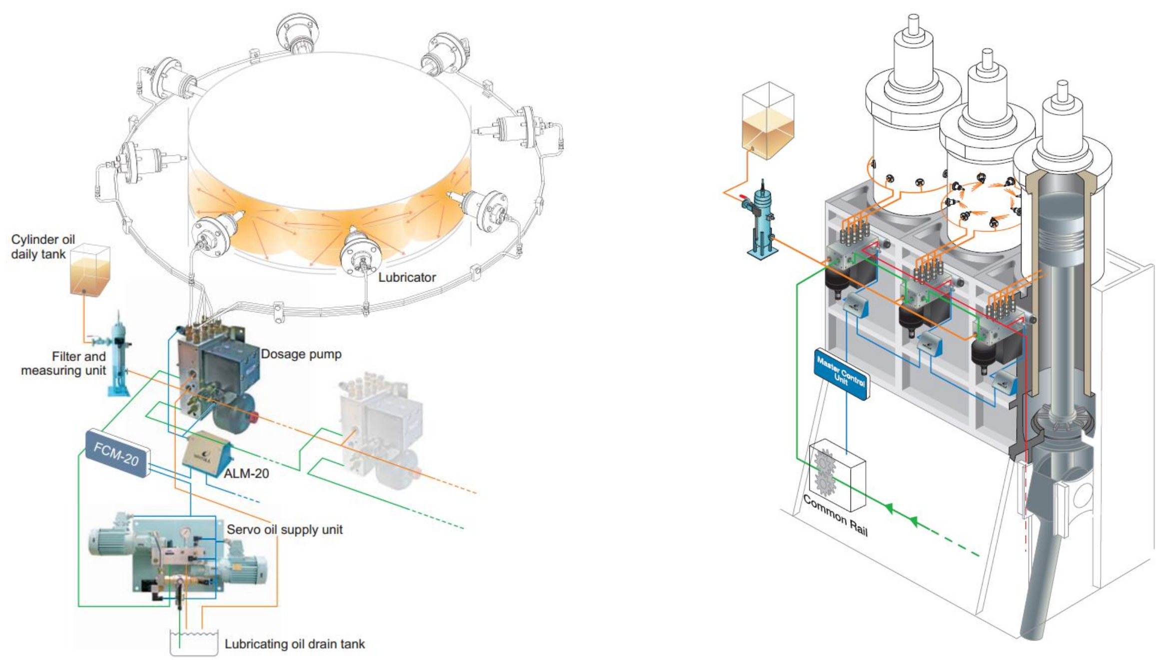


Figure 1-2  Wartsila Pulse Lubrication System[9].

Each of these 3 lubricators govern cylinder oil feed rate based on engine load as opposed to engine speed.  The feed rate is altered by instantaneously adjusting the injection frequency. Injection timing of all three lubricators occur as the ring pack crosses the lubrication port.

Doosan's Alpha Lubricator operates at maximum flow rate of 75% of that of the corresponding mechanical lubricator.  Associated wear testing, by Doosan, found that an Alpha lubricated engine cylinder wore at a rate of 0.05 mm/1000 hrs.  The equivalent mechanically lubricated engine wore at a rate of 0.1 mm/1000 hrs[7].

MAN Diesel claims that their Alpha lubricator decreases lube oil consumption, decreases cylinder wear, and decreases emissions[8].

Each of these systems utilizes a lubricator unit mounted on each cylinder, see Figure 1-3. A common rail system supplies oil to the lubricators and maintains a constant pressure throughout the system. The lubricators are largely composed of a fast response solenoid valve that can open and close relative to crank positioning. Crank position is determined by an encoder that is mounted to the crank. After the solenoid opens, oil flow is split between the lubrication ports located on the cylinder. Oil then passes through non-return nozzles into the cylinder.

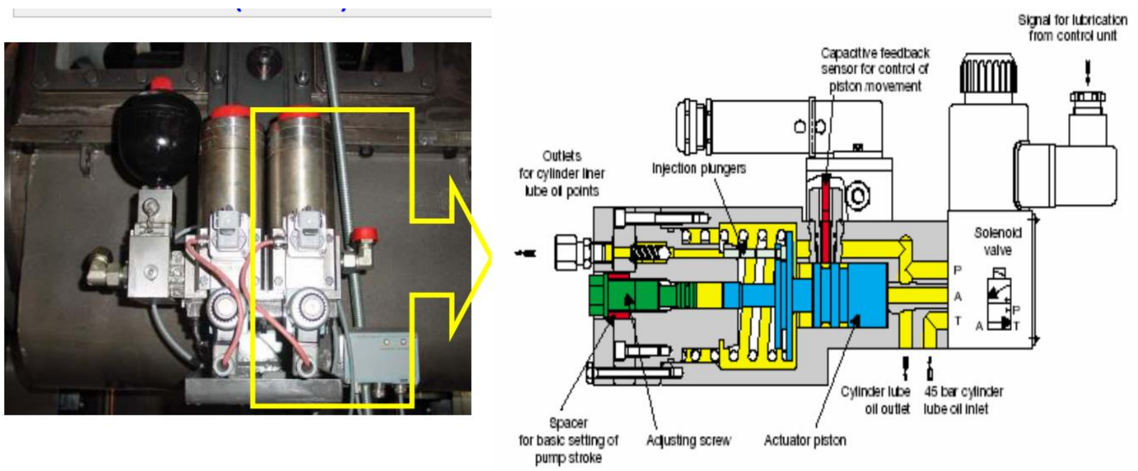


**Figure 1-3 Doosan Lubricator[7].**

Installation of the retrofit Alpha lubricators require slight modification to the cylinder wall, shown in Figure 1-4. The lubrication ports are bored to accept the geometry of the injection nozzles and a horizontal groove is ground into the cylinder wall. The cylinder groove is likely ground to allow for flow when the rings block the port.

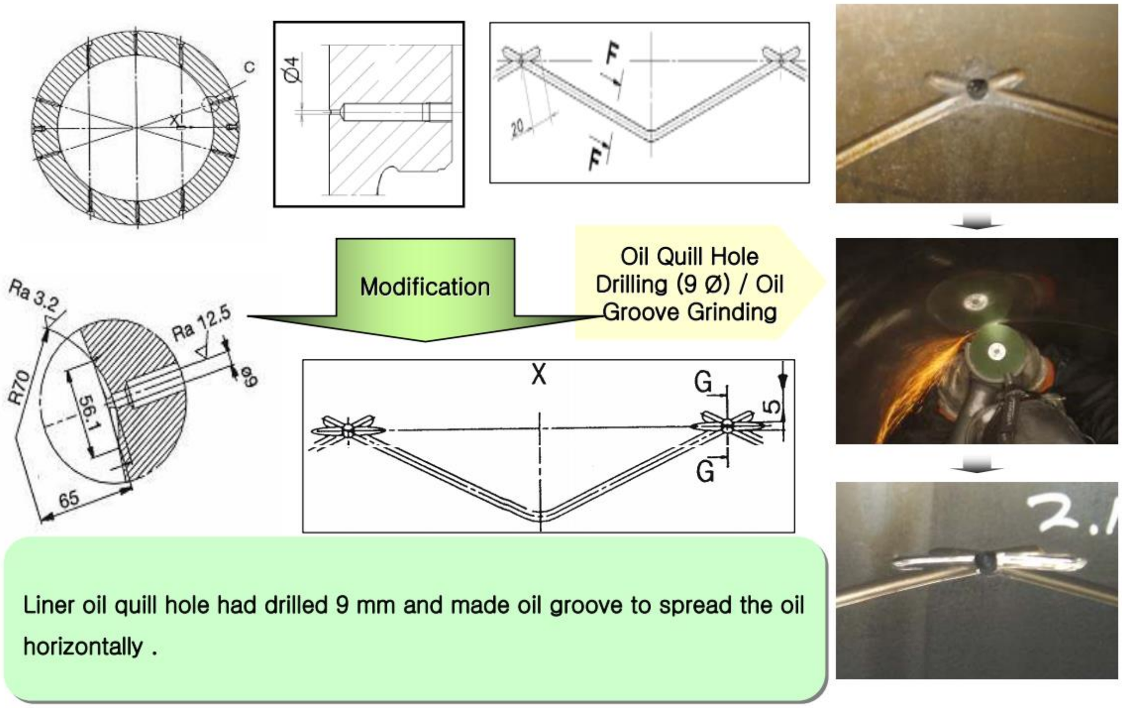


**Figure 1-4 Doosan cylinder liner modification[7].**

### 1.1.4 Injector Selection for Power Cylinder Oil Injection

Few commercial injectors currently exist that have the capability to inject viscous lubricating oil, the responsiveness to inject at the optimal time of a LBNGE's cycle, and the integrity to operate at pressures required for fast injection into the cylinder. Five classes of injectors/valves, see Figure 1-5, were investigated: fast response solenoid valves, indirect diesel injectors, direct diesel injectors, direct gasoline injectors, and compressor oil injectors.

| Solenoid Valves | Indirect Injector | Direct Diesel Injector | Direct Gasoline Injector | Compressor Oil Injector Design |
|---|---|---|---|---|

Figure 1-5 Injector options.

Table 1-1 outlines the positives and negatives of each injector for ECL implementation.

Table 1-1 Injector selection matrix.

| | Pros | Cons |
|---|---|---|
| **Fast Response Solenoid Valves** | • Fast Response<br>• Commercially available<br>• Precise control (easy variability of injection time, frequency, and injection) | • Never been tested with combustion chamber injection<br>• Require check valves for backflow prevention |
| **Indirect Diesel Injectors** | • Fast Response<br>• Commercially available<br>• Designed for combustion chamber injection<br>• Accurate Dosage Operates at ideal lube system pressures<br>• Simple system, minimal setup required for injectors and inline pumps that feed oil to the injectors | • Limited injection control (not electronically controlled)<br>• Requires mechanical gearing of the inline pumps to the crank shaft for precise injection timing<br>• To adjust injection frequency, gear ratio must be adjusted<br>• Injectors have not been tested with oil<br>• Nozzle is designed to spray fuel (not ideal for lubricant injection) |

| | Pros | Cons |
|---|---|---|
| **Direct Diesel Injectors** | • Fast Response<br>• Commercially available<br>• Designed for combustion chamber injection<br>• Precise control (easy variability of injection time, frequency, and injection)<br>• Injectors have successively injected oil at the EECL | • Designed for pressures far above pressures required for oil injection ( >9000 psi)<br>• Minimum operating pressures likely very high<br>• Nozzle is designed to atomize fuel (not ideal for lubricant injection) |
| **Direct Gasoline Injectors** | • Fast Response<br>• Commercially available<br>• Designed for combustion chamber injection<br>• Precise control (easy variability of injection time, frequency, and injection)<br>• Operates at relatively low pressures ( >3000 psi) | • Injectors have not been tested with oil<br>• Nozzle is designed to atomize fuel (not ideal for lubricant injection) |
| **Compressor Oil Injectors** | • Fast Response<br>• Accurate Dosage<br>• Designed for lube port injection<br>• Precise control (easy variability of injection time, frequency, and injection)<br>• Operate at relatively low pressures<br>• Operates with an oil medium | • Currently commercially unavailable<br>• Requires custom design<br>• Extensive lead time for injector development |

Of the five classes of injectors/valves, fast response solenoid valves and compressor oil injectors were investigated further (see Section 2.1 and Section 2.2, respectively).

## 1.2 Power Cylinder Lubrication

Power cylinder lubrication serves several functions:

- Reduces friction.
- Reduces wear.
- Provides sealing.
- Transfers heat from the lubricating surfaces.
- Removes internally generated debris from surfaces.
- Inhibits corrosion.

Friction generated between the cylinder liner, rings, piston, skirt, and rod bearing contribute to the overall power cylinder friction. Power cylinder friction is the major contributor to mechanical friction loss in the internal combustion engine[5]. Though cylinder friction is relatively significant, the overall frictional losses of an engine only account for 4% - 15% of the total energy (IMEP) produced by the engine. Quantifying power cylinder friction is difficult due to its relatively small contribution to the overall engine production.

### 1.2.1 Power Cylinder Friction Testing

Power cylinder friction can be experimentally determined by motoring tests or firing tests. Motoring tests require the mechanical turning of an engine and are significantly simpler to administer than firing tests. The frictional contributions of engine components, using a motoring test, are determined by a variety of methods. One of the simplest methods uses a motorized dynamometer. The dynamometer correlates frictional changes with the changes in torque required to maintain constant motor speed. The accuracy of motoring tests is widely debated. Researchers found motoring test accuracy to be anywhere from a significant under-approximation[10] to an 85% accurate approximation[11] of the actual frictional effects in operating engines.

Firing tests provide more realistic friction testing results, as thermal and chemical contributions from combustion are accounted for in friction testing.  In firing tests, frictional impact is often determined by calculating the changes in engine performance using a frictional mean effective pressure (FMEP) approach.  The FMEP approach takes the difference between the engine's IMEP and break mean effective pressure (BMEP) to find the frictional contribution. Several techniques for determining a component's frictional contribution are employed in friction testing. Techniques for quantifying power cylinder friction are as follows:

- Component removal- Friction is initially evaluated on the engine before friction-contributing components are removed.  The overall change in friction is attributed to the removed component.  This technique is not always possible as some engine components are required for operation.  This technique is not always accurate as the removal of one component can change the frictional impact of another.
- Difference testing- Two designs of a friction-contributing component are developed. Each design is tested.  The difference in measured friction between the designs indicate the frictional effect of the design change.
- Analytical modeling- Predicts the frictional contribution of each component.  The models are verified using the component removal and difference testing techniques.

### 1.2.2 Frictional Contribution of the Power Cylinders to Overall Engine Friction

Richardson quantified the contribution of power cylinder friction in diesel engines using the power cylinder quantification techniques[5] explained above; his results are displayed in Figure 1-6.

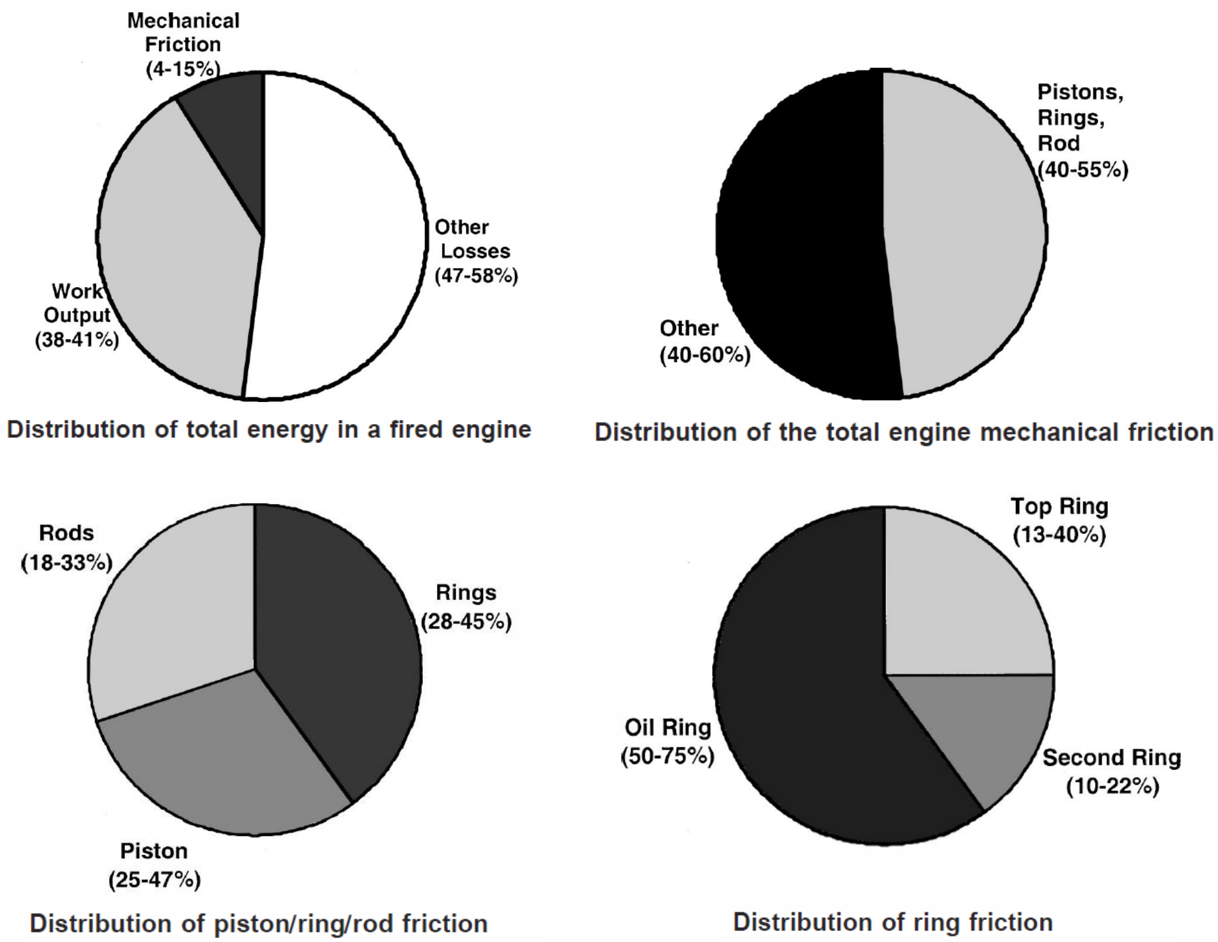


**Figure 1-6 Mechanical friction contribution in diesel engines[5].**

Richardson found that power cylinder lubrication contributed to about half of all friction present in internal combustion engines. The frictional contributions that Richardson found for each component in the power cylinder are shown in Table 1-2.

**Table 1-2 Percent frictional contributions of diesel engines[5].**

| | % Power Cylinder | % Total Energy | % Work Output |
|---|---|---|---|
| **Piston/Rings/Rods** | 100 | 1.6 - 8.3 | 4.1 - 20.9 |
| **Rods** | 18 - 33 | 0.3 - 2.7 | 0.7 - 6.8 |
| **Piston** | 25 - 47 | 0.4 - 3.9 | 1.0 - 9.8 |
| **Rings** | 28 - 45 | 0.4 - 3.7 | 1.1 - 9.4 |
| **Top Compression Ring** | 3.6 - 18.0 | 0.1 - 1.5 | 0.1 - 3.8 |
| **Second Compression Ring** | 2.8 - 9.9 | 0.1 - 0.8 | 0.1 - 2.1 |
| **Oil** | 14 - 34 | 0.2 - 2.8 | 0.6 - 7.0 |

### 1.2.3 Cylinder Liner Surfacing Impacts on Friction and Wear

Surface treatment of the cylinder liner is one method to decrease power cylinder friction and wear. Cylinder liner surface topography impacts engine performance, running-in duration, oil consumption, and exhaust gas emissions[12]. Optimal surface topography of cylinder liners requires a balance between smoothness and roughness. The smoothness of the liner reduces the coefficient of friction between the cylinder and rings; however, if the surface is overly smooth oil will fail to coat the cylinder efficiently. Two surfacing methods that have effectively decreased cylinder friction and wear are burnishing and plateau honing. Burnishing utilizes pressure to create dimples (oil pockets) in the cylinder. Plateau honing creates a smooth wear-resistant plateaued surface with deep intersecting valleys that act as oil resevoirs[12].

### 1.2.4 Lubricating Oil Viscosity and Condition

The properties and condition of lubricating oil play a vital impact on the reduction of power cylinder friction and wear. The major rheological property of lubricating oil that influences its effectiveness is its viscosity. Lubricating oil's viscosity is a function of both temperature and shear rate[13]. Lubricating oil, a non-Newtonian fluid, experiences shear thinning effects. An ideal lubricating oil viscosity is viscous enough to reduce wear, yet thin enough to reduce friction. The selection of lubricating oil is engine specific due to discrete engine operating conditions that may affect oil viscosity.

Another major contributor that impacts lube oil effectiveness is oil condition. Degradation of lubricating oil, due to the pick-up of both internal and external contaminants, reduces its effectiveness over time[14].

### 1.2.5 Ring Pack Design and Lubrication

The piston and ring pack are designed to reduce friction within the cylinder while minimizing pressure loss in the combustion chamber. The ring pack refers to the vertical assembly of rings on the piston (see Figure 1-7). Two varieties of rings comprise the ring pack, compression rings and oil rings.

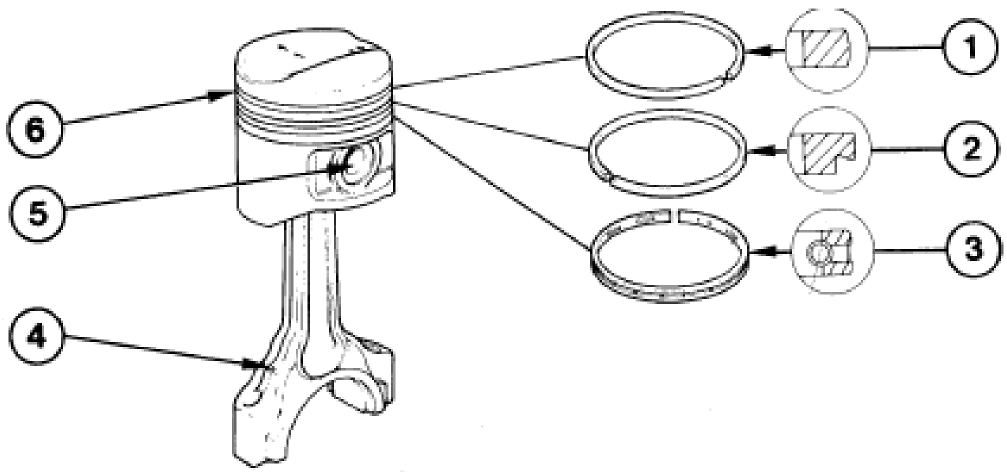


**Figure 1-7 General Piston Assembly[15].**

Compression rings are generally the uppermost rings of the pack. The compression rings' primary function are to create a seal between the piston and cylinder. These rings also reduce the friction between the piston assembly and the cylinder. The outer profile of the compression rings are designed to accomplish one of three things: 1) squeeze oil past the ring, 2) scrape oil along the cylinder surface, or 3) balance squeeze and scrape mechanisms. Generally the top compression ring is designed with either a chamfered or barrel-shaped profile, this coerces squeezing effects. The lowest compression ring is generally designed as a scraper. If the piston contains intermediate compression rings, the rings are commonly tapered to balance squeeze and scrape effects.

The oil ring(s) is designed to hold oil in high lubricated areas and distribute oil in low lubricated areas. The oil rings primary purpose is to maintain lubrication along the entire piston stroke.  Oil rings generally have a convex outer profile to retain oil.  Holes are bored through the oil ring(s) and the piston (directly behind the oil ring).  These holes allow oil to travel through the piston to lubricate the piston bearings and/or cylinder wall.  Most 4-stroke engines (without cylinder lubrication ports) utilize oil "splash" passing through the piston and oil ring(s) as the primary means of lubricating the cylinder.

Several researchers have developed models to simulate the friction present in the ring pack of an engine[16,17,18,19,20].  Jeng's model[16,17] is a one-dimensional analysis that can assumes either a fully flooded ring pack or lubricant starved ring pack.  Figure 1-8 displays the results of Jeng's model.

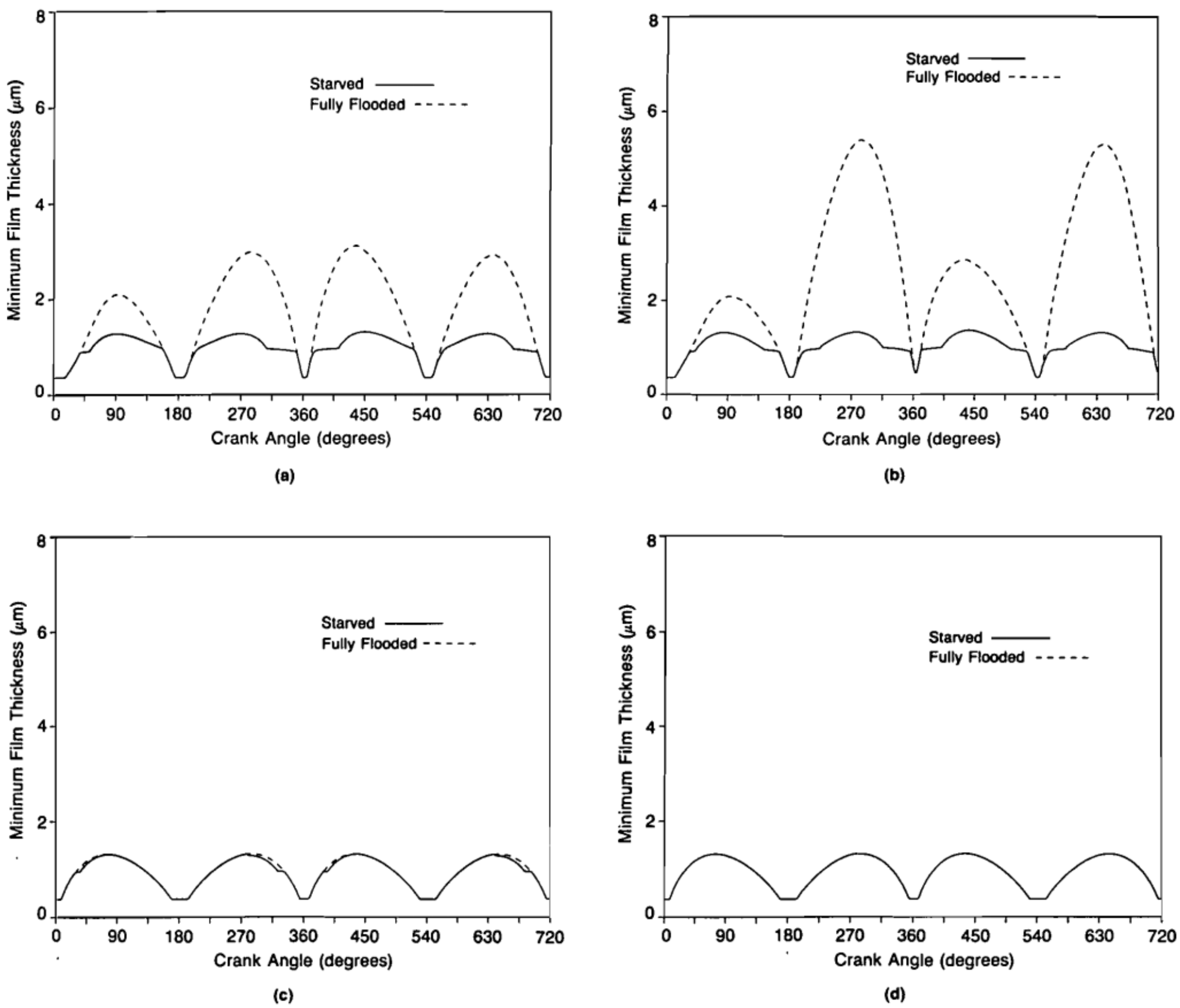


Comparisons of minimum film thickness for fully flooded and starved lubrication conditions.
(a) first compression ring
(b) second compression ring
(c) upper rail of oil control ring
(d) lower rail of oil control ring

**Figure 1-8 Effect of crank angle on oil film thickness between rings and cylinder[17].**

Jeng's results display the significance that a fully flooded ring pack has on the minimum film thickness between ring and cylinder. The minimum film thickness impacts both cylinder friction and wear.

Ma's ring pack model[18,19] takes a more realistic approach in that it does not assume a fully flooded ring pack. Ma uses an oil transport analysis which accounts for the ring locations, ring axial directions, and oil accumulation in front of each ring to determine the oil availability of each ring in the ring pack. Ma's model exhibited similar behavior to Jeng's model. The quantification of film thickness differed between the models, but the relative relationship between minimum film thickness and crank angle were similar.

### 1.3 Lubricant Based Exhaust Emissions

Natural gas engines are generally regarded as clean burning. Natural gas, composed of 70%-90% methane on average[21], nearly burns completely into CO2 and H2O and produces little particulate matter (PM). Particulate matter is defined as any material collected on a filter after diluting the exhaust gas with clean filtered air to a temperature between 315 K to 325 K. Particulate matter, small liquid or solid particles suspended in the air, is attributed to several human health concerns[22]. The Environmental Protection Agency (EPA) notes the following health concerns from inhalation of PM smaller than 10 microns in diameter:

- Premature death in people with heart or lung disease.
- Nonfatal heart attacks.
- Irregular heartbeat.
- Aggravated asthma.
- Decreased lung function.
- Increased respiratory symptoms, such as irritation of the airways, coughing or difficulty breathing.

A previous study published in 2011[4], determined the travel of cylinder lubricating oil after injection into the power cylinder. The lubricating oil, composed of long chain hydrocarbons

(HCs), had six theoretical pathways to travel after injection into the cylinder. Figure 1-9, displays these pathways.

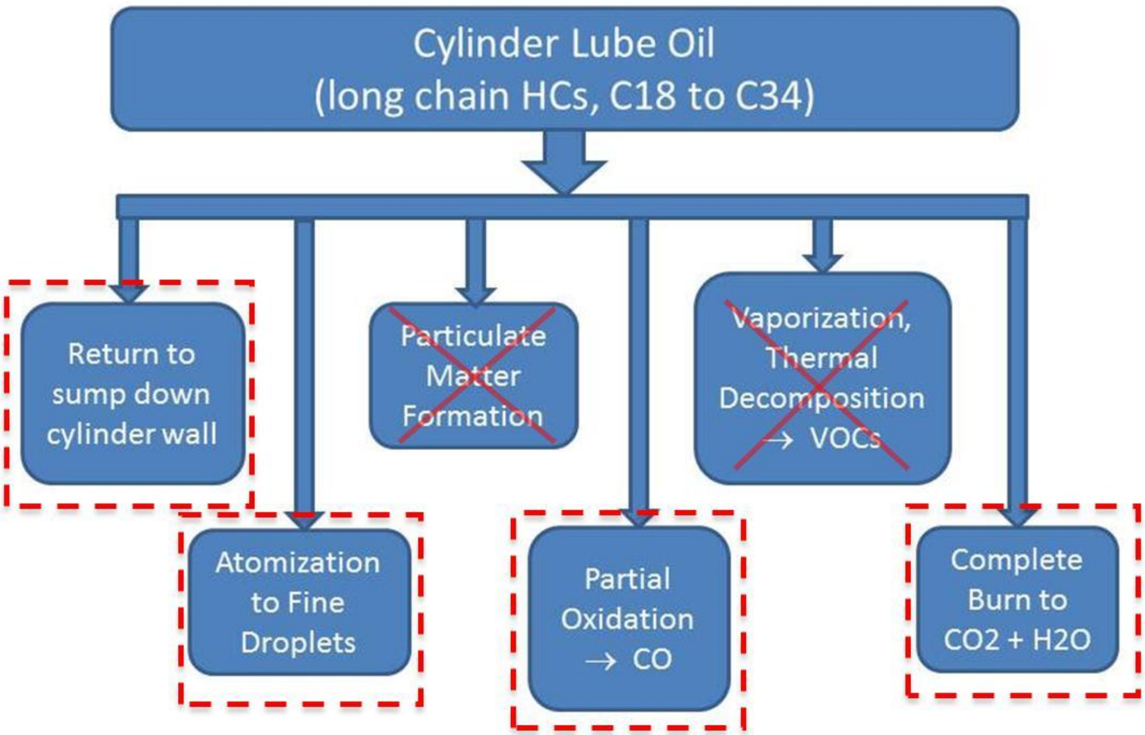


**Figure 1-9 Cylinder lube oil carryover[4].**

The pathway descriptions are as follows:

- Return to sump down cylinder wall. The cylinder lube oil is scraped into the sump, unburned and mixes with the sump oil supply.
- Atomization to fine droplets. The cylinder oil passes into the exhaust unburned and remains in the form of organic compounds (OCs). The composition of the OCs are: (1) atomized lubricating oil that passes through the cylinder unaltered; (2) broken down hydrocarbons smaller than lubricating oil, yet large enough to condense on the filter; or (3) a combination of (1) and (2).

- Elemental Carbon (EC) PM formation. The cylinder oil is incompletely burned during combustion. Solid PM is formed in rich zones during combustion. The partially broken down lube oil is passed into the exhaust as soot (strings of carbon molecules).
- Partial Oxidation to carbon monoxide (CO). The cylinder oil is incompletely burned during combustion to form CO, which passes into the exhaust.
- Vaporization thermal decomposition to volatile organic compounds (VOCs). VOCs are generally defined as non-methane, non-ethane hydrocarbons, excluding $CH_2O$.
- Complete burn to carbon dioxide ($CO_2$) and water ($H_2O$). The cylinder oil is completely burned during combustion and passes into the exhaust as $CO_2$ and $H_2O$.

Of the 6 pathways outlined, Olsen, et. al. found four to be probable. Lubricating oil either returned to the sump, atomized into fine droplets, partially oxidized into CO, or completely burned into $CO_2$ and $H_2O$. Of the four probable lube oil paths, oil return to the sump was considered preferential, complete burn was acceptable, and atomization or partial oxidation was undesirable.

Little evidence of EC PM formation or vaporization of the lubricating oil. Gaseous emissions, including CO, $CH_20$, and VOCs, showed only weak and inconsistent correlations with changes in cylinder lube rate. OC PM emissions, however, showed a strong correlation to power cylinder lube rate. Under engine loads of 70% and 100%, PM increased linearly with lube rate (see Figure 1-10 and Figure 1-11); nearly 100% of collected PM was OC. The volume of OC found in the exhaust represented over 7% of the injected cylinder lubricating oil (7% carryover). A summary of the 2011 study is shown in Table 1-3.

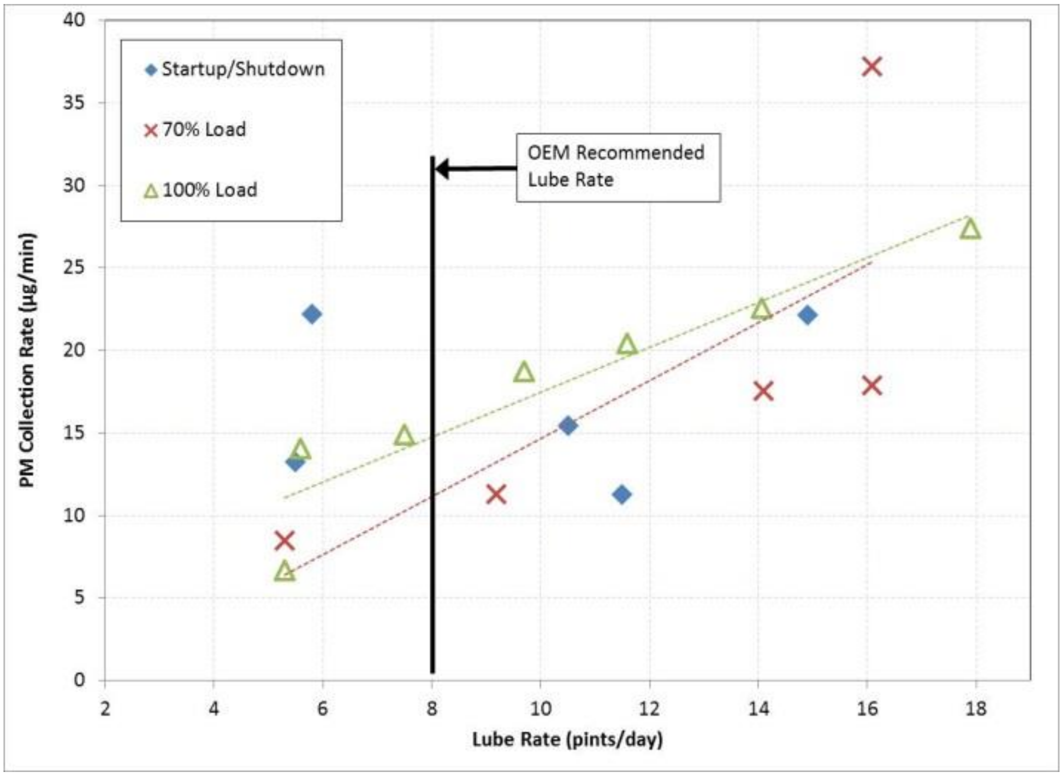


Figure 1-10  OC PM vs. power cylinder lube rate[4].

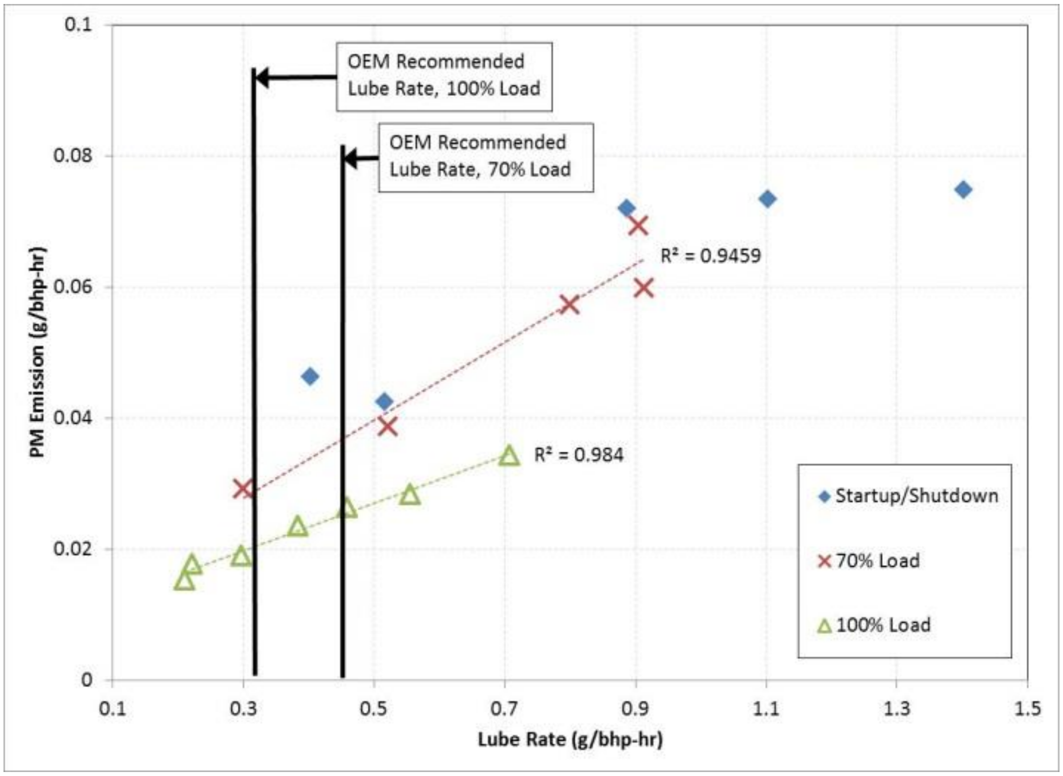


Figure 1-11  OC PM vs. power cylinder lube rate[4].

Table 1-3 Lube oil carryover summary[4].

| | Percent Change with Increasing Lube Rate | | | | |
|---|---|---|---|---|---|
| Test Map | Lube Rate | PM | CO | CH2O | VOC |
| 100% Load | 238% | 310% | 13% | 8% | 10% |
| 70% Load #1 | 204% | 339% | 29% | 1% | -6% |
| 70% Load #2 | 218% | No Data | -1% | 7% | 3% |

### 1.3.1 Effect of Lubricant on Exhaust After-treatment

Exhaust after-treatment has become common as pollutant emission regulations have increased. The installation of oxidation catalysts is a common after-treatment method used for emissions reduction. Oxidation catalysts are typically used to reduce CO, formaldehyde, and/or VOCs from engine emissions[4].

Oxidation catalysts are generally composed of a porous γ-alumina coating on a ceramic or stainless steel substrate. The high surface area γ-alumina provides support for the precious metal (platinum and/or palladium) layer that coats the alumina. The precious metal provides catalytic sites for oxidation to occur.

The use of precious metals in these catalysts makes this after-treatment process a significant financial investment. Ensuring the longevity of an oxidation catalyst is critical in reducing operating costs and harmful emissions of engines.

The lifetime of an oxidation catalyst depends on its continued efficiency at reducing a specified emissive species. Oxidation catalysts generally lose their efficiency to degradation through two means: thermal deactivation and catalyst poisoning[4]. Thermal deactivation occurs when precious metal sites sinter, reducing the number of available oxidation sites available. Thermal deactivation generally occurs over the initial 100-200 hours of operation[23]. Catalyst poisoning is a more gradual process that has attributed to contact with sulfur, phosphorous, zinc, and calcium compounds. Sulfur generally originates from fuels; however, current sulfur standards for natural gas minimize sulfur's effect on catalyst poisoning. Phosphorous, zinc, and calcium compounds derive from lubricating oil and have been shown to cause significant degradation in catalyst efficiency in 4-stroke engines[24,25]. For 2 stroke LBNGEs, with cylinder lube ports, the effect of catalyst poisoning is likely more severe.

## 1.4 Cylinder Lubrication Verification Methods

Verifying cylinder lubrication is an important and challenging task in engine development. Several verification methods have been investigated including: qualitative, electrical, and fluorescent methods.

### 1.4.1 Qualitative Methods

Qualitative methods are the simplest and most economical methods for verifying cylinder lubrication; however, these methods provide the least amount of insight to cylinder lubrication. Two basic qualitative methods are the cigarette paper method and the wick method.

The cigarette paper method has been used in the field to ensure sufficient cylinder lubrication on operating LBNGEs. This method requires the removal of a cylinder head directly after an engine's operation. After the head removal, cigarette paper is placed upon the cylinder liner in numerous locations. If the cigarette paper saturates and sticks to the cylinder wall, the cylinder is considered well-lubricated. If the cigarette paper does not saturate and does not adhere to the cylinder wall, the cylinder is considered under-lubricated. Although only qualitative, the cigarette paper method economically establishes whether an engine cylinder is lubricated sufficiently.

The wick method, conducted similar to the cigarette paper method, utilizes a wick to absorb cylinder oil.  Pre-weighted wicks contact multiple locations on the cylinder wall after the cylinder head removal.  The end weights of the wicks are recorded.  A qualitative assessment of the wicks' saturation can determine whether the cylinder is well-lubricated or under-lubricated.

A theoretical advantage of the wick method over the cigarette paper method is that quantification of the lubricant film thickness could be assessed.  Film thickness could easily be calculated if the oil density, the change of wick mass, and the surface area of the wicking surface were known. In this regard the wick method could be considered semi-quantitative. However, high uncertainties would likely contribute to inaccurate film thickness quantification.  Accurate film thickness quantification would require meticulous consistency by the experimenter.  The experimenter would need to consistently wick the same cylinder surface area, understand the percentage of oil that is absorbed by the wick (removed from the cylinder), and precisely record wick masses. The wick method was conceived during this work. It has not been employed experimentally.

### 1.4.2 Electrical Methods

Electrical methods for verifying cylinder oil film thickness have several advantages over qualitative methods. The primary advantages are that the oil film thickness can be quantified and the lubrication can be verified while the engine is in operation.  Three electronic methods have been used for cylinder lubrication verification are the resistance method, the inductance method, and the capacitance method.

The resistance method involves electrically insulating the whole, or part, of a piston-ring from the rest of the piston and passing a current through the ring to the liner[26,27,28,29]. The intention of this method is to correlate changes in the resistance of the ring/liner junction with the thickness of the intervening oil-film[30].

In experimentation of the resistance method[30], however, many individual short-circuits occurred between the liner and rings. These short circuits prevented the assessment of quantitative film thickness measurements. Although unsuccessful at quantifying film thickness, this method did provide a qualitative approach to relative film thickness. In areas of lower film thickness, more short circuits occurred. This behavior was witnessed around top dead center (TDC) and bottom dead center.

Another resistance technique[30] used an arrangement that could be described as a resistance transducer to estimate film thickness. In this experiment a piston ring was pinned at one end to the piston (the cathode). An anode valve, with anode attached to the free end of the ring, was positioned on the opposite end of the pinned section of the ring. As the engine operated, the diameter of the ring fluctuated, due to liner geometry and oil film thickness. As the ring diameter changed, the distance between the anode and cathode changed. This distance change resulted in a change of resistance of the anode valve. A strong understanding of the liner geometry allowed for a correlation to be made between anode valve position and cylinder film thickness.

Inductance methods utilize the principle that the inductance of a coil decreases as the distance between the coil and a magnet increases. Self-inductance proximity transducers have been used to measure cylinder oil film thickness[31]. Transducers mounted on opposing sides of the piston, behind a compression ring, monitored the distance between the piston and the back of the ring. Cylinder oil film thickness was deduced by monitoring the distances between piston and ring while the engine was in operation. Two problems persisted in using the transducers in this application: 1) the output was non-linear and 2) the method was not reliable due to the low thermal stability which made calibration difficult.

Other inductance methods have determined oil film thickness by monitoring the piston end gap[29]. An estimation of average cylinder oil film thickness was made by mounting an inductance transducer to the end face of a ring and monitoring the changes in ring gap. Disadvantages of this method were that the method was very temperature sensitive and that any geometric inaccuracies in bore circularity added significant error to the measurements.

Capacitance methods utilize the principle that the capacitance of two parallel plates varies inversely with plate separation. Capacitance methods for lubrication verification have utilized a custom constructed transducer either mounted to the cylinder liner[32] or piston ring[33]. The capacitance transducers were composed of a thin, electronically insulated electrode wire.

In the cylinder liner installed transducer method[32], three transducers were mounted vertically in-line with one another along the cylinder wall. The capacitance was determined as the grounded rings passed the transducers. This method permitted observation of each ring in the pack and the strong resolution allowed for the determination of the orientation of each ring as it passed the transducer. Three major difficulties were experienced with this method though:

- Rotation of the rings during operation made it impossible to record a true ring profile. A true profile required the ring to pass each transducer at the same ring point.
- Electrical short circuits occurred when the film thickness was less than .5 µm.

- Cavitation on the outlet side of the ring reduced the dielectric constant of the film gap, which distorted the estimated film thickness measurement.

In the ring installed transducer method[33], a transducer was mounted in each of the top two compression rings. This allowed for film thickness to be measured over the entire stroke, and also recorded ring twist.

### 1.4.3 Fluorescence Methods

Fluorescent methods for cylinder lubrication verification utilize a liquid's inherent properties to absorb radiation of a certain wavelength and then emit radiation of a different wavelength. The intensity of the fluoresced wavelength relates to thickness of the liquid film.

Though many liquids, including engine oil, have inherent fluorescence, dyes are usually added to the fluid to increase fluorescent intensity. Two devices commonly used to induce fluorescence are Ultraviolet (UV) emitters and high frequency pulse lasers.

UV induced fluorescence is most commonly used in the automotive industry for leak detection. UV induced fluorescence has also been used to quantify fluid film thickness[34]; however, laser induced fluorescence (LIF) is generally regarded as having a higher accuracy for quantifying film thickness.

LIF has been used in engine research to image fuel film thickness[35], and lubricant film thickness[36]. A charge coupled device (CCD) camera or a photomultiplier tube are commonly used to pick up the fluoresced light between laser pulses. Lubricant film thickness has been quantified by LIF in research engines that utilize optical cylinders constructed from fused silica[35] or quartz[37]. In addition to optical engines, LIF, utilizing optical fiber probes installed into cylinder liners, has successfully quantified oil film thickness in operating engines[36,38]. Optical fibers composed of single or multiple optical strands act as a medium for the emitted and fluoresced light. The optical fibers can be installed flush with the cylinder liner and attach to a laser and/or oscilloscope.

### 1.4.4 Current Large Bore Cylinder Lubrication Research

Extensive research on large bore cylinder oil film behavior is currently under development as part of the HERCULES BETA project. The HERCULES BETA project, funded by the European Union and Switzerland, aims at finding technological solutions for compliance of future emission regulations in the marine engine industry. Research is led by MAN Diesel and Wärtsilä. The HERCULES BETA project's major focus areas[9] are:

- Development of a test rig for intensive studies of the lubricating oil film between a piston ring segment and cylinder liner segment under various conditions.
- Development of sensors and methods for dynamic cylinder lubricating oil film thickness measurements on the Wärtsilä RTX4 test engine.
- Development of a mathematical model for advanced simulation of lubricating oil film behavior.

## 2 Timed Lubricator Design

Two designs of ECLs were developed, each with their own detriments and benefits. Both ECLs were designed to deliver a nominal flow rate (6 drops/min) of oil into each feed path, as specified in the GMV engine owner's manual. There are 2 feed paths per cylinder. For the 4-cylinder GMV test engine at the Engines and Energy Conversion Laboratory (EECL), this flow rate equates to 8 pints/day. The ECLs were designed to sustain this flow rate by injecting an equal amount of oil once per cycle. This equated to an injection volume of 2.2 μL in the test engine. All system design calculations are provided in Appendix 1.

### 2.1 ECL Design I

ECL Design I was designed to provide timed lube oil injection, as well as, accomplish the following:

- Minimize modification to the test engine or any of its components.
- Employ the stock check valves that were used in the mechanical system.
- Use system components that were available by outside vendors. No custom design required.
- Monitor the system pressure and temperature.
- Operate from controls developed in-house.

ECL Design I, shown in Figure 2-1, integrates pressure control, flow control, safety, and monitoring equipment.

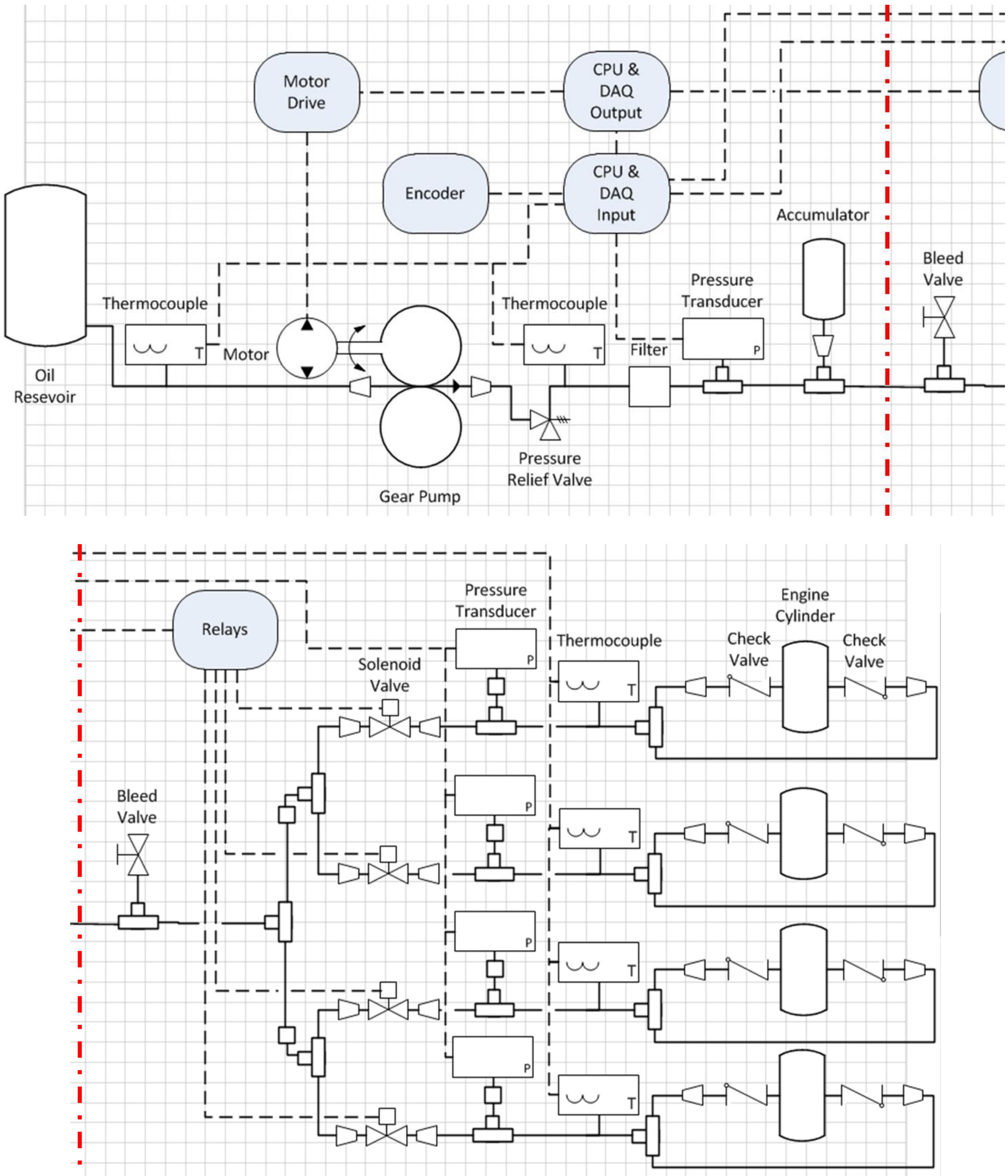


**Figure 2-1 ECL Design I Schematic.**

This system's primary components were a positive displacement pump and solenoid valves. A Beinlich ZPDA series positive displacement pump provided oil pressure to the system. This gear pump offered precise dosing due to its low displacement volume (0.1 mL/rev), low operating speeds (10-200 rpm), and high pressurizing capability, (2900 psi). Assuming no losses, the pump needed to operate at 27 rpm to provide the test engine's nominal lubrication rate. Powering this pump was a Pacific Scientific servo motor and driver, series PMA23B and series PC830, respectively. The motor had a torque rating of 7.2 Nm, with a power rating of 0.62 kW. The motor driver used a 0-10 V analog input signal to direct the motor speed. PacSci 800Tools software communicated with the motor driver. Figure 2-2 displays the command windows and inputs that were used to govern motor speed. An omega PX309 pressure transducer with a 0-1000 psi range, was located downstream of the pump (between the filter and accumulator in Figure 2-1) output a 4-20 mA signal to a National Instruments PXI Data Acquisition system (DAQ). The DAQ system then controlled the output voltage to the motor driver.

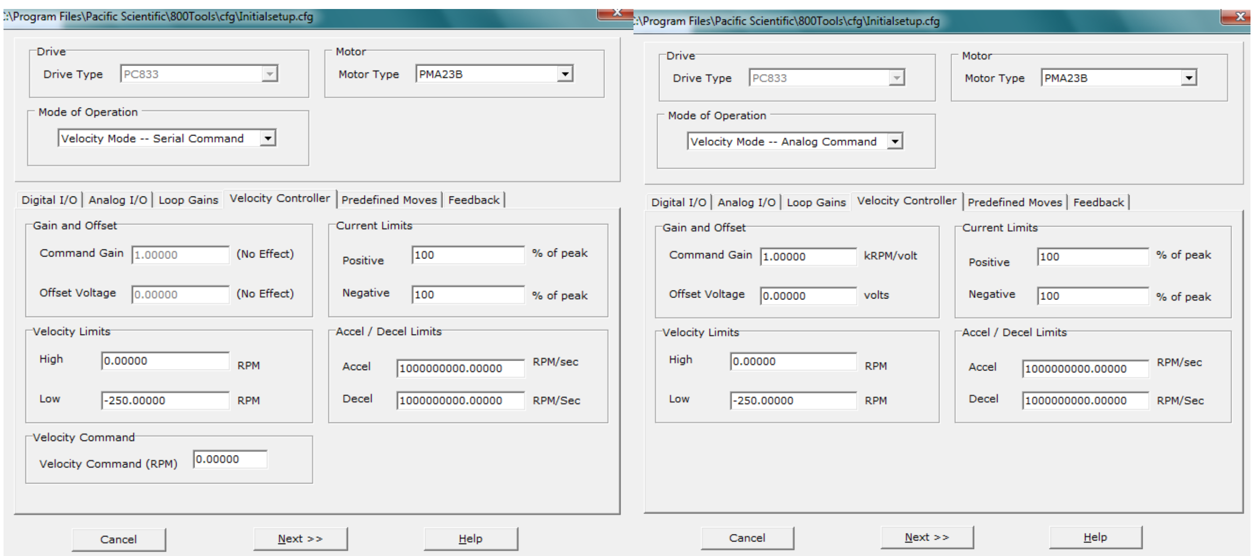


| | |
|---|---|
| Motor control for constant speed | Motor control for constant pressure |

**Figure 2-2 PacSci 800Tools command windows**

Flow control was accomplished using Lee Extended Performance Solenoid Valves, see Figure 2-3. One valve was installed on each cylinder for independent injection control. These valves appeared to be ideal due to their fast operating speeds (500 Hz), high pressure rating (800 psi), and ample maximum flow rate (2.3 mL/s). Using Lee performance data and engine parameters it was calculated that the time necessary to provide the nominal injection volume into each cylinder was 2.6 ms. Each valve was powered by a Lee Spike and Hold Driver, which initially sent a spike voltage (12 V) to open the valve before dropping the voltage (2 V) to hold the valve open. This driver prevented overheating of the solenoid coils. An encoder, mounted to the engine crank, communicated crank positioning to the DAQ, allowing for accurate injection timing.

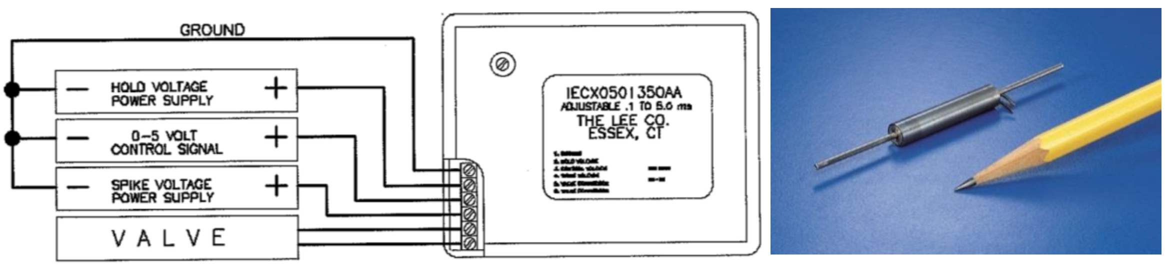


**Figure 2-3 Lee Spike and Hold Driver (left) and High Performance Solenoid Valve (right).**

Real time flow monitoring of the system would have been ideal but due to budgetary restraints could not be accomplished. However, a Max Machinery Model 213 piston flow meter was specified for its low flow rate capabilities (1 mL/min), high pressure rating (3000 psi), ability to operate within an oil medium, and high resolution (1000 pulses/mL). In lieu of a flow meter, flow monitoring largely derived from extensive bench testing calibrations of the solenoid valves to correlate their flow rate with changes in pressure, open duration, and injection interval. Secondary flow rate monitoring was calculated on engine by utilizing a digital scale with a resolution of 2 grams to continuously monitor the oil reservoir mass. The change in reservoir mass was recorded over each point. The difference in reservoir mass coupled with known density of oil allowed for calculation of the average flow rate of the point. This secondary flow rate measurement was used as confirmation of the solenoid calibrations during engine testing.

A pressure relief valve was installed downstream of the pump for overpressure protection. A 7 micron filter removed unwanted particulate in the oil. A diaphragm accumulator located downstream of the pump decreased pulsations within the system. A bleed valve, located at the apex of the system, bled air from the system during start-up. Stainless steel tubing channeled oil flow from the pump to the engine cylinders.

Thermocouples and pressure transducers, installed throughout, monitored the system. Thermocouples, installed upstream/downstream of the pump and downstream of each solenoid valve, monitored changes in oil temperature in the system. Omega PX309 pressure transducers (0-1000 psi range), positioned downstream of each solenoid valve, ensured effective solenoid and check valve operation.

A program written in Labview controlled and monitored the ECL, see Figure 2-4. Pressure control of the system was split into two modes: Manual Pressure (%) and Pressure Setpoint (psi). Manual pressure control commanded the pump to rotate at a constant rpm. The input for manual pressure control was a percentage of the maximum allowed rotational speed, which was input within the servo driver. Manual pressure control was used for calibration of the system. Pressure setpoint control maintained constant pressure within the system. A proportional-integral-derivative (PID) controller minimized pressure fluctuations in the system. PID values were determined experimentally.

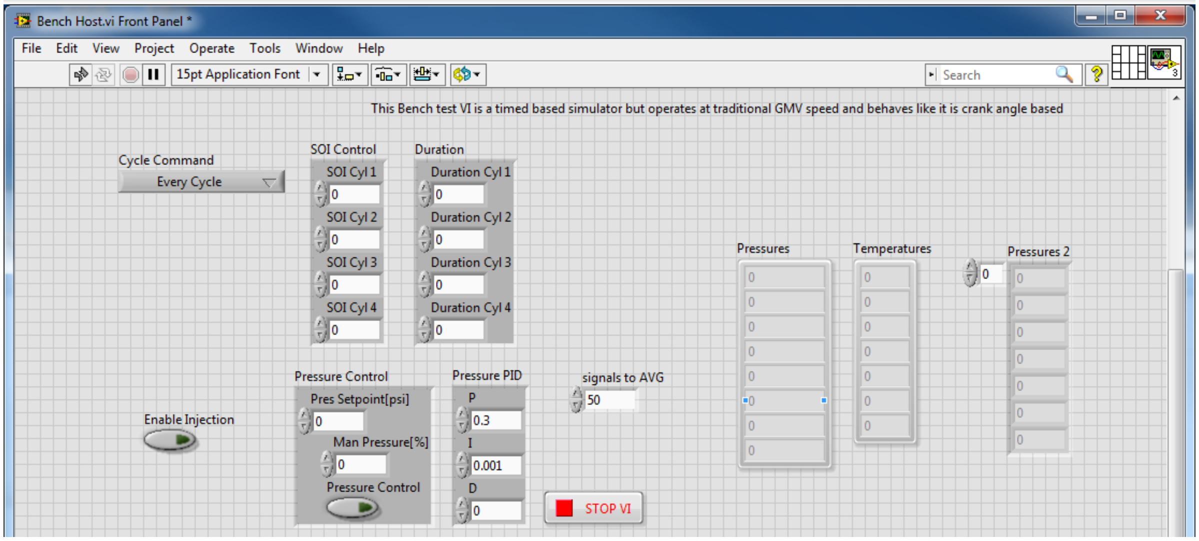


**Figure 2-4 ECL control program.**

Injection was controlled within Labview by adjusting the solenoid opening time and duration. Both the opening time and the duration inputs used the units of crank position degrees, where 0 and 360 degrees correspond to the top dead center (TDC) of cylinder 1. This program allowed for the independent control of each injector. The cycle command in Labview adjusted the injection interval (every cycle, every other cycle, etc.).

### 2.1.1 Pump-Injector Calibration

Bench-testing enabled calibration of the pump and solenoid valves in the system. Bench-testing also determined the optimal system pressure and identified contrasts between individual solenoid valve performances. Oil exiting the system was collected in beakers. Beaker mass was recorded before and after each experiment; the change in beaker mass over time was used to calculate the flow rate. Experiments lasted 10 minutes, unless noted otherwise. Experiments employing the solenoid valves, were at 5 Hz (300 injections/min), equating to one injection per cycle, unless noted otherwise. The solenoid valves were designated A-E; the solenoid drivers were designated 1-4. The following bench-tests were conducted:

a) Motor-Pump Calibration. Using a gate valve downstream of the pump, the pump outlet pressure was adjusted from 0 psig to 700 psig. The pump speed varied between 10-60 rpm. Resulting flow rates were recorded and showed that pump leakage was independent of pump speed and equated to less than one (mL/min) from 0-700 psi outlet pressure.

b) Solenoid-driver impact on flow rate. Two drivers were tested on one solenoid valve to quantify driver impact on valve flow rate. Driver impact on valve flow rate was negligible.

c) Effect of driver hold voltage on flow rate. Adjustment of the hold voltage had no impact on flow rate. This result was likely caused by malfunctioning of the drivers' hold voltage command. However, experimentation found that the open durations required for injection were short enough that no large change in solenoid coil temperature ever occurred.

d) Effect of open duration on flow rate. A linear relationship between valve flow rate and open duration was found.

e) Effect of open duration on flow rate with oil injection every other cycle (150 injections per minute). Oil injection every other cycle gave a slightly higher oil volume per injection. Increased stability of the system pressure, due to fewer injection events, was attributed with the increased injection volume.

f) Effect of backpressure on flow rate. For this experiment, oil was injected through a check valve and into a pressurized reservoir (Figure 2-5). The reservoir pressure, compressed using a compressed air connection to 50 psi, corresponded with the expected cylinder pressure as the ring pack crossed the lube port on the engine. The check valve, used in experimentation, was borrowed from the Trabon force feed system and had a cracking pressure of 50 psi.  These pressures equated to a steady backpressure of 100 psi. Results, counter intuitively, showed that flowrate increased with the addition of backpressure.  This result was attributed to the effect of upstream pressure on the opening time of the solenoid valves.  The solenoid valves operated by translating a plunger upstream to open a flow channel.  At low differential pressures, the opening time for the solenoid valves was likely relatively low.

**Figure 2-5  Benchtop experiment f) setup.**

g) Optimal injection pressure for maximum flow rate.  Maximum flow rate was observed at a differential pressure of 200 psi.  This pressure balanced opening speed of the valve with oil velocity exiting the valve during injection.

h) Nominal lube rate (8 pints/day, .67 mL/min) testing on engine.  Before engine testing, a final calibration of the system was conducted while installed on the inactive engine.  The data was consistent with the off-engine bench-test results.

The corresponding graphs for bench-testing are located in the same order as noted above in Appendix II.

## 2.2 ECL Design II

ECL Design II is similar to ECL Design I in several ways. Design II, displayed in Figure 2-6, utilizes the same pressure control system as Design I. Pressure control is composed of a servo motor, driver, and pressure transducer. Design I's pressure transducer is replaced with an Omega PX319 pressure transducer with a pressure range of 0-3000 psi to accommodate higher system pressures. The same servo motor, driver, pump filter, accumulator, pressure relief valve, and bleed valve are used in both designs.

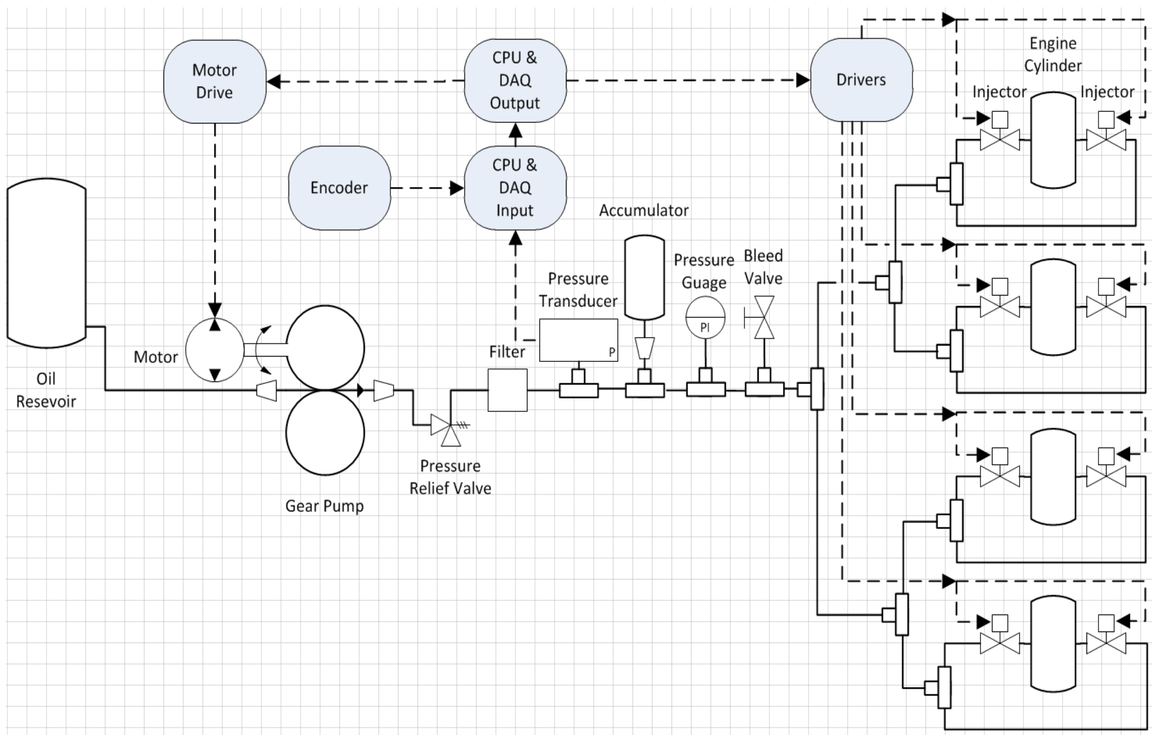


Figure 2-6 ECL II schematic.

The system pressure downstream of the filter is monitored with an Omega PGF series pressure gage with a 0-3000 psi range.

Unlike ECL Design I, Design II utilizes injectors on each lube port (2 injectors per cylinder). The injectors are Hoerbiger XperLUBE injectors (see Figure 2-7). These injectors are custom designed to meet the performance required for power cylinder oil injection. The injectors are designed for fast response (< 1ms open/close), low injection volume (1.2 µL minimum), substantial backpressure (100 psi), and high oil pressure (725-2200 psi). These injectors are powered by an R&D SDM injector driver supplied by Hoerbiger, shown in Figure 2-7.

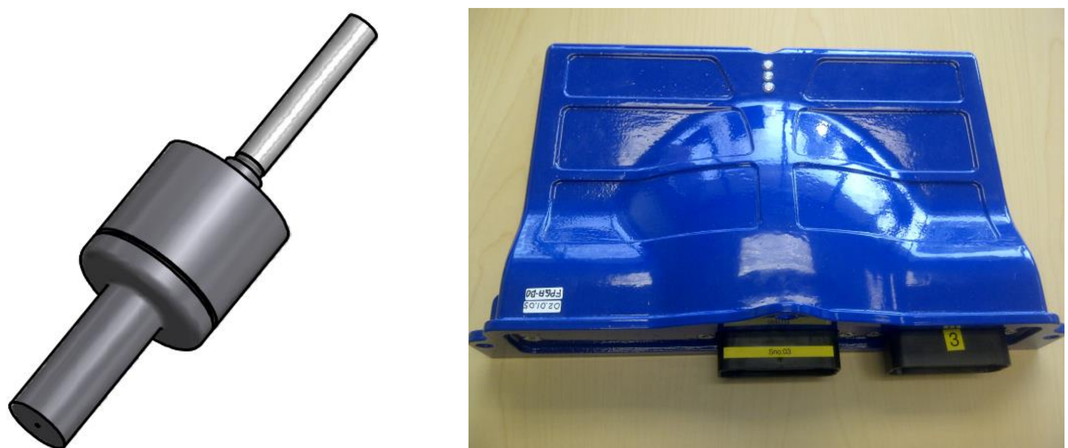

| Hoerbiger XperLUBE Injector | SDM Injector Driver |
|---|---|

**Figure 2-7 Hoerbiger XperLUBE injector and SDM driver.**

Positioning of an injector on each lube port provides several benefits. This positioning permits the removal of the system check valves, ensures equal flow to each lube port, and significantly reduces dead volume in the system.

The dead volume between the injector and inner cylinder wall is reduced by nearly 12,500% (calculations provided in Appendix I), from ECL Design I to II. If nominal injections occur in intervals of 1 injection per every 4 cycles, the dead volume equates to less than 12 injection volumes. The calculated volumetric compression of the oil equates to less than 4% of the injected volume.

To increase the flow rate measurement accuracy of the ECL, two different methods of flow rate measurement are used. (1) The same mass scale measurement method utilized in design I. However, a more precise scale is incorporated. An A&D Newton EJ balance with a 4100 g capacity, 0.1 g readability, 0.1 g repeatability, 1 second stabilization time, and RS-232 serial interface is used. This scale increases accuracy 20x (for small changes in mass) compared to the scale used in ECL Design I testing. (2) The average rotational velocity of the pump is normalized and is used to calculate the average flow rate of the pump. Leakage losses within the pump are accounted for by utilizing the pump calibration data that was determined in ECL Design I bench-testing.

### 2.2.1 Injector Mounting

Additional reduction in dead volume is accomplished by mounting a capillary into each lube port. The capillary inside the lube port has an outer diameter equal to that of the original lube port (.215 inches) and an inner diameter of .04 inches (~1mm). This reduces the cross-sectional area of the lube port by over 2500%.

The inner diameter of the capillary was selected through calculation (see Appendix I) and experimentation. In calculation, inner capillary diameters less than 1 mm gave unacceptable pressure drops due to high surface tension. In experimentation, six, four inch length tubes of varying inner diameters were tested with water and engine oil at room temperature. Three experiments were conducted for each liquid and determined the following: 1) If dripping occurred when the flooded tube was held vertically with a finger covering the upper end of the tube, 2) If leakage occurred in the vertically positioned, uncovered tube, 3) The angle of the tube, with respect to the ground, which dripping commenced. A protractor measured the tube angle. Results for the capillary testing are displayed in Table 2-1.

**Table 2-1 Inner capillary diameter experimental results.**

| | Water | | | Engine Oil | | |
|---|---|---|---|---|---|---|
| **Tube ID (inches)** | **Vertical Vacuum Drip?** | **Vertical Drip?** | **Minimum Drip Angle (°)** | **Vertical Vacuum Drip?** | **Vertical Drip?** | **Minimum Drip Angle (°)** |
| **.188** | No | Yes | 2 | No | Yes | 3 |
| **.069** | No | Yes | 15 | No | Yes | 22 |
| **.040** | No | Yes | 25 | No | Yes | 70 |
| **.030** | No | Yes | 50 | No | No | N/A |
| **.020** | No | No | N/A | No | No | N/A |
| **.010** | No | No | N/A | No | No | N/A |

In addition to decreasing the dead volume, the capillary insert provides mounting and sealing from the injector to the lube port (Figure 2-8). A male NPT to straight thread fitting threads onto the 1/8 NPT threaded port that utilizes for the mechanical lubricator check valve attachment and seal. Adjustment of the translational positioning of insert in the cylinder is necessary because of relative differences in the lube port molding. Straight threading, located on the insert capillary, attaches to the fitting and accommodates for translational adjustment in the cylinder to ensure that the capillary tip is flush with the inner cylinder wall. A jam nut locks the insert capillary into final position. An O-ring, set against the jam nut and fitting, seals the cylinder with the insert. The insert capillary threads into the injector housing and compresses an O-ring against the injector for sealing. An O-ring groove is machined into the outer end of the insert capillary. The injector compresses into the injector housing using bolts and an insert end cap. The inserts were machined in house with assistance from a local machine shop.

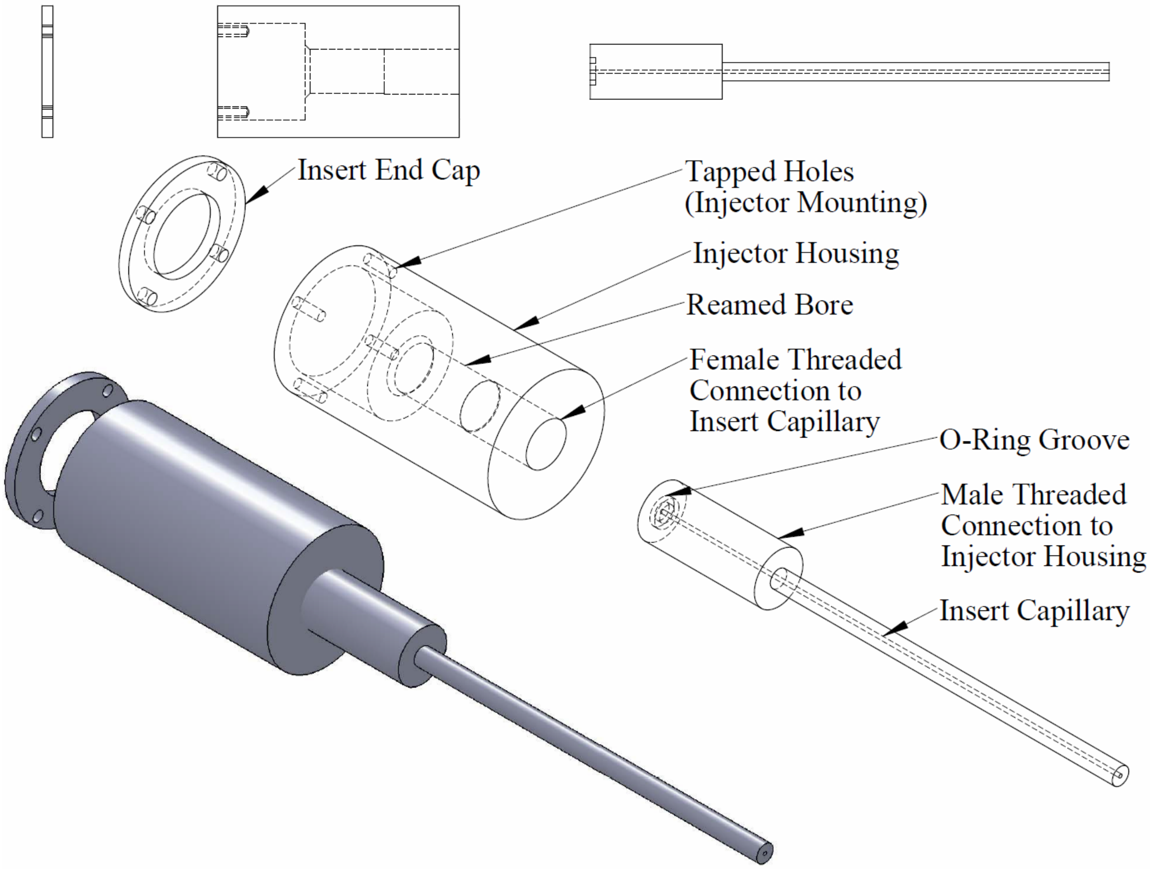


**Figure 2-8 ECL II lube port insert**

A model of the engine cylinder with the lube port inserts is shown in Figure 2-9.

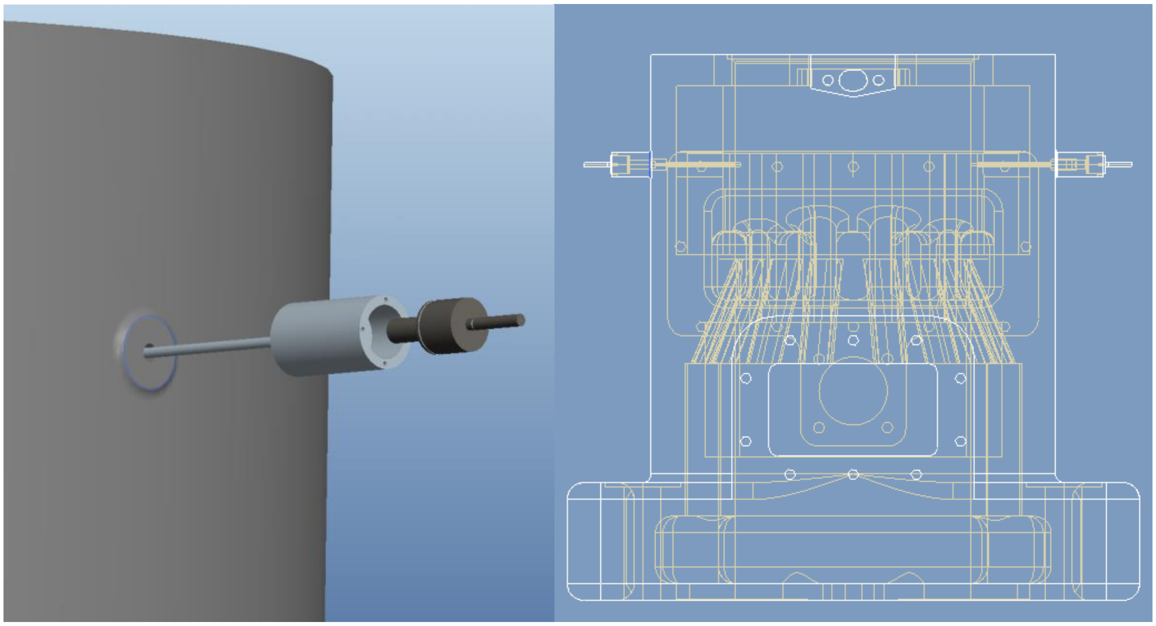

**Figure 2-9  Insert attachment to the cylinder.**

### 2.2.2 Cylinder Modification

Three of the eight lube ports on the test engine were modified to mount the injector inserts. Eccentricity between the lube port and its counterbored section (threaded to accept 1/8 NPT) required cylinder modification to mount the injector inserts.  The three threaded ports were bored with a 7/16" piloted counterbore (see Figure 2-10).  A custom machined pilot allowed the original counterbore to be re-bored concentrically to the lube port.  The pilot also prevented chips from entering the cylinder during boring.  After re-boring the cylinder, the ports were tapped to accept 1/4 NPT fittings.

Figure 2-10  Piloted Counterbore.

### 2.2.3 Fuel-Arm Pushrod Modification

A geometrical issue presented itself with the ECL II design that was a nonissue with ECL Design I.  On each engine cylinder, one lube port was positioned directly behind the pushrod for the fuel rocker arm.  With only a one inch clearance, the injector position interfered with the pushrod.  To accommodate the positioning of the new injectors, each pushrod was adapted with a notch. Figure 2-11 shows the original rocker arm configuration and the modified rocker arm.

| | |
|---|---|
| Original Rocker Arm | Notched Rocker Arm |

**Figure 2-11  Pushrod alteration.**

# 3 Experimental Equipment

## 3.1 Test Engine

A 4-cylinder Cooper-Bessemer GMV-4TF large bore natural gas, 2-stroke engine carried out the testing, see Figure 3-1. The Cooper Bessemer, located at Colorado State University's Engines and Energy Conversion Laboratory (EECL), was instrumented to record over 100 different engine parameters at each test point. The engine was slow speed (300 rpm) and had a 14 inch bore and stroke. The rated load for the engine was 440 bhp, corresponding to a 67.6 psi BMEP. The engine output shaft connected to a computer-controlled, water brake dynamometer for precise load control. The engine operated lean with direct fuel injection. The Cooper-Bessemer had pre-chamber heads, with pre-combustion chambers installed. Ignition timing was controlled by an Altronic CPU2000 ignition system. The ignition system maintained a peak pressure location at 18° above top dead center (ATDC).

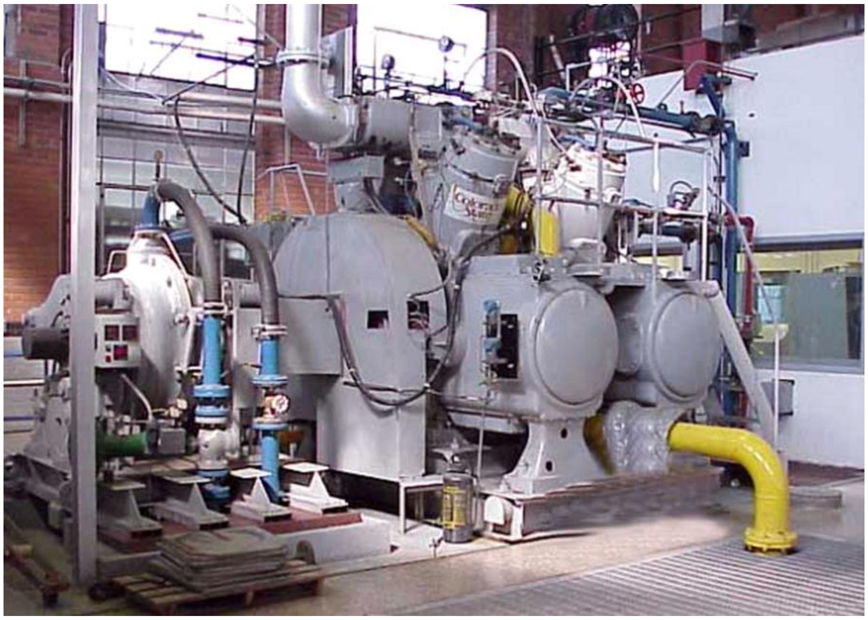

**Figure 3-1 Cooper-Bessemer GMV-4TF at the CSU EECL**

Air supply for the engine was provided via a turbocharger simulator, consisting of a Gardner Denver screw compressor and a backpressure valve. Through computer control, the air and exhaust manifold pressures were controlled to simulate any turbocharger set-point.

### 3.1.1 Mechanical Lubricator

The force-feed lubricator installed on the test engine at the Engines and Energy Conversion Laboratory was produced by Trabon, shown in Figure 3-2.

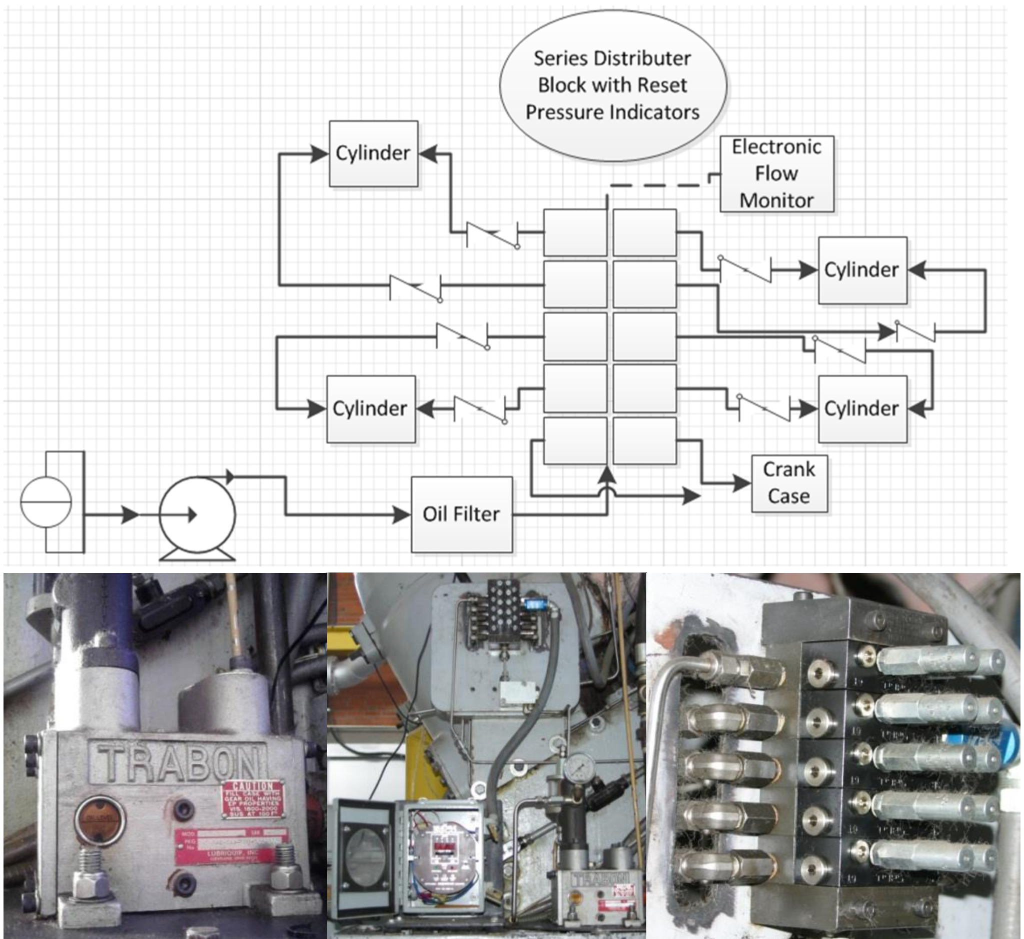


| | | |
|---|---|---|
| Piston Pump | Divider Block | Divider Block Assembly |

**Figure 3-2 Trabon force feed lubricator.**

This lubricator was primarily composed of a piston pump and a divider block assembly. The crank-powered piston pump metered oil to the divider block assembly. The lubrication rate of the system was altered via an adjustment bolt located on the pump; this bolt altered the stroke length of the piston. Lube oil, after exiting the pump, passed into the divider block assembly. A Sloan Brother lube rate monitor tied into the divider block assembly to accurately quantify lube flow rate.

## 3.2 Exhaust Concentration Measurements

Exhaust gas analyzers, shown in Figure 3-3, determined the emissions exiting the test engine. A Rosemount 5-gas analyzer determined CO, $CO_2$, THC, NOx, and $O_2$ concentrations in the exhaust. Three of the 5-gas instruments (CO, CO2, and NOx) were replaced with Siemens instruments. Table 3-1 summarizes the 5-gas instrumentation. A Fourier transform infrared (FTIR) spectrometer (see Figure 3-3) measured numerous other emissive species, including ethane, ethylene, propane, and formaldehyde. Applicable EPA and ASTM measurement methods were employed for operation of the emissions analyzers. A Varian CP – 4900 gas chromatograph determined the natural gas composition entering the test engine.


| 5-Gas Analyzer | FTIR Spectrometer |
| --- | --- |

**Figure 3-3 Exhaust Analyzers.**

Table 3-1 Characteristics of instrumentation in 5-gas analyzer system[4].

| | Device | Measurement Technology | Minimum Concentration Range | Maximum Concentration Range | Linearity |
|---|---|---|---|---|---|
| **CO** | Ultramat 6 | IR | 0 – 10.0 ppm | 0 – 10000 ppm | < 0.5% of full-scale value |
| **$CO_2$** | Ultramat 6 | IR | 0 – 5.0 ppm | 0 – 30 % | < 0.5% of full-scale value |
| **THC** | NGA 2000, FID | FID | 0 – 1.0 ppm | 0 – 10000 ppm | < +/- 1% of full scale |
| **$NO_x$** | NOx MAT 600 | Chemiluminescence | 0 – 1.0 ppm | 0 – 3000 ppm | < 0.5% of full-scale value |
| **$O_2$** | NGA 2000, PMD | Paramagnetic | 0 – 1.0 ppm | 0 – 100 % | +/- 1% of full scale |

A mini dilution tunnel was used to measure particulate emissions of the test engine, see Figure 3-4.

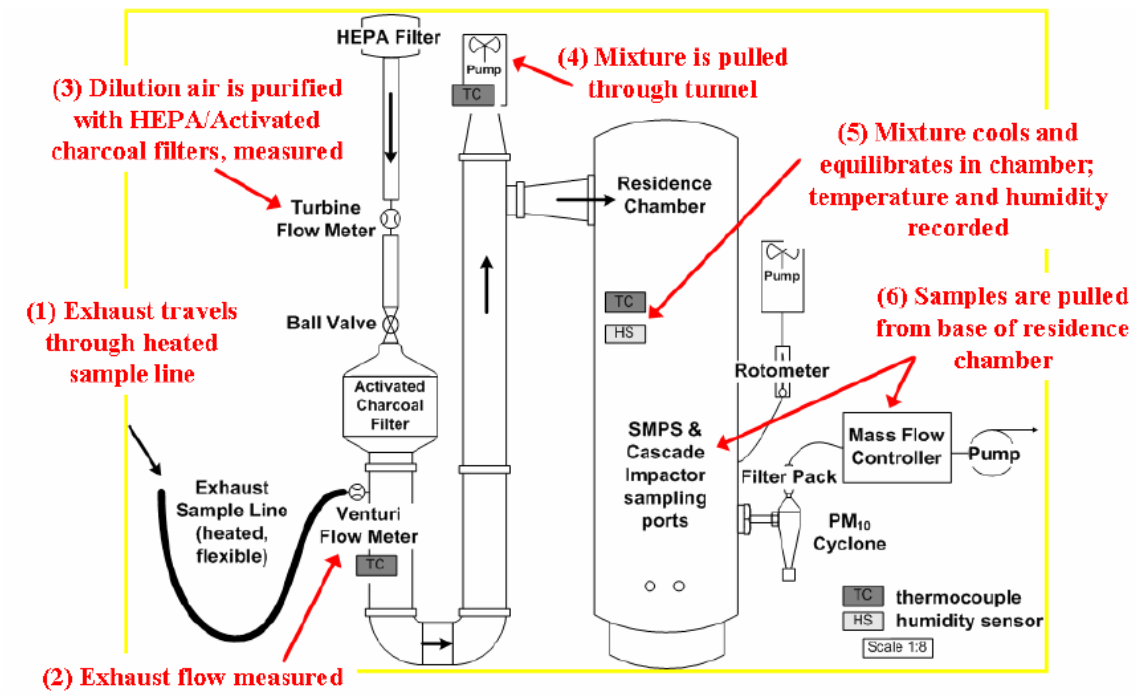


Figure 3-4 Dilution tunnel schematic.

The dilution tunnel, consistent with ISO 8178, pulled exhaust air through a heated sample line and inserted it into a tunnel, where it mixed with laboratory air (1). The exhaust air was received through a 3/8" PM probe located approximately 4 feet downstream of a large radius, 90° exhaust elbow. The elbow was part of the 10" exhaust line that runs from the engine manifold. The probe is located at the centerline of the exhaust line and was angled parallel to maximize exhaust collection. The probe diameter was sized to isokinetically sample exhaust at nominal operating conditions; the exhaust velocity in the main exhaust line was approximate to the exhaust velocity in the probe. This sizing minimized momentum effects at the probe inlet. The probe then attached to a heated sample line which guided flow into the dilution tunnel. A venturi measured the exhaust flow rate (2). Laboratory air traveled through a high efficiency particulate air (HEPA) filter and an activated charcoal filter. A turbine flow meter measured laboratory air flow rate (3). A ball valve, located on the laboratory air line adjusted the dilution ratio (adjustable between 5 and 100). A vacuum pump pulled both the laboratory and emissive air through the tunnel (4). A second vacuum pump pulled the now diluted exhaust through a residence chamber (5); the residence chamber equilibrated and cooled the diluted exhaust. The residence chamber (320 L) created a vortex that wound down into a cyclone (6). The cyclone was designed to drop relatively heavy particulate greater than 10 microns in diameter ( $\geq PM_{10}$) out of the diluted exhaust. Optimal cyclone flow rate was 28 lpm (1 cfm). The diluted exhaust was pulled though the cyclone via a third vacuum pump. A rotameter, with a range of 10-100 SCFH, measured the flow rate through the cyclone. A choke flow orifice, attached to the filter assembly, maintained a consistent flow rate of approximately 60 SCFH. The filter assembly, located downstream of the cyclone collected the remaining PM in the exhaust. The filter assembly was composed of a Teflon filter held in a 47 mm delrin cassette that is housed inside a stainless steel filter holder. Ball valves were located upstream and downstream of the filter holder and were used to stop flow when Teflon filters were changed. The difference in pre-test and post-test mass of the Teflon filter signified the particulate sample taken, and was used in calculation of total PM emissions.

Several modifications were made to the dilution tunnel, prior to testing, to optimize sample accuracy. All piping connections were resealed, and the system was pressure tested to 5 psi. A second turbine flow meter was installed in parallel to the existing turbine flow meter on the dilution air line. The purpose of this second flow meter was to accurately measure dilution air flow at low dilution ratios. Ball valves were fitted on both turbine flow meter lines so that only one remained open at a time. The sample probe was reinstalled into the exhaust line to ensure its correct positioning. Dilution air filters were also replaced.

# 4 Experimental Procedures

## 4.1 Mechanical Lubricator Testing

Mechanical lubricator testing was conducted to validate the findings of Olsen[4] on power cylinder lube oil carryover. To test the effect of cylinder lubrication rate on exhaust emissions, the test engine's load (100%) and speed (300 rpm) were held constant.

A sweep of the mechanical lubricator flow rate was conducted. The lube rate sweep consisted of 6 data points taken from 5.7-18.4 pints/day. The points were taken after start-up and had durations of 15 minutes per data point. The first point taken was at a constant lube rate of 18.4 pints/day; subsequent points were taken in descending lube rate order. Between points, the PM filter on the dilution tunnel was changed. The average time between data points was 15 minutes. This time allowed emissions to stabilize after the lubrication rate was altered.

## 4.2 Optimum Injection Angle Testing

The injection angles at each cylinder were relative to the optimal injection angle (OIA). The OIA was, theoretically, the angle that the top compression ring on each piston passed the lubrication port on its upstroke. The OIA was found by manually turning over the engine while using an Autel MV208 borescope to view the piston rings through each port; the corresponding angle, for each cylinder, was determined by identifying the corresponding gear tooth on the flywheel. The tooth count on the flywheel began, in addition to the encoder, at the TDC of Cylinder 1. The following equation calculated the angle:

$$\theta = \frac{The\ corresponding\ flyweel\ tooth\ as\ the\ top\ compression\ ring\ passes\ the\ lube\ port}{Total\ number\ of\ flywheel\ teeth} \times 360°$$

The piston rings were identified, through the lube port, by their reflectivity to the borescope's LED light.  Figure 4-1 is a stillshot of the top compression ring crossing the lubrication port.

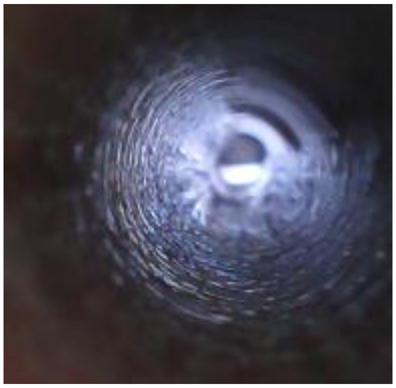

Figure 4-1  Compression ring passing the lube port.

Results from OIA testing are displayed in Table 4-1.  The OIAs for cylinders 1 and 2 were 180° apart from cylinders 3 and 4, respectively.  Since the TDC of cylinder 1 and 2 were known to be 180° apart from the TDC of cylinder 3 and 4, respectively, the OIAs were likely presumed correctly.

Table 4-1  Injection Timing.

| Cylinder # | OIA.  Top compression ring passing the lube port (θ ATDC of cylinder 1) | Bottom compression ring passing the lube port (θ ATDC of cylinder 1) | TDC (θ ATDC of cylinder 1) |
|---|---|---|---|
| **1** | 294 | 312 | 0 |
| **2** | 353 | 11 | 63 |
| **3** | 115 | 133 | 180 |
| **4** | 174 | 192 | 243 |

## 4.3 ECL I Testing

The engine and emission analyzer parameters for ECL I testing duplicated the engine parameters of the mechanical lubricator testing.

Timed lubricator testing was scheduled for two days. Day 1 testing would determine the optimal injection time (OIT) for the timed lubrication system. This was necessary as the injection delay of the system was unknown due to the system complexity. Delays caused by solenoid opening time, oil compression, check valve cracking, and lube port flow to the cylinder wall could all contribute to delayed injection. The low tolerance necessary for optimal injection made experimental evaluation of system delay advantageous. OIT would be determined by creating an injection sweep across the entire crank cycle, and comparing PM emissions at each angle.

An initial injection sweep, at 45º intervals from OIA was used to find the approximate OIT. The goal was to have this sweep identify the injection interval where PM emissions were lowest; subsequent data points would be taken within this interval to precisely determine the OIT.

Day 2 of engine testing would be used to create a lube rate sweep at the OIA. This data would then be compared to the mechanical lubricator lube rate sweep to determine the benefits of timed injection.

## 4.4 Lubrication Verification

Two economical methods of verifying cylinder lubrication were administered after mechanical lubricator engine testing. The two verification methods were the cigarette paper method and UV induced fluorescence.

Two bench-top experiments were conducted to verify the UV induced fluorescence method, shown in Figure 4-2.

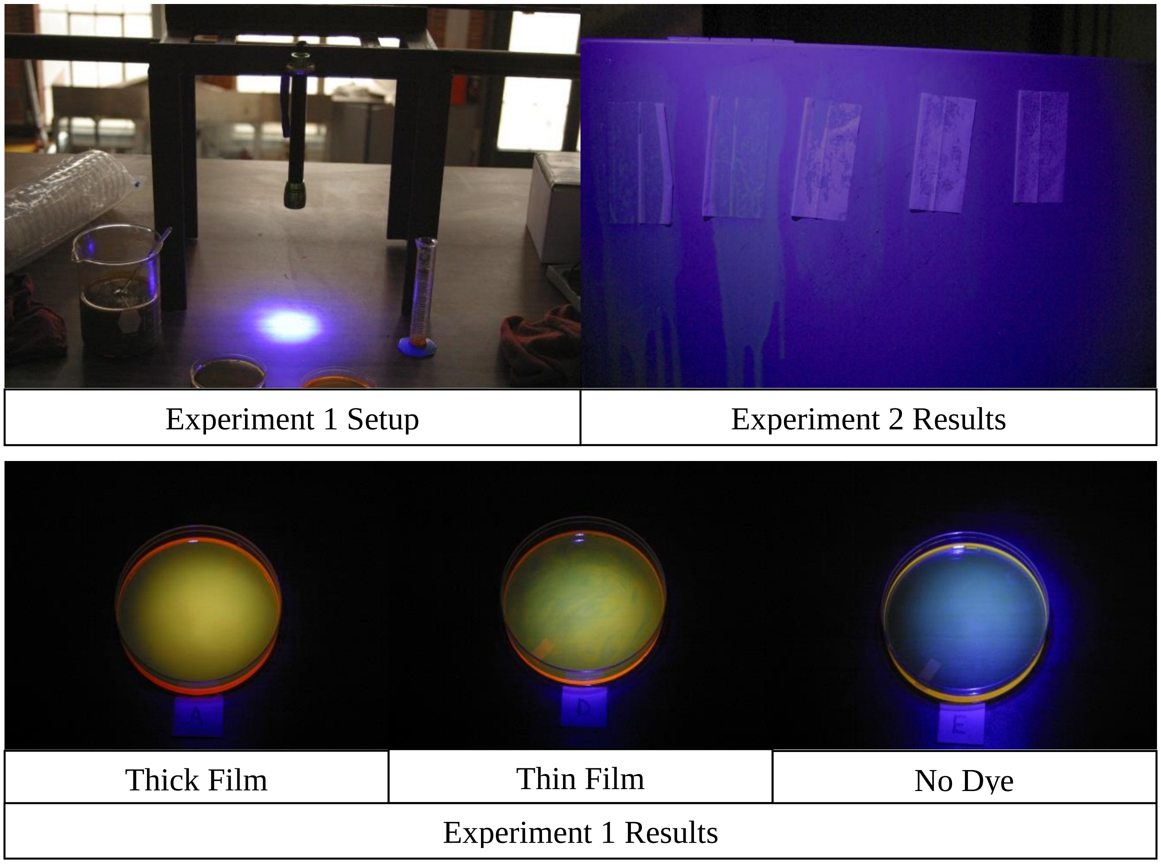


**Figure 4-2 UV Fluorescence Experiments**

Both experiments used Dye-Lite Leak Detection Dye at a dilution ratio of ½ oz. dye/gallon oil. A Spectronics UV flashlight illuminated the dyed oil. Experiment 1 confirmed that the fluorescent intensity of the oil/dye solution was dependent on oil film thickness. Experiment 2, conducted on a vertical face (similar to the engine cylinders), confirmed that UV fluorescence method could be used in conjunction with the cigarette paper method to give a qualitative representation of cylinder lubrication.

After confirmation of the UV fluorescence method, Dye-Lite leak detection dye was added to the power cylinder lubrication reservoir at a dilution ratio of approximately ½ oz. dye/gallon oil. After engine testing of the mechanical system a cylinder head was removed, and the cylinder was examined for lubrication. The UV flashlight identified relatively high and low lubricated areas on the cylinder wall.

# 5 Results and Discussion

## 5.1 Mechanical Lubricator Results

Figure 5-1 and Figure 5-2 are plots of the lubrication rate and the corresponding PM emissions data.  Data points and the original equipment manufacturer (OEM) lube rate are located on the graphs.

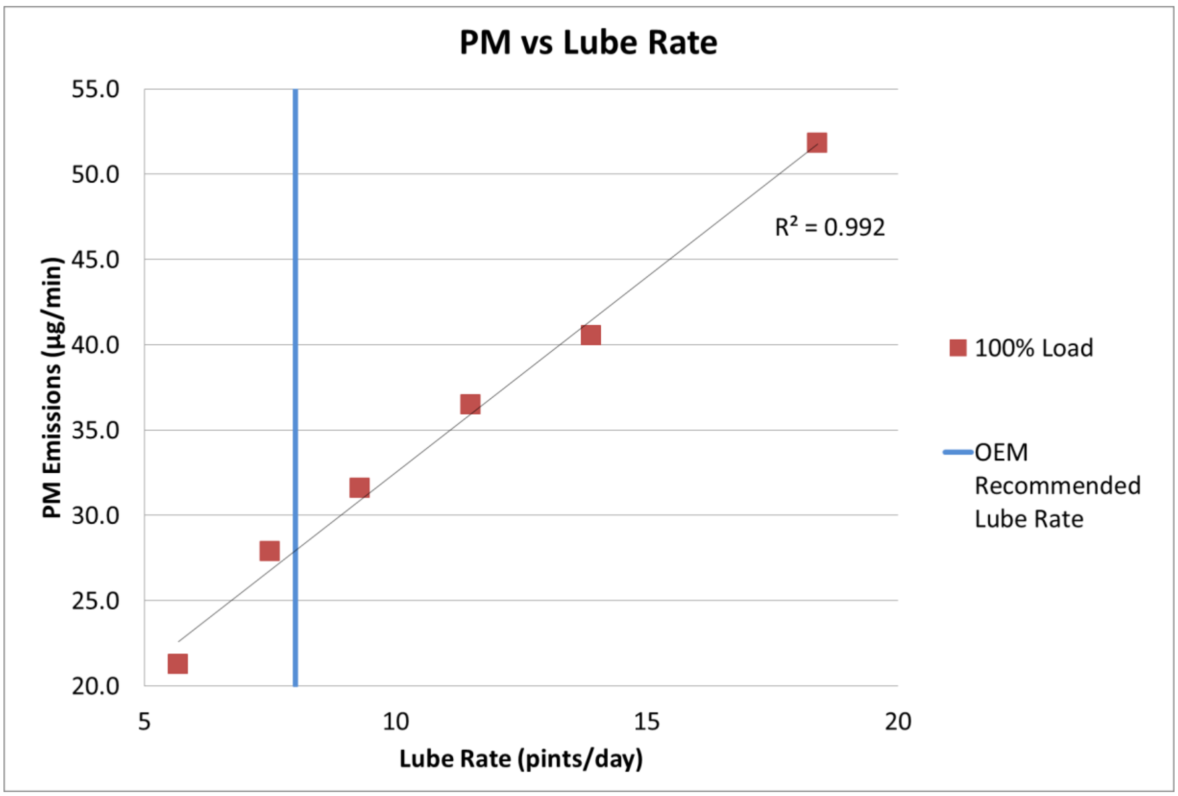


Figure 5-1  PM vs. lube rate.

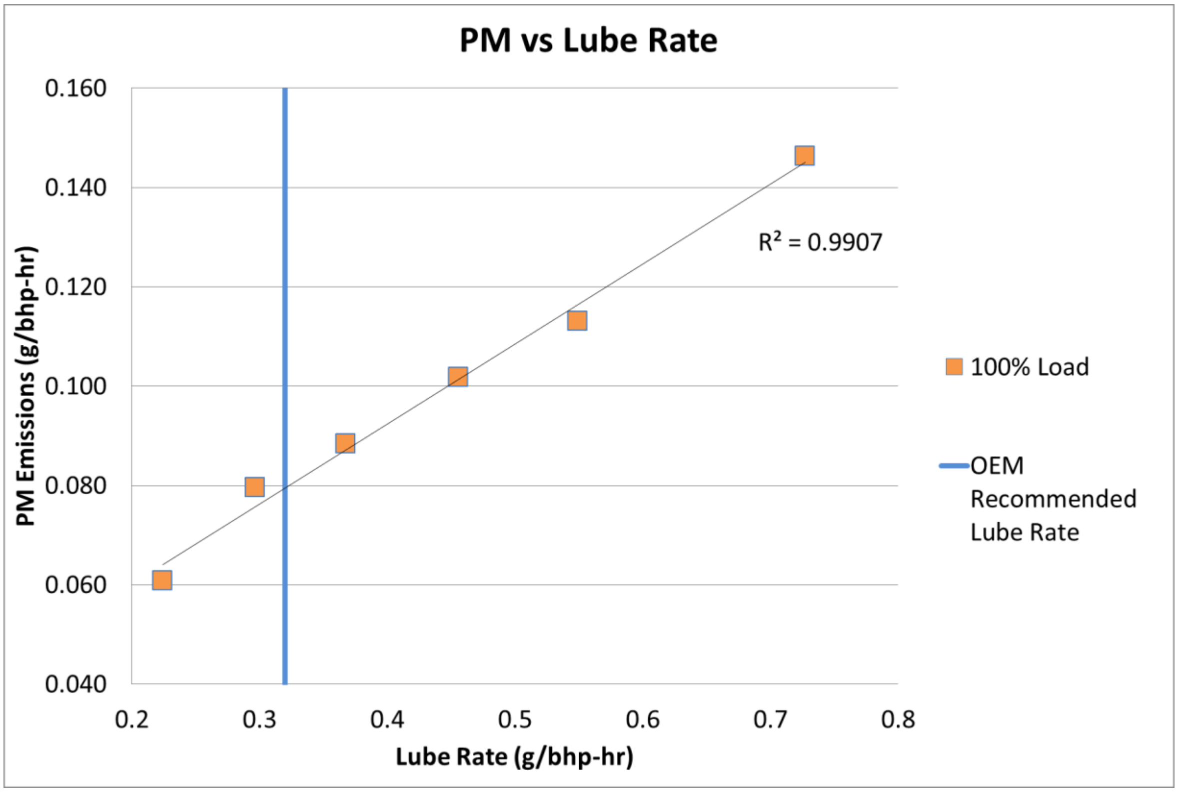


**Figure 5-2 Normalized PM vs. lube rate.**

A normalized graph (Figure 5-2), using brake specific units, displays a linear correlation between PM emissions and lubrication rate. It is insightful to compare the results with regulated PM limits for stationary compression ignition (diesel) engines. The PM regulated limits for engines between 750 and 1200 hp for 2011-2014 and 2015+ model years are 0.075 and 0.020 g/bhp·hr, respectively.[39] All of the PM values are above the 2011-1014 level and nearly all of the PM values are above the 2015+ level. Thus, PM levels are significant compared with current regulation limits for compression ignition engines.

The carryover of injected power cylinder lubricant that was present in PM form in the exhaust was 25% at the nominal lube rate. Figure 5-3 displays the lubricant carryover relative to the lubrication rate.

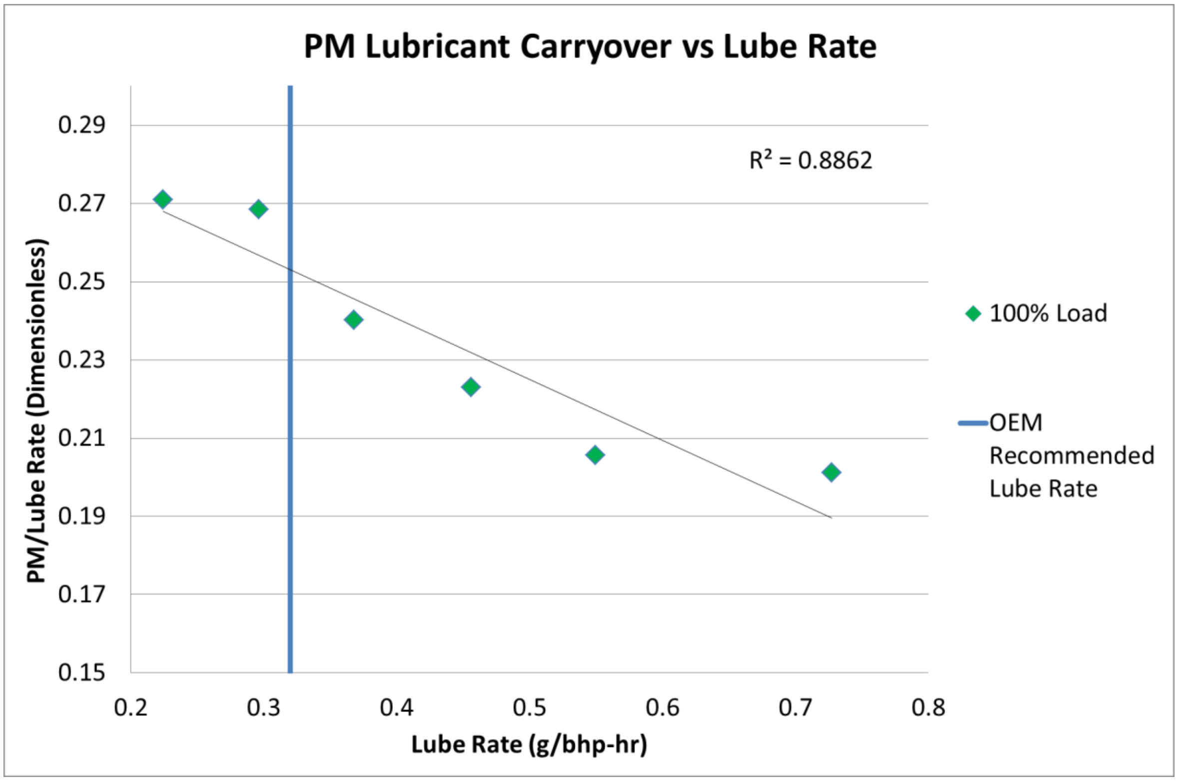


**Figure 5-3 Mechanical lubricator PM carryover vs. lube rate.**

Figure 5-3 in conjunction with Figure 5-2 shows that the percentage of PM lubricant carryover linearly decreases as the lubrication rate increases, even though overall PM emissions increase. Therefore, with increased lube rate, a higher volume of PM is emitted, but a lower percentage of the injected cylinder oil carries over into the exhaust in PM form. The inverse linear relationship between lubricant carryover and lube rate may signify that a higher percentage of power cylinder lubricant returns to the sump at increased flow rates.

The lubrication rate's effect on CO, VOCs, $CH_2O$, Formaldehyde, Ethylene, and NOx emissions were also analyzed. Results of this analysis are displayed in Figure 5-4, Figure 5-5, and Figure 5-6, respectively.

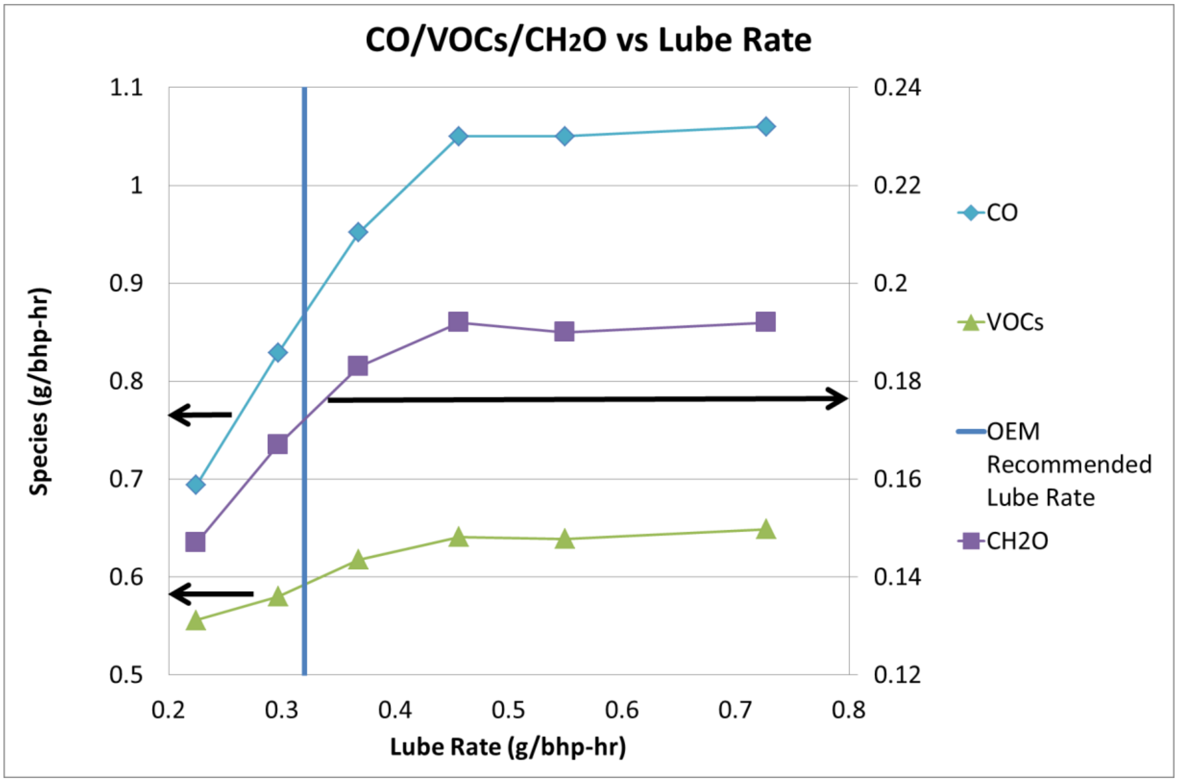


Figure 5-4  CO, VOCs, CH2O emissions vs. lube rate.

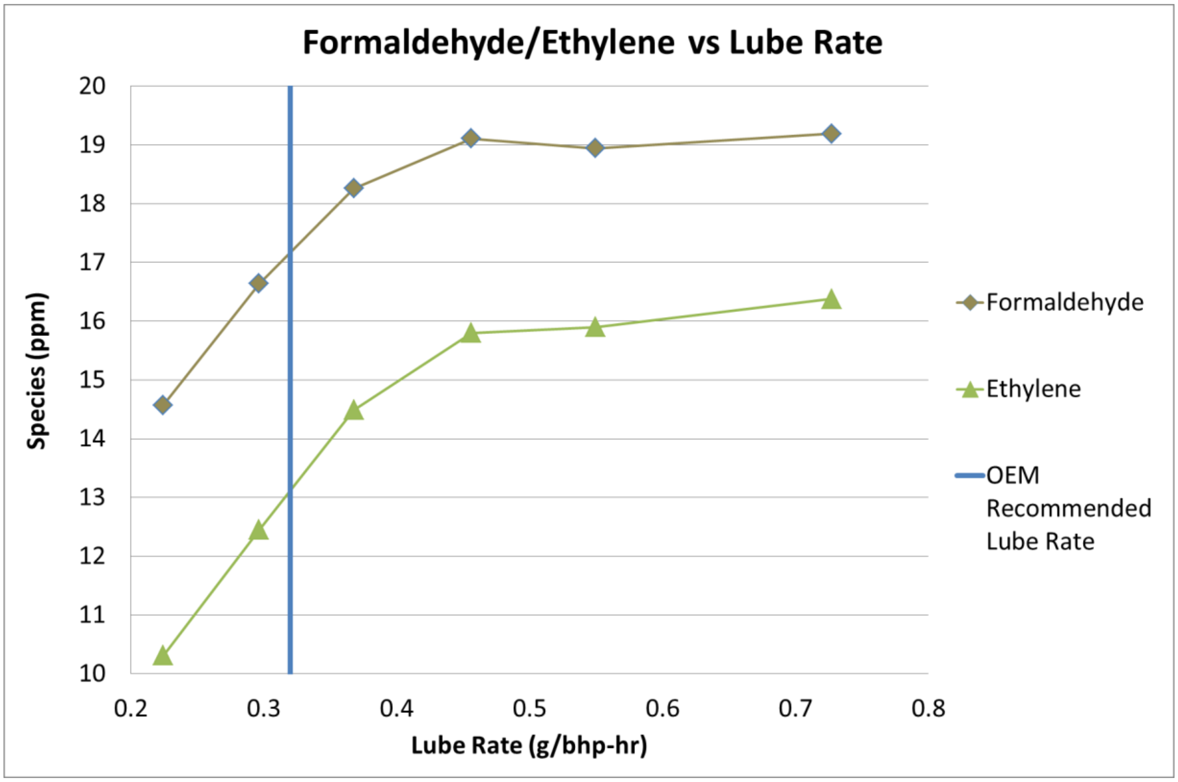


Figure 5-5  Formaldehyde, Ethylene vs. lube rate.

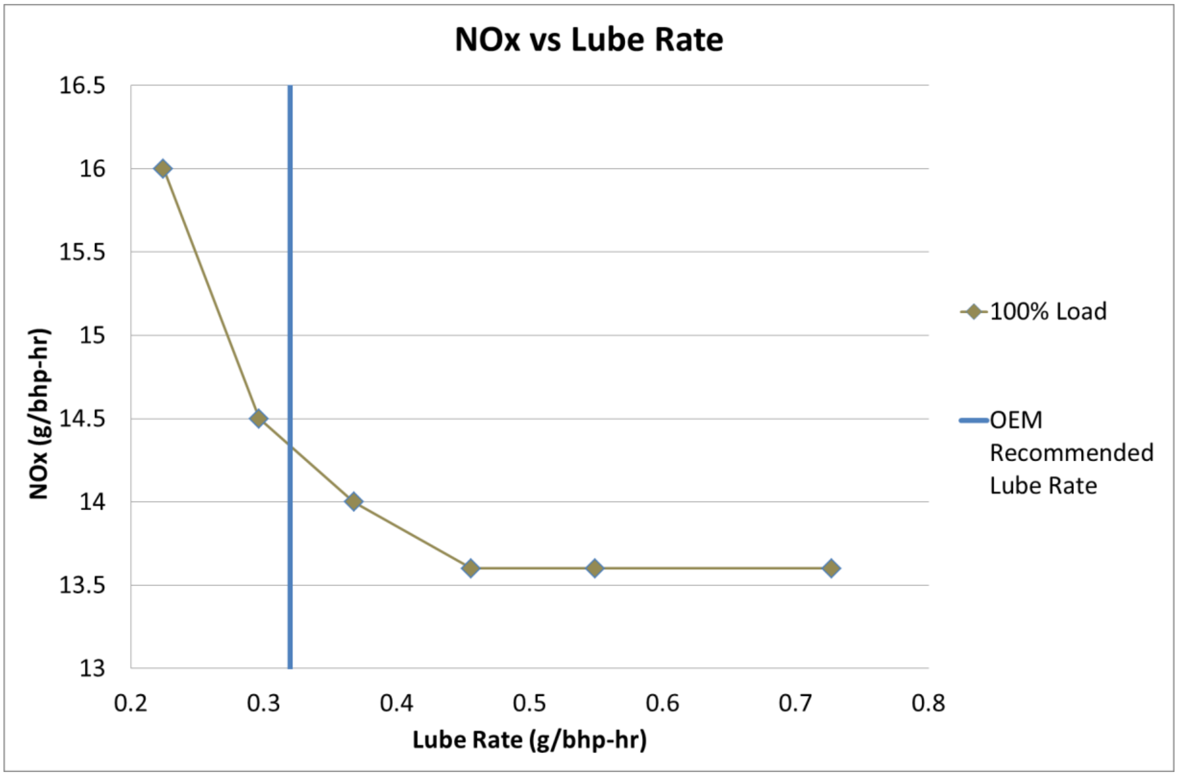


Figure 5-6 NOx vs lube rate.

CO, VOCs, CH2O, formaldehyde, and ethylene emissions all displayed a similar relationship with cylinder lubrication rate. Each of these five emissions increased linearly with lubrication rate for lube rates ranging from .22-.45 g/bhp-hr. At higher lubrication rates (.45-.73 g/bhp-hr), lube rate showed little correlation to these five emissive species. NOx emissions linearly decreased at lower lubrication rates, before remaining constant at higher lube rates.

An exhaust temperature analysis is displayed in Figure 5-7 and Figure 5-8.

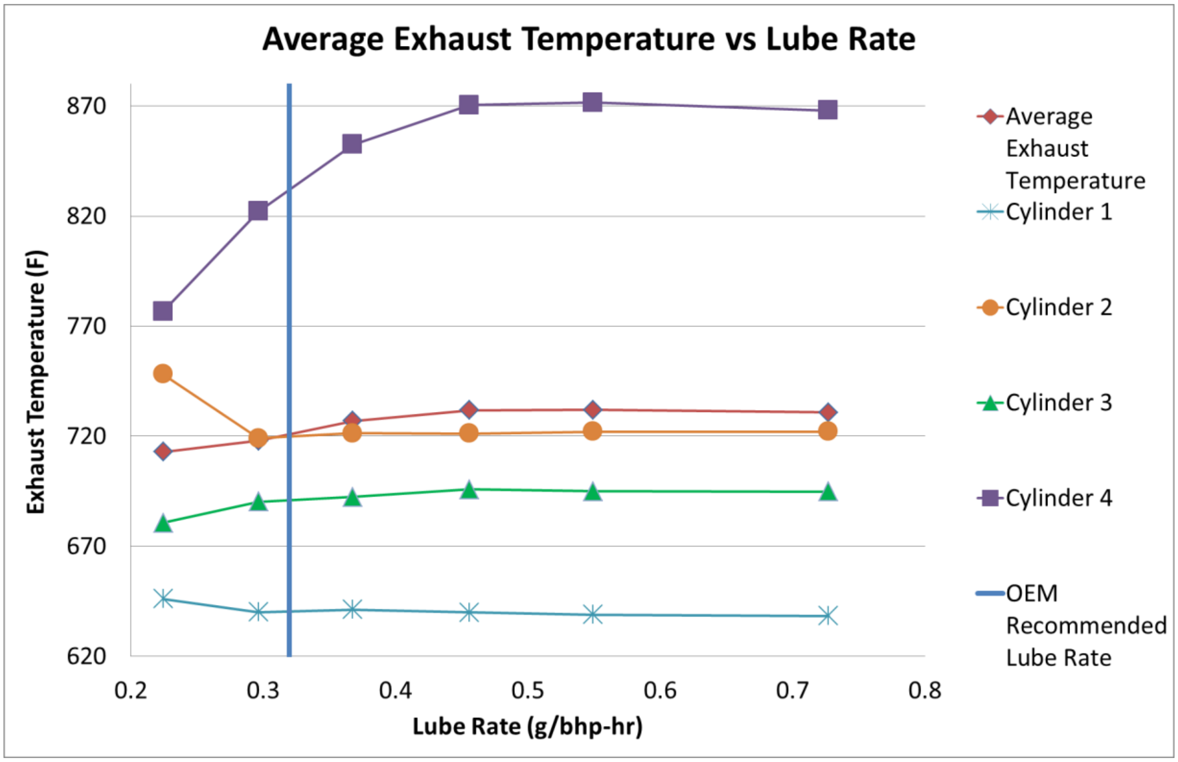


Figure 5-7 Exhaust Temperature vs. Lube Rate.

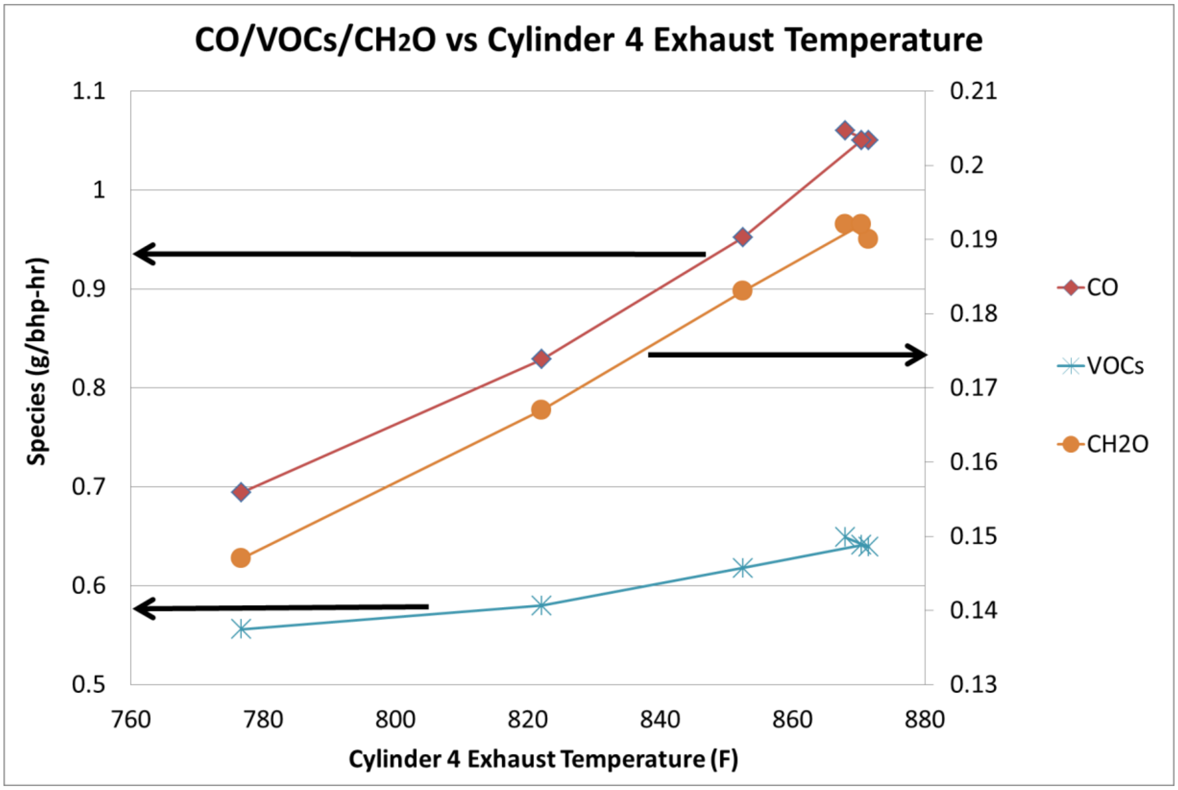


Figure 5-8 Cylinder 4 Exhaust Temperature vs CO, VOCs, $CH_2O$

The exhaust temperature analysis provides more insight on the gaseous emission results. Average exhaust temperature displayed the same pattern as the gaseous emissions (with the exception of NOx). Cylinder 4 exhaust temperature heavily contributed to the average exhaust temperature profile. Cylinder 4 operated at relatively very high exhaust temperatures at the beginning of the day before approaching nominal exhaust temperatures mid-day. It is unknown why Cylinder 4 operated so hot. It is very unlikely that reducing the lubrication rate reduced the temperature of Cylinder 4. Therefore, gaseous emissions were significantly effected during testing; however, changes in gaseous emissions likely resulted from Cylinder 4's high exhaust temperature profile. Table 5-1 summarizes the impact of increased cylinder lubrication rate and Cylinder 4 exhaust temperature on exhaust emissions.

**Table 5-1 Summary of impact of lubrication rate and Cylinder 4 exhaust temperature on emissions.**

| | Percent Change with Increasing Lube Rate | | | | | | | | |
|---|---|---|---|---|---|---|---|---|---|
| **Lube Rate Range (g/bhp-hr)** | **Lube Rate** | **PM** | **Cylinder 4 Exhaust Temp** | **CO** | **VOCs** | **$CH_2O$** | **Formal-dehyde** | **Ethylene** | **NOx** |
| .22-.45 | 103 | 67 | 12 | 51 | 15 | 31 | 31 | 53 | -15 |
| .45-.73 | 59 | 44 | 0 | 1 | 1 | 0 | 0 | 4 | 0 |

### 5.1.1 Comparison with Prior Research

Prior research by Olsen[4] utilized the same engine test-bed and mechanical lubricator to characterize lube oil carryover in 2011. Conclusions of that study were as follows:

- PM increased linearly with power cylinder lube rate.
- Lubricant carryover, in the exhaust as PM, equated to 7% at nominal lube rate.
- No strong correlation between gaseous emissions and lube rate was made.

Reevaluation of the 2011 data found that PM carryover decreased linearly with lube rate, as shown in Figure 5-9.

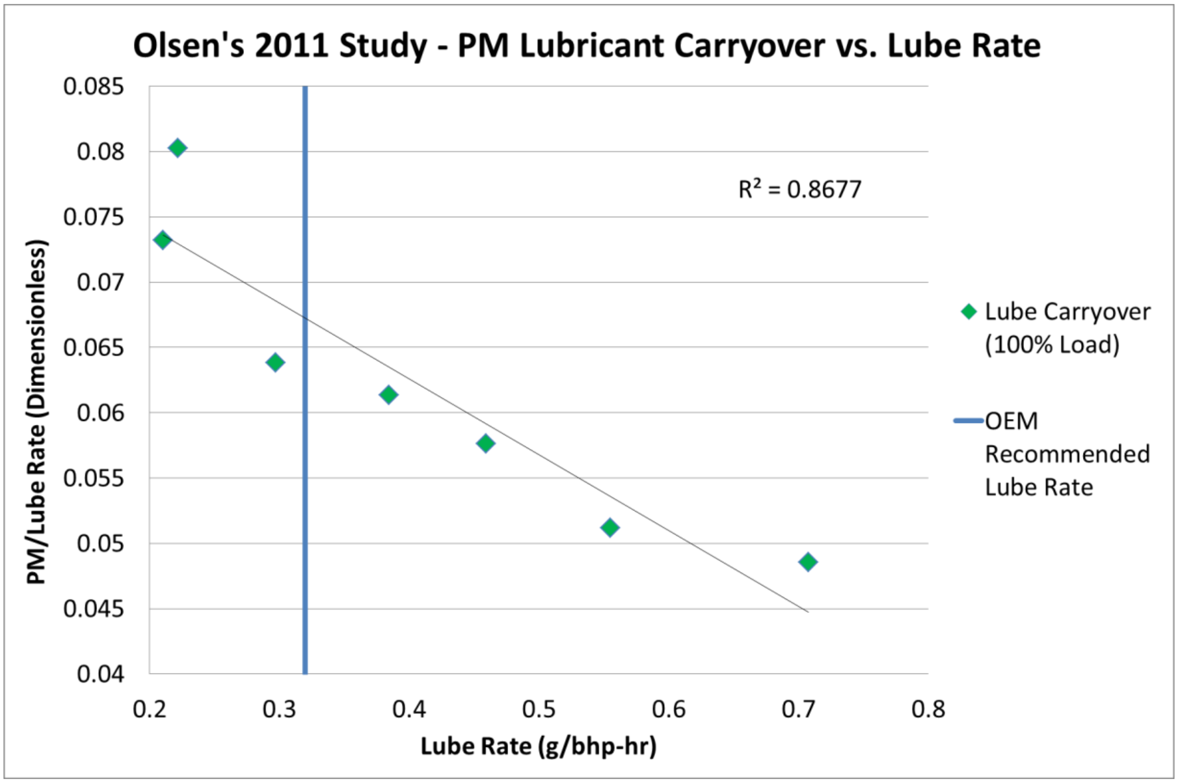


**Figure 5-9 Olsen et al. 2011 study[4]- carryover vs. lube rate.**

Results of this study correlate with those found by Olsen et al. in 2011. This study does, however, find that the 2011 study may have significantly underestimated the impact of PM lubricant carryover. Carryover was found to be about 400% larger in the current study.

The attributed reason for this carryover discrepancy is the dilution tunnel modification. Both studies utilized the same dilution tunnel. However, before recent modifications to the dilution tunnel it is likely that the tunnel contained leaks. Leaks would have increased the actual dilution ratio above the calculated dilution ratio. This underestimate of dilution ratio would lead to an underestimate in PM lubricant carryover. The higher precision in the PM linear fits of this study, compared to that of the 2011 study, support this argument.

## 5.2 ECL I Results

Day 1 engine testing's initial OIT sweep showed no relationship between injection timing and PM emissions. Figure 5-10 displays the lubricant carryover in reference to the injection timing. The initial 8 points taken are the uppermost points in the graph. Repeat injection points are the lowest points in the graph.

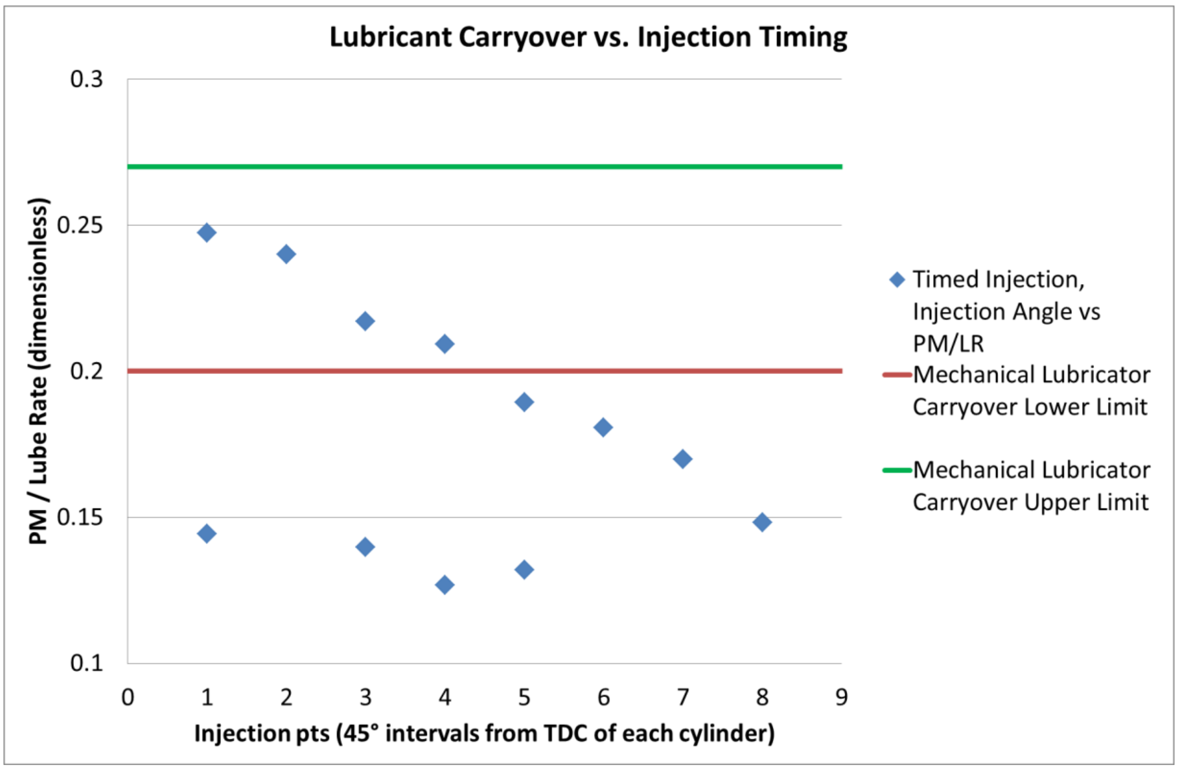


Figure 5-10 ECL I Lubricant carryover vs. injection timing.

Figure 5-10 displays the low repeatability of the points. Lubricant carryover decreased consistently throughout the day, independently of injection timing, shown in Figure 5-11.

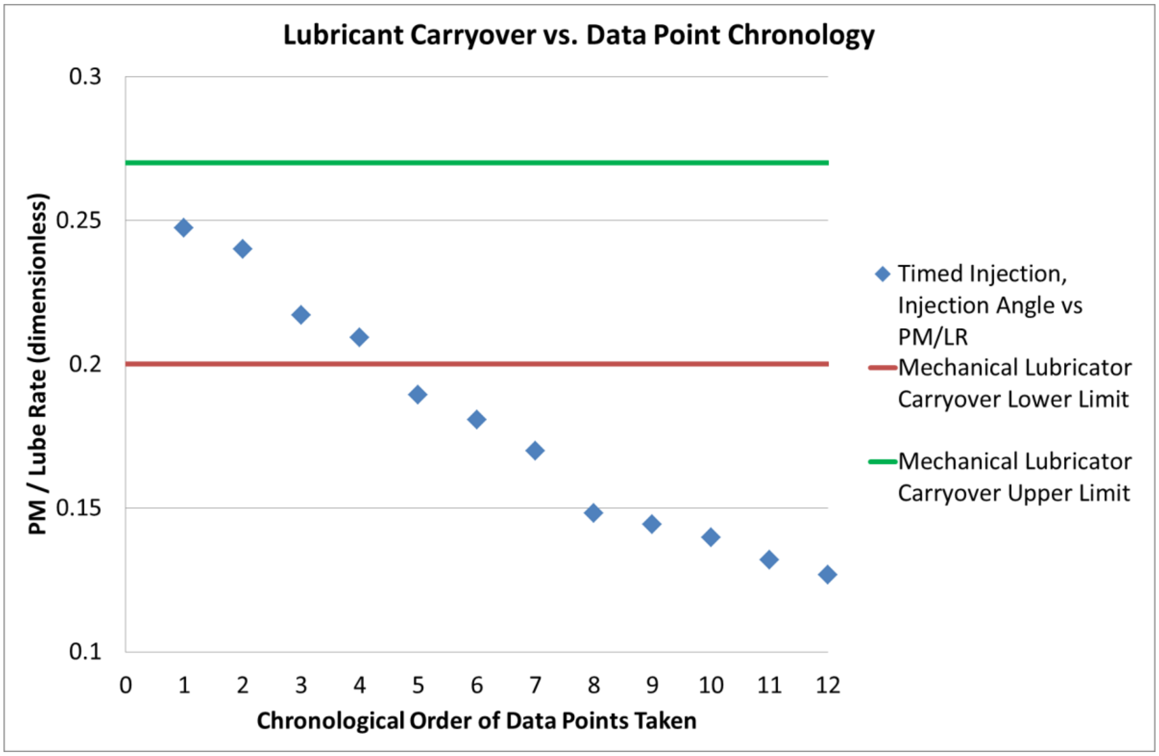


**Figure 5-11 ECL I lubricant carryover vs. data point chronology.**

The poor results from the Day 1engine testing raised concerns over the benefits of a second day of testing with ECL I. The budget for the second day of engine testing was conserved until the faults in ECL I were resolved.

Analysis of the entire ECL system showed that the possible faults for Day 1's humble results were as follows:

- The high dead volume downstream of the oil injector (injection lines). The volume of the oil likely compressed by an amount greater than 1 injection due to the differential pressure between the solenoid valve and cylinder. This may have resulted in a delayed injection when the lube ports were at a relatively high pressure.
- The dead volume in the lube ports. The lube port dead volume was significantly higher than dead volume elsewhere in the system. This may have resulted in delayed injection if

the lube oil was pushed back into the check valve at relatively high cylinder pressures. It is also possible that lube oil in the lube ports leaked into the cylinder when cylinder pressure was low, thus delivering oil to the cylinder at an arbitrary time.

- The solenoid valves did not provide consistent flow to the cylinders. Flow rate slowly increased throughout the day. The solenoid valves either developed slow leaks or increased in opening speed as the day progressed; both scenarios result in inconsistency in the injection timing. Regardless of the scenario, the solenoid valves proved to be flawed for this application.
- The solenoid valve bench-top flow calibrations did not match the on-engine flow. This resulted in imprecise lube rate measurements.
- Poor check valve response. For the system to function properly the check valves must open and close as fast as the solenoid valve. If it is slow to open then the start of injection timing is delayed. If it is slow to seat then the end of injection timing is delayed. If the valve does not fully seat before the next cycle then the system would provide a continuous, yet variable flow rate to the cylinder.

## 5.3 Lubrication Verification

### 5.3.1 Mechanical Lubricator Lubrication Verification

In both cigarette paper testing and UV fluorescence testing the cylinder was deemed significantly under-lubricated. No saturation of the cigarette paper occurred anywhere in the cylinder. UV induced fluorescence showed that the only visible lubrication in the cylinder was either inside the lube ports or directly beneath the ports (in-line). Figure 5-12 displays pictures of the lubrication examination.

| Engine Cylinder | UV Fluorescence Testing / Lube Port Close-up |
| --- | --- |

**Figure 5-12 Cylinder lubrication pictures.**

This result was likely witnessed because the last data point taken during the lubrication sweep had a lubrication rate equal to 70% of the OEM recommended rate.

## 5.4 Conclusions

Lubricant oil carryover was quantified on a Cooper Bessemer GMV 4TF, 2-stroke LBNGE using three different lubricators. A lubrication rate sweep on a mechanical force-feed lubricator determined the following:

- Mass based PM emissions increased linearly with lubrication rate.
- PM lubricant carryover inversely decreased with lubrication rate. At nominal lube rates, lubricant carryover equated to 25%. Lubricant carryover equated to 20% at a lube rate equal to 225% OEM recommended rate. At a lube rate of 70% OEM recommended rate, carryover equated to 27%.
- A change in gaseous emissions was witnessed during testing; however, gaseous emissions were likely impacted by unstable exhaust temperatures as opposed to changes in lubrication rate.

- Post-test lubrication verification determined that at lubrication rates of 70% OEM the power cylinders were lubricant starved.

Two electronically controlled power cylinder lubricators (ECLs) were designed to provide timed power cylinder oil injection. The ECLs were designed and constructed to inject oil into the ring pack on the upstroke of the piston.

ECL design I utilized a positive displacement pump and high speed solenoid valves to control injection. Design I focused on minimizing engine alteration, integrating components of the traditional mechanical lubrication system, and utilizing commercially available hardware. The following was determined with regards to the ECL Design I:

- ECL Design I did not successfully provide timed injection to the power cylinders. This was evidenced by observed insensitivity of lube oil carryover to injection crank angle. Possible contributing causes for the flawed results were the following: high dead volumes downstream of the solenoid valves, ill-suited solenoid valves, slow check valve response, and inaccurate volumetric flow rate measurements.

ECL design II utilized many of the components from ECL design I; although compressor injectors replaced design I's solenoid valves. ECL II focused on eliminating system dead volume, decreasing injection delay, and accurately measuring system flow rate.

## 5.5 Recommendations for Future Research

The following is recommended before commercial implementation of an ECL:

- Experimentation of ECL design II.

- An injection sweep to determine system delay and optimal injection time.
- A lubrication rate sweep at optimal injection time.

- Analysis of ECL design II lubrication rates on exhaust emissions.
- The development of improved power cylinder lubrication verification methods.
- A long-term wear study comparing traditional mechanical lubricators with an ECL.
- Improved commercial design of an ECL that:
  - Improves functionality.
  - Reduces engine alteration.
  - Reduces manufacturing cost.
  - Reduces retrofit time and cost.
  - Protects the engine in cases of ECL hardware malfunction.

# 6 References

[1] Energy Information Administration, Office of Oil and Gas, 2007, “Natural Gas Compressor Stations on the Interstate Pipeline Network: Developments Since 1996,” n.d., from http://www.eia.gov/pub/oil_gas/natural_gas/analysis_publications/ngcompressor/ngcompressor.pdf.

[2] McCarthy, Jim., 2009, “Air Regulations Impacting the Natural Gas Industry- 2009 Air Quality Regulatory Update,” *2009 Gas machinery Conference,* Atlanta, GA.

[3] Tice, John K., 2009, “Exhaust Gas After-treatment: Catalyst Systems,” *2009 Gas Machinery Conference,* Atlanta, GA.

[4] Olsen, Daniel B., Arney, and G., Reining, A., 2011, “Oxidation Catalyst Performance Considerations: Catalyst Temperature, Space Velocity, and Fouling,” *2011 Gas Machinery Conference*, Nashville, TN.

[5] Richardson, D. E., 2000, “Review of Power Cylinder Friction for Diesel Engines,” ASME, **122**, pp. 506-519.

[6] Graco Inc., 2008, n.d., from http://www.youtube.com/watch?v=zZcX4-8oz-U.

[7] Doosan Engine. “Adaptive Cylinder Oil Control System: ALPHA Lubricator,” Alpha Lubricator Brochure, from http://www.scribd.com/doc/48632327/ALPHA-LUBRICATOR.

[8] 2007. MAN Diesel. “Alpha Lubricator: Alpha Adaptive Cylinder Oil Control (Alpha ACC),” Alpha Lubricator Brochure, from http://www.mandieselturbo.com/files/news/filesof11363/1-3%20Alpha%20Lubricator.pdf.

[9] Christensen, Ole., 2010, “Cylinder Lubrication of Two-Stroke Crosshead Marine Diesel Engines,” Wartsila Technical Journal, 02.2010, pp. 39-48.

[10] Uras, H. M. and Patterson, D.J., 1983. “Measurement of Piston and Ring Assembly Friction Instantanious IMEP Method,” SAE Paper 830416.

[11] Furuhama, S., Takijuchi, M., and Tomizawa, K., 1981, “Effect of Piston and Piston Ring Designs on the Piston Friction Forces in Diesel Engines,” SAE Paper 810977.

[12] Grabon, W., Pawlus P., and Sep, J., 2010, “Tribological Characteristics of One-Process and Two-Process Cylinder Liner Honed Surfaces Under Reciprocating Sliding Conditions,” Tribology International, **43**, pp. 1882-1892.

[13] Taylor, R. I., Brown, M. A., Thompson, D. M., and Bell, J. C., 1994, “The Influence of lubricant Rheology on Friction in the Piston Ring-Pack,” SAE Paper 941981.

[14] Truhan, John J., Qu, Jun, and Blau, Peter J., 2005, "The Effect of Lubricating Oil Condition on the Friction and Wear of Piston Ring and Cylinder Liner Materials in a Reciprocating Bench Test," Wear, **259**, pp. 1048-1055.

[15] Ford Manuals, n.d., from http://www.fordmanuals.org/page-1004.html.

[16] Jeng, Yeau-Ren, 1992, "Theoretical Analysis of Piston-Ring Lubrication Part I—Fully Flooded Lubrication," Tribology Transactions, **45**(4), pp. 696-706.

[17] Jeng, Yeau-Ren, 1992, "Theoretical Analysis of Piston-Ring Lubrication Part II—Starved Lubrication and Its Application to a Complete Ring Pack," Tribology Transactions, **45**(4), pp. 707-714.

[18] Ma, M-T, Sherrington, I., and Smith E.H., 1997, "Analysis of Lubrication and Friction for a Complete Piston-Ring Pack with an Improved Oil Availability Model—Part 1: Circumferentially Uniform Film," Journal of Engineering Tribology, **211**(J), pp. 1-15.

[19] Ma, M-T, Sherrington, I., and Smith E.H., 1996, "Analysis of Lubrication and Friction for a Complete Piston-Ring Pack with an Improved Oil Availability Model—Part 2: Circumferentially Variable Film," Journal of Engineering Tribology, **211**(J), pp. 17-27.

[20] Stanley, R., Taraza, D., Henein, N., and Bryzik, W., 1999, "A Simplified Friction Model of the Piston Ring Assembly," SAE Paper 1999-01-0974.

[21]NaturalGas.org, 2012, n.d., from http://www.naturalgas.org/overview/background.asp.

[22] Environmental Protection Agency, 2012, n.d., from http://www.epa.gov/pm/health.html.

[23] DeFoort, M., Olsen, D., and Willson, B., 2002, "Performance Evaluation of Oxidation Catalysts for Natural Gas Reciprocating Engines," *2002 Gas Machinery Conference,* Nashville, TN.

[24] Andersson, J., Antonsson M., Eurenius, L., Olsson, E., and Skoglundh, M., 2007 "Deactivation of Diesel Oxidation Catalysts: Vehicle- and Synthetic Aging Correlations," Applied Catalyst B: Environmental, **72**, pp. 71-81.

[25] Williams, S., Neseri, M., Aleixo, J., and Sandelin, K., 2006, "Field Experience and Laboratory Analysis of Oxidation Catalyst on Dual Fuel Engines", *ASME ICE Spring Technical Conference*, Paper ICES2006-1362, Aachen, Germany.

[26] Courtney-Pratt, B.E. and Tudor, G.K., 1946, "An Analysis of the Lubrication Between the Piston-Rings and Cylinder-Wall of a Running Engine," Proc. I Mech. E., pp. 155, 293.

[27] Furuhama, S. and Sumi T. 1961, "A Dynamic Theory of Piston-Ring Lubrication, 3rd Report: Measurement of Oil-Film Thickness," Bull. JSME, **4**(16), pp. 744.

[28] Rhodes, M.L.T., 1980, “Piston Research and Development Techniques,” *AED Group Symposium,* UK.

[29] Dow, T.A., Schiele, C.A., and Stockwell, R.D., 1983, “Technique for Experimental Evaluation of Piston-Ring/Cylinder Film Thickness,” Journal of Lubrication Technology, **105**, pp. 353.

[30] Sherringtion, I. and Smith, E.H., 1985, “Experimental Methods for Measuring the Oil-Film Thickness Between the Piston-Rings and Cylinder-Wall of Internal Combustion Engines,” Tribology International,” **85**(6), pp. 315-320.

[31] Wing, R.D. and Saunders, O., 1972, “Oil-Film Temperature and Thickness Measurements on the Piston-Rings of a Diesel Engine,” Proc. I. Mech. E., **186**(1).

[32] Hamilton, G.M. and Moore, S.L., 1974, “Measurement of the Oil-Film Thickness Between the Piston-Rings and Liner of a Small Diesel Engine,” Proc. I. Mech. E., **188**(53).

[33] Shin, K., Tateishi, Y., and Furuhama, S., 1983, “Measurement of Oil-Film Thickness Between Piston-Ring and Cylinder,” SAE paper 830068.

[34] Johnson, M. F. G., Schluter, R. A., and Bankoff, S. G., 1997, “Fluorescent Imaging for Global Measurement of Liquid Film Thickness and Dynamic Contact Angle in Free Surface Flows,” Rev. Sci. Instrum., **68**(11), pp. 4097-4102.

[35] Jermy M.C., Noel T., and Doherty, W.G., 2004, “Laser Induced Fluorescence Measurements of the Thickness of Fuel Films on the Combustion Chamber Surface of a Gasoline SI Engine,” DAMSE, School of Engineering, Cranfield University, UK.

[36] Arcoumanis C., Lindenkamp H., and Preston, H., 1998, “Measurements of Lubricant Film Thickness in the Cylinder of a Firing Diesel Engine using LIF,” SAE Paper 982435.

[37] Smith, J. D. and Sick V., 2005, “Crank-Angle Resolved Imaging of Biacetyl Laser-Induced Fluorescence in an Optical Internal Combustion Engine,” Applied Physics B, **81**, pp. 579-584.

[38] Ghandi, Jaal B., 2000, “Single- and Dual-Fiber Fluorescence Probes: Application to Oil-Film Measurements in an Internal Combustion Engine,” Applied Optics, 39(30), pp. 5456-5464.

[39] Environmental Protection Agency, 2006, “Standards of Performance for Stationary Compression Ignition Internal combustion Engines; Final Rule”, 40 CFR Parts 60, 85 et al., Federal Register, 71(132).

# APPENDIX I – CALCULATIONS

# ECL I DESIGN CALCULATIONS

Timed Lube System Injection Calculations

INPUTS:

Engine Inputs

$Q_e$ = 3.875 [l/day] Engine Lube Rate

$\omega_e$ = 300 [rev/min] Engine speed

N = 4 [-] Number of cylinders

$t_{injallow}$ = 0.005 [s] Allowable time to inject oil into cylinder

$P_c$ = 50 [psi] Cylinder Pressure at lube port during injection

$D_c$ = 14 [in] Cylinder Inner diameter

$D_p$ = 354.584 [mm] Piston Diameter

$L_{rp}$ = 9.525 [mm] Distance Between piston rings

$N_{ports}$ = 2 Number of lube ports per cylinder

Lubrication Inputs

SG = 0.885 Specific Gravity

X = 0.45 Viscosity Compensation Factor- From Lee Chart

$f_v$ = 1.5 Viscosity factor- From Beinlich Pump Chart, dependant on discharge pressure

$\mu$ = 0.117 [pa-s] Oil Viscosity

$\rho$ = 885 [kg/m$^3$] Oil Density

$\beta$ = 1.5 [GPa] Bulk modulus SAE 30 Oil, Fluid Power System Dynamics, Durfee and Sun

Pump Inputs

$V_p$ = 0.1 [cm$^3$] Fixed displacement per pump revolution

$P_i$ = 14.7 [psi] Inlet pump pressure

$P_o$ = 300 [psi] Outlet Pump pressure

$\eta_{ptot}$ = 0.7 [-] Overall Pump efficiency- Beinlich chart, dependant on Discharge Pressure

$\eta_{vol}$ = 0.96 Volumetric efficiency, Beinlich chart, dependant on discharge Presser

$\omega_p$ = 27 [rev/min] Pump speed

Solenoid Valve inputs for Lee Valve

$N_{cycle}$ = $1 \times 10^8$ [rev] Solenoid Expected Cycle lifetime

$t_{resp}$ = 0.8 [millisec] Solenoid Response time

K = 75700 [ml/min-psi$^{.5}$] Liquid Flow Constant, Given by Lee

Lohms = 4100 Valve Rating

Piping Inputs

$d_{line}$ = 0.0625 [in] 1/8 inch Inside diameter of PTFE tubing entering cylinder

$L_{line}$ = 44 [in] Tubing length from end of solenoid to cylinder

$d_{inst}$ = 0.069 [in] 1/8 inch SS tubing inside diameter of instrument line

$L_{inst}$ = 9 [in] Length of instrument line

$L_{ports}$ = 8 [in] Length of lube ports

$d_{ports} = \frac{3}{16}$ Diameter of lube ports

CALCULATIONS:

Flow Calculations

$$\rho_1 = \rho \cdot \left| 0.001 \cdot \frac{g/ml}{kg/m^3} \right|$$

$$\omega_{e1} = \omega_e \cdot \left| 0.016666667 \cdot \frac{rev/s}{rev/min} \right|$$

$$Q_{e1} = Q_e \cdot \left| 0.6944 \cdot \frac{ml/min}{l/day} \right|$$

$$Q_{e2} = Q_e \cdot \left| 0.011007172 \cdot \frac{gph}{l/day} \right|$$

$$Q_{e3} = Q_e \cdot \left| 0.000694444 \cdot \frac{l/min}{l/day} \right|$$

$$Q_{e4} = Q_e \cdot \left| 1.15741 \times 10^{-8} \cdot \frac{m^3/s}{l/day} \right|$$

$$Q_c = \frac{Q_{e1}}{N}$$ Cylinder Lube Rate

$$V_{rev} = Q_{e1} \cdot \frac{1 \quad [rev]}{\omega_e}$$ Lube injection volume per crank revolution

$$V_{inj} = \frac{V_{rev}}{N}$$ Lube injection volume per cylinder

$$V_{inj,port} = \frac{V_{inj}}{N_{ports}}$$

$$t_{rev} = \frac{1 \quad [rev]}{\omega_{e1}}$$ crank revolution time

$$t_{rev1} = t_{rev} \cdot \left| 1000 \cdot \frac{millisec}{s} \right|$$

$$Q_{inj} = \frac{V_{inj}}{t_{injallow}}$$ Volumetric flow rate required required for injection

$$Q_{inj1} = Q_{inj} \cdot \left| 0.000001 \cdot \frac{m^3/s}{ml/s} \right|$$

$$Q_{inj2} = Q_{inj} \cdot \left| 60 \cdot \frac{ml/min}{ml/s} \right|$$

$$V_{p1} = V_p \cdot \left| 0.000001 \cdot \frac{m^3}{cm^3} \right|$$

$$V_{p2} = V_p \cdot \left| 1 \cdot \frac{ml}{cm^3} \right|$$

$$V_{p3} = V_p \cdot \left| 0.061023744 \cdot \frac{in^3}{cm^3} \right|$$

$$\dot{m}_{port} = \frac{Q_c}{N_{ports}} \cdot \rho_1$$

Piping (Dead Volume) Calculations

$A_{line} = d_{line}^{2} \cdot \pi \cdot 0.25$ Inside area of 1/8 inch tubing

$A_{inst} = d_{inst}^{2} \cdot \pi \cdot 0.25$ Inside area of instrument line

$A_{ports} = d_{ports}^{2} \cdot \pi \cdot 0.25$ Inside area of lube ports

$V_{line} = L_{line} \cdot A_{line}$ Volume between solenoid and cylinder, 1/8 inch

$V_{inst} = L_{inst} \cdot A_{inst}$ Volume of instrument line, 1/8 inch SS

$V_{ports} = A_{ports} \cdot L_{ports}$ Volume of lube ports

$$V_{line1} = V_{line} \cdot \left| 16.387064 \cdot \frac{mL}{in^3} \right|$$

$$V_{inst1} = V_{inst} \cdot \left| 16.387064 \cdot \frac{mL}{in^3} \right|$$

$$V_{ports1} = V_{ports} \cdot \left| 16.387064 \cdot \frac{mL}{in^3} \right|$$

$$V_{dead} = V_{line1} + V_{inst1}$$

$$V_{dead,tot} = V_{dead} + V_{ports1}$$

$N_{inj,cyl} = \frac{V_{dead}}{V_{inj}}$ Ratio of dead volume to injection volume, Number of injections to fill dead volume

$N_{inj,comp} = \frac{\Delta V_{dead}}{V_{inj}}$ Number of injections to fill compression of oil

$t_{inj,cyl} = \frac{V_{dead}}{Q_c}$ Time for oil to pass from solenoid to cylinder

$\Delta P_{sol} = P_o - P_c$ Pressure Change across solenoid

$$\Delta P_{sol1} = \Delta P_{sol} \cdot \left| 6895 \cdot \frac{Pa}{psi} \right|$$

$$BETA1 = \beta \cdot \left| 1 \times 10^{9} \cdot \frac{Pa}{GPa} \right|$$

$\Delta V_{line} = \frac{\Delta P_{sol1} \cdot V_{line1}}{BETA1}$ Change in volume of engine oil past solenoid valves

$\Delta V_{inst} = \frac{\Delta P_{sol1} \cdot V_{inst1}}{BETA1}$ Change in volume of engine oil past solenoid valves

$\Delta V_{ports} = \frac{\Delta P_{sol1} \cdot V_{ports1}}{BETA1}$ Change in volume of engine oil past solenoid valves

$\Delta V_{dead} = \Delta V_{line} + \Delta V_{inst}$ Change in volume of engine oil past solenoid valves

Pump Calculations

$$\omega_{preq} = Q_{e1} \cdot \frac{1 \ \ [rev]}{V_{p2}}$$ Pump speed required to satisfy flow

$$P_{o1} = P_o \cdot \left| 6895 \cdot \frac{pa}{psi} \right|$$

$$P_{i1} = P_i \cdot \left| 6895 \cdot \frac{pa}{psi} \right|$$

$$P_{i2} = P_i \cdot \left| 0.068947579 \cdot \frac{bar}{psi} \right|$$

$$P_{o2} = P_o \cdot \left| 0.068947579 \cdot \frac{bar}{psi} \right|$$

$$P_{c1} = P_c \cdot \left| 6895 \cdot \frac{pa}{psi} \right|$$

$$\Delta_{P,p} = P_{o2} - P_{i2}$$ Pump differential pressure

$$Q_p = V_p \cdot \frac{\omega_p}{1 \ \ [rev]}$$ Actual Volumetric Flow rate determined by pump speed

$$Q_{p1} = Q_p \cdot \left| 1 \cdot \frac{ml/min}{cm^3/min} \right|$$

$$\dot{W}_p = \frac{\Delta_{P,p} \cdot Q_{e3} \cdot f_v}{600 \cdot \eta_{ptot}}$$ Required Power Consumption

$$\dot{W}_{p1} = \dot{W}_p \cdot \left| 1000 \cdot \frac{w}{kw} \right|$$

$Z = 1$ [n-m-rev/min-kW] Unit conversion factor for $T_{erf}$

$$T_p = \frac{\dot{W}_p \cdot 9550 \ \ [n\text{-}m\text{-}rev/min\text{-}kw]}{\omega_p}$$ Torque required to run pump

$$T_{p1} = T_p \cdot \left| 8.851 \cdot \frac{lbf-in}{n-m} \right|$$

$$\eta_{mech} = \frac{\eta_{ptot}}{\eta_{vol}}$$

Valve Calculations

$$t_{valvelife} = \frac{N_{cycle}}{\omega_e}$$ Solenoid Valve Projected lifetime if used nonstop in engine

$$t_{valvelife1} = t_{valvelife} \cdot \left| 0.000694444 \cdot \frac{day}{min} \right|$$

$$Q_v = \frac{K \cdot X}{Lohms} \cdot \left[ \frac{P_o - P_c}{SG} \right]^{0.5}$$ Maximum Solenoid Flowrate

$$t_{vopen} = \frac{V_{inj}}{Q_v}$$ Time required for full oil injection to flow out of fully open solenoid

$$t_{vopen1} = t_{vopen} \cdot \left| 60000 \cdot \frac{millisec}{min} \right|$$

$$t_{minvalveinjection} = 2 \cdot t_{resp} + t_{vopen1}$$ Minimum amount of time required by solenoid to inject oil portion into cylinder

Ring Pack Oil Flow Calculations

$$D_h = \frac{4 \cdot L_{rp1} \cdot L_{rg}}{2 \cdot (L_{rp1} + L_{rg})}$$ Hydrualic diameter of ring packing

$$L_{rp1} = L_{rp} \cdot \left| 0.001 \cdot \frac{m}{mm} \right|$$

$$L_{rg} = \frac{D_{c1} - D_{p1}}{2}$$ Distance between piston and cylinder

$$D_{c1} = D_c \cdot \left| 0.0254 \cdot \frac{m}{in} \right|$$

$$D_{p1} = D_p \cdot \left| 0.001 \cdot \frac{m}{mm} \right|$$

$$Re_{Dh} = \frac{\rho \cdot vel_{rp} \cdot D_h}{\mu}$$ Reynolds Number for flow between ring pack

$$vel_{rp} = \frac{Q_{inj1}}{\pi \cdot D_h^{\ 2} \cdot 0.25}$$ Oil velocity in Ringpack

$$Q_{allow,rp} = \frac{P_{o1} - P_{c1}}{R_{eq}}$$ Allowable flow to enter ring pack

$$Q_{allow,rp1} = Q_{allow,rp} \cdot \left| 1000000 \cdot \frac{ml/s}{m^3/s} \right|$$

$$R_{op} = 128 \cdot \mu \cdot \frac{L_{cd}}{\pi \cdot D_h^{\ 4}}$$ Resistance of oil flow between two piston rings

$$L_{cd} = D_{c1} \cdot \frac{\pi}{2}$$ Circumferential length from lube port to lube port

$$R_{eq} = \left[ 6 \cdot \frac{1}{R_{op}} \right]^{-1}$$ Total resistance of oil flow between ring packing

$$V_{rp} = L_{rg} \cdot L_{rp1} \cdot L_{cd}$$ Volume between compression rings

$$V_{rp1} = V_{rp} \cdot \left| 1 \times 10^9 \cdot \frac{mm^3}{m^3} \right|$$

## SOLUTIONS:

| | | |
|---|---|---|
| $A_{inst}$ = 0.003739 [in$^2$] | $A_{line}$ = 0.003068 [in$^2$] | $A_{ports}$ = 0.02761 [in$^2$] |
| $\beta$ = 1.5 [GPa] | BETA1 = 1.500E+09 [Pa] | $\Delta P_{sol}$ = 250 [psi] |
| $\Delta P_{sol1}$ = 1.724E+06 [Pa] | $\Delta V_{dead}$ = 0.003176 [mL] | $\Delta V_{inst}$ = 0.0006337 [mL] |
| $\Delta V_{line}$ = 0.002542 [mL] | $\Delta V_{ports}$ = 0.00416 [mL] | $\Delta P_{,p}$ = 19.67 [bar] |
| $D_c$ = 14 [in] | $D_{c1}$ = 0.3556 [m] | $D_h$ = 0.0009646 [m] |
| $d_{inst}$ = 0.069 [in] | $d_{line}$ = 0.0625 [in] | $D_p$ = 354.6 [mm] |
| $D_{p1}$ = 0.3546 [m] | $d_{ports}$ = 0.1875 [in] | $\eta_{mech}$ = 0.7292 [-] |
| $\eta_{ptot}$ = 0.7 [-] | $\eta_{vol}$ = 0.96 [-] | $f_v$ = 1.5 [kw-min/bar-l] |
| K = 75700 [ml/min-psi$^{.5}$] | Lohms = 4100 [-] | $L_{cd}$ = 0.5586 [m] |
| $L_{inst}$ = 9 [in] | $L_{line}$ = 44 [in] | $L_{ports}$ = 8 [in] |
| $L_{rg}$ = 0.000508 [m] | $L_{rp}$ = 9.525 [mm] | $L_{rp1}$ = 0.009525 [m] |
| $\mu$ = 0.117 [pa-s] | $\dot{m}_{port}$ = 0.2977 [g/min] | N = 4 [-] |
| $N_{cycle}$ = 1.000E+08 [rev] | $N_{inj,comp}$ = 1.416 | $N_{inj,cyl}$ = 1232 |
| $N_{ports}$ = 2 | $\omega_e$ = 300 [rev/min] | $\omega_{e1}$ = 5 [rev/s] |
| $\omega_p$ = 27 [rev/min] | $\omega_{preq}$ = 26.91 [rev/min] | $P_c$ = 50 [psi] |
| $P_{c1}$ = 344738 [pa] | $P_i$ = 14.7 [psi] | $P_{i1}$ = 101353 [pa] |
| $P_{i2}$ = 1.014 [bar] | $P_o$ = 300 [psi] | $P_{o1}$ = 2.068E+06 [pa] |
| $P_{o2}$ = 20.68 [bar] | $Q_{allow,rp}$ = 0.000003362 [m$^3$/s] | $Q_{allow,rp1}$ = 3.362 [ml/s] |
| $Q_c$ = 0.6727 [ml/min] | $Q_e$ = 3.875 [l/day] | $Q_{e1}$ = 2.691 [ml/min] |
| $Q_{e2}$ = 0.04265 [gph] | $Q_{e3}$ = 0.002691 [l/min] | $Q_{e4}$ = 4.485E-08 [m$^3$/s] |
| $Q_{inj}$ = 0.4485 [ml/s] | $Q_{inj1}$ = 4.485E-07 [m$^3$/s] | $Q_{inj2}$ = 26.91 [ml/min] |
| $Q_p$ = 2.7 [cm$^3$/min] | $Q_{p1}$ = 2.7 [ml/min] | $Q_v$ = 139.6 [ml/min] |
| $Re_{Dh}$ = 4.478 [-] | $\rho$ = 885 [kg/m$^3$] | $\rho 1$ = 0.885 [g/ml] |
| $R_{eq}$ = 5.127E+11 [pa-s/m$^3$] | $R_{op}$ = 3.076E+12 [pa-s/m$^3$] | SG = 0.885 [-] |
| $t_{injallow}$ = 0.005 [s] | $t_{inj,cyl}$ = 4.108 [min] | $t_{minvalveinjection}$ = 2.564 [millisec] |
| $T_p$ = 0.06687 [n-m] | $T_{p1}$ = 0.5918 [lbf-in] | $t_{resp}$ = 0.8 [millisec] |
| $t_{rev}$ = 0.2 [s] | $t_{rev1}$ = 200 [millisec] | $t_{valvelife}$ = 333333 [min] |
| $t_{valvelife1}$ = 231.5 [day] | $t_{vopen}$ = 0.00001606 [min] | $t_{vopen1}$ = 0.9635 [millisec] |
| $vel_{rp}$ = 0.6138 [m/s] | $V_{dead}$ = 2.764 [mL] | $V_{dead,tot}$ = 6.383 [mL] |
| $V_{inj}$ = 0.002242 [ml] | $V_{inj,port}$ = 0.001121 [ml] | $V_{inst}$ = 0.03365 [in$^3$] |
| $V_{inst1}$ = 0.5515 [mL] | $V_{line}$ = 0.135 [in$^3$] | $V_{line1}$ = 2.212 [mL] |
| $V_p$ = 0.1 [cm$^3$] | $V_{p1}$ = 1.000E-07 [m$^3$] | $V_{p2}$ = 0.1 [ml] |
| $V_{p3}$ = 0.006102 [in$^3$] | $V_{ports}$ = 0.2209 [in$^3$] | $V_{ports1}$ = 3.62 [mL] |
| $V_{rev}$ = 0.00897 [ml] | $V_{rp}$ = 0.000002703 [m$^3$] | $V_{rp1}$ = 2703 [mm$^3$] |
| $\dot{W}_p$ = 0.000189 [kw] | $\dot{W}_{p1}$ = 0.189 [w] | X = 0.45 [-] |
| Z = 1 [n-m-rev/min-kW] | | |

# ECL II DESIGN CALCULATIONS

```
"Matt Luedeman
1-8-13
Thesis Calculations
Critical Dead Volume"

"ASSUMPTIONS:
1. Wall Temperature of Insert constantly remains at the temperature of the coolant
2. Specific heat of oil is constant
3. Oil thermal conductivity is constant
"

"INPUTS:"

"Insert Inputs:"
{ID_tube=.04 [in]  "Insert Inner Diameter"}
L_tube=200 [mm]  "Lube Port Insert Length"

"Oil Inputs:"
nu=132  [Centistoke]  "Oil Dynamic Viscosity- Determined from chart and average oil Temperature"
rho=885 [kg/m^3]  "Oil Density"
BETA=1.5 [GPa]  "Bulk modulus SAE 30 Oil, Fluid Power System Dynamics, Durfee and Sun"
C_p_oil=1800 [J/kg-K]  "Oil specific heat"
k_oil=.1872  [W/(m-K)]  "Thermal Conductivity of oil [http://mailman.egr.msu.edu/mailman/public/thermal/2001-May/000412.html]"

"Other Inputs:"
theta_inj=18 [degrees]  "Injection Duration"
Q_port=1 [pint/day]  "Cylinder Lube Rate"
N_engine=300 [rev/min]  "Engine speed"
T_cool= 344 [K]  "Engine coolant temperature"
T_oil_in=300 [K]  "Oil temperature"
Inj_int= 4 [rev/1]  "Injection interval (Revolutions/Injection)"
g=9.81 [m/s^2]  "Gravity Force"
V_dead_orig=6.4 [mL]  "Dead volume of original design"
P_cyl=60 [psi]  "Cylinder pressure during injection"
P_oil=725 [psi]  "Oil pressure of timed lube system"


"CALCULATIONS:"

"Insert Flow Calculations:"
Q_port1=Q_port*convert(pint/day,m^3/s)
Q_port2=Q_port*convert(pint/day,mL/s)
Vel=Q_port1/A_tube1  "Average velocity of oil in insert"
ID_tube1=ID_tube*convert(in,mm)
ID_tube2=ID_tube*convert(in,m)
A_tube=ID_tube1^2*.25
A_tube1=A_tube*convert(mm^2,m^2)
V_tube=A_tube*L_tube
V_tube1=V_tube*convert(mm^3,m^3)
V_tube2=V_tube*convert(mm^3,mL)
V_dead=V_tube2  "Dead Volume in system, injector to cylinder wall"
Red_dead=1-((V_dead-V_dead_orig)/V_dead) "Reduction in dead volume from original design"
Red_dead1=Red_dead*convert(dim,%)
L_tube1=L_tube*convert(mm,m)
Re=Vel_inj*ID_tube2/nu1  "Reynolds Number"
f=64/Re  "Friction Factor"
h_f=f*(L_tube1/ID_tube2)*(Vel_inj^2/(2*g)) "Head Loss in Insert"
DELTAP_insert=rho*g*h_f  "Pressure Loss Through Insert"
DELTAP_insert1=DELTAP_insert*convert(Pa,psi)

"Engine Calculations:"
N_engine1=N_engine*convert(rev/min,rev/s)
```

```
"Injection Calculations:"
t_inj=(theta_inj/(360 [degrees/rev]))/N_engine1  "Time duration of injection"
t_inj1=t_inj*convert(s,millisec)
F_inj=N_engine1/Inj_int  "Injection frequency"
V_inj=Q_port2/F_inj  "Volume of Injection"
Inj_dead=V_tube2/V_inj  "Number of Injections that it takes for an oil particle to entirely move through dead volume"
t_dead=Inj_dead/F_inj  "Time oil particle is present in dead volume"
Q_inj=V_inj/t_inj
Q_inj1=Q_inj*convert(mL/s,m^3/s)
Vel_inj=Q_inj1/A_tube1

"Oil  Calculations:"
nu1=nu*convert(centistoke,m^2/s)
mu=nu1*rho  "Kinematic Viscosity"

"Oil compression Calculations:"
DELTAP_inj=P_oil-P_cyl  "Pressure Change across injector"
DELTAP_inj1=DELTAP_inj*convert(psi, Pa)
BETA1=BETA*convert(GPa, Pa)
DELTAV_comp=(DELTAP_inj1*V_dead)/BETA1 "Volumetric change in volume of engine oil in dead volume due to
..compression"
Red_V_inj_comp=1-((V_inj-DELTAV_comp)/V_inj)  "Reduction in injected volume due to oil compression"
Red_V_inj_comp1=Red_V_inj_comp*convert(dim,%)
P_inj=DELTAP_inj-DELTAP_insert1  "Relative injection pressure at cylinder wall"

"Heat Transfer Calculations:"
{k_sleeve=k_('Carbon_steel', Temperature)
k_insert=k_('Stainless_AISI304', Temperature)
q=m_dot_port*c_p_oil*(T_oil_out-T_oil_in)  "Q=Heat transfer into oil,   "}
m_dot_port=Q_port1*rho
Nus_D=3.66  "Nusselt number for Laminar, fully developed, uniform surface temperatured insert [Incropera, Frank P.; DeWitt,
..David P. (2002). Fundamentals of Heat and Mass Transfer (5th ed.). Hoboken: Wiley. pp. 486, 487.]"
h=(Nus_D*k_oil)/ID_tube2  "Oil convective heat transfer coefficient"
{T_oil_av=(T_oil_in+T_oil_out)/2  "Average oil temperature in the insert"
DELTAT_lm=((T_cool-T_oil_out)-(T_cool-T_oil_in))/(LN((T_cool-T_oil_out)/(T_cool-T_oil_in)))  "Average temperature
..difference over the insert length"
h=((m_dot_port*C_p_oil)/(pi*ID_tube2*L_tube1))*((T_oil_out-T_oil_in)/DELTAT_lm)}
```

## SOLUTIONS:

$A_{tube}$ = 0.2581 [mm$^2$]
$A_{tube1}$ = 2.581E-07 [m$^2$]
$\beta$ = 1.5 [GPa]
BETA1 = 1.500E+09 [Pa]
$C_{p,oil}$ = 1800 [J/kg-K]
$\Delta P_{inj}$ = 665 [psi]
$\Delta P_{inj1}$ = 4.585E+06 [Pa]
$\Delta P_{insert}$ = 1.230E+06 [Pa]
$\Delta P_{insert1}$ = 178.3 [psi]
$\Delta V_{comp}$ = 0.0001578 [mL]
f = 4.898 [-]
$F_{inj}$ = 1.25 [1/s]
g = 9.81 [m/s$^2$]
h = 674.4 [W/m$^2$-K]
$h_f$ = 141.6 [m]
$ID_{tube}$ = 0.04 [in]
$ID_{tube1}$ = 1.016 [mm]
$ID_{tube2}$ = 0.001016 [m]
$Inj_{dead}$ = 11.78 [1]
$Inj_{int}$ = 4 [rev/1]
$k_{oil}$ = 0.1872 [W/(m-K)]
$L_{tube}$ = 200 [mm]
$L_{tube1}$ = 0.2 [m]
$\mu$ = 0.1168 [kg/m-s]
$\dot{m}_{port}$ = 0.000004847 [kg/s]
$\nu$ = 132 [Centistoke]
nu1 = 0.000132 [m$^2$/s]
$Nus_D$ = 3.66 [-]
$N_{engine}$ = 300 [rev/min]
$N_{engine1}$ = 5 [rev/s]
$P_{cyl}$ = 60 [psi]
$P_{inj}$ = 486.7 [psi]
$P_{oil}$ = 725 [psi]
$Q_{inj}$ = 0.4381 [mL/s]
$Q_{inj1}$ = 4.381E-07 [m$^3$/s]
$Q_{port}$ = 1 [pint/day]
$Q_{port1}$ = 5.476E-09 [m$^3$/s]
$Q_{port2}$ = 0.005476 [mL/s]
Re = 13.07 [-]
$Red_{dead}$ = 124 [-]
$Red_{dead1}$ = 12400 [%]
$Red_{V,inj,comp}$ = 0.03601 [-]
$Red_{V,inj,comp1}$ = 3.601 [%]
$\rho$ = 885 [kg/m$^3$]
$\theta_{inj}$ = 18 [degrees]
$T_{cool}$ = 344 [K]
$t_{dead}$ = 9.425 [s]
$t_{inj}$ = 0.01 [s]
$t_{inj1}$ = 10 [millisec]
$T_{oil,in}$ = 300 [K]
Vel = 0.02122 [m/s]
$Vel_{inj}$ = 1.698 [m/s]
$V_{dead}$ = 0.05161 [mL]
$V_{dead,orig}$ = 6.4 [mL]
$V_{inj}$ = 0.004381 [mL]
$V_{tube}$ = 51.61 [mm$^3$]
$V_{tube1}$ = 5.161E-08 [m$^3$]
$V_{tube2}$ = 0.05161 [mL]

SOLUTIONS:

| 1..10 | $ID_{tube}$ [in] | $P_{inj}$ [psi] | $\Delta P_{insert1}$ [psi] | $Inj_{dead}$ [1] | $Red_{dead1}$ [%] | $Red_{V,inj,comp1}$ [%] |
|---|---|---|---|---|---|---|
| Run 1 | 0.01 | -44990 | 45655 | 0.7363 | 198400 | 0.2251 |
| Run 2 | 0.02 | -2188 | 2853 | 2.945 | 49600 | 0.9002 |
| Run 3 | 0.03 | 101.4 | 563.6 | 6.627 | 22044 | 2.026 |
| Run 4 | 0.04 | 486.7 | 178.3 | 11.78 | 12400 | 3.601 |
| Run 5 | 0.05 | 592 | 73.05 | 18.41 | 7936 | 5.627 |
| Run 6 | 0.06 | 629.8 | 35.23 | 26.51 | 5511 | 8.102 |
| Run 7 | 0.07 | 646 | 19.02 | 36.08 | 4049 | 11.03 |
| Run 8 | 0.08 | 653.9 | 11.15 | 47.12 | 3100 | 14.4 |
| Run 9 | 0.09 | 658 | 6.959 | 59.64 | 2449 | 18.23 |
| Run 10 | 0.1 | 660.4 | 4.566 | 73.63 | 1984 | 22.51 |

| 1..10 | $Inj_{int}$ [rev/1] | $P_{inj}$ [psi] | $Inj_{dead}$ [1] | $Red_{V,inj,comp1}$ [%] |
|---|---|---|---|---|
| Run 1 | 1 | 620.4 | 47.12 | 14.4 |
| Run 2 | 2 | 575.8 | 23.56 | 7.202 |
| Run 3 | 3 | 531.2 | 15.71 | 4.801 |
| Run 4 | 4 | 486.7 | 11.78 | 3.601 |
| Run 5 | 5 | 442.1 | 9.425 | 2.881 |
| Run 6 | 6 | 397.5 | 7.854 | 2.401 |
| Run 7 | 7 | 352.9 | 6.732 | 2.058 |
| Run 8 | 8 | 308.3 | 5.89 | 1.8 |
| Run 9 | 9 | 263.7 | 5.236 | 1.6 |
| Run 10 | 10 | 219.1 | 4.712 | 1.44 |

| 1..15 | $\theta_{inj}$ [degrees] | $\Delta P_{insert1}$ [psi] | $P_{inj}$ [psi] |
|---|---|---|---|
| Run 1 | 18 | 178.3 | 486.7 |
| Run 2 | 17 | 188.8 | 476.2 |
| Run 3 | 16 | 200.6 | 464.4 |
| Run 4 | 15 | 214 | 451 |
| Run 5 | 14 | 229.3 | 435.7 |
| Run 6 | 13 | 246.9 | 418.1 |
| Run 7 | 12 | 267.5 | 397.5 |
| Run 8 | 11 | 291.8 | 373.2 |
| Run 9 | 10 | 321 | 344 |
| Run 10 | 9 | 356.7 | 308.3 |
| Run 11 | 8 | 401.3 | 263.7 |
| Run 12 | 7 | 458.6 | 206.4 |
| Run 13 | 6 | 535 | 130 |
| Run 14 | 5 | 642 | 22.97 |
| Run 15 | 4 | 802.5 | -137.5 |

| 1..10 | $\nu$ [Centistoke] | $P_{inj}$ [psi] |
|---|---|---|
| Run 1 | 13 | 647.4 |
| Run 2 | 26 | 629.9 |
| Run 3 | 39 | 612.3 |
| Run 4 | 52 | 594.7 |
| Run 5 | 65 | 577.2 |
| Run 6 | 78 | 559.6 |
| Run 7 | 91 | 542.1 |
| Run 8 | 104 | 524.5 |
| Run 9 | 117 | 506.9 |
| Run 10 | 130 | 489.4 |

## APPENDIX II - BENCH-TEST GRAPHS

## ECL I BENCH TEST GRAPHS

a) Motor-Pump Calibration

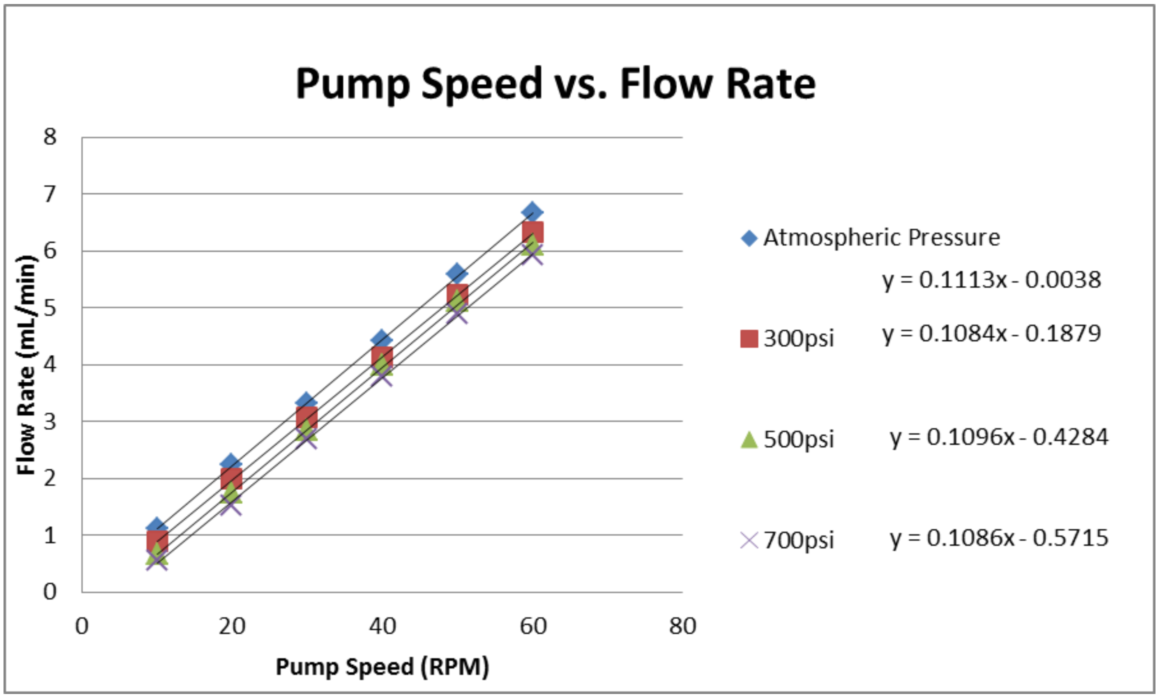


b) Solenoid Driver Impact on flow rates

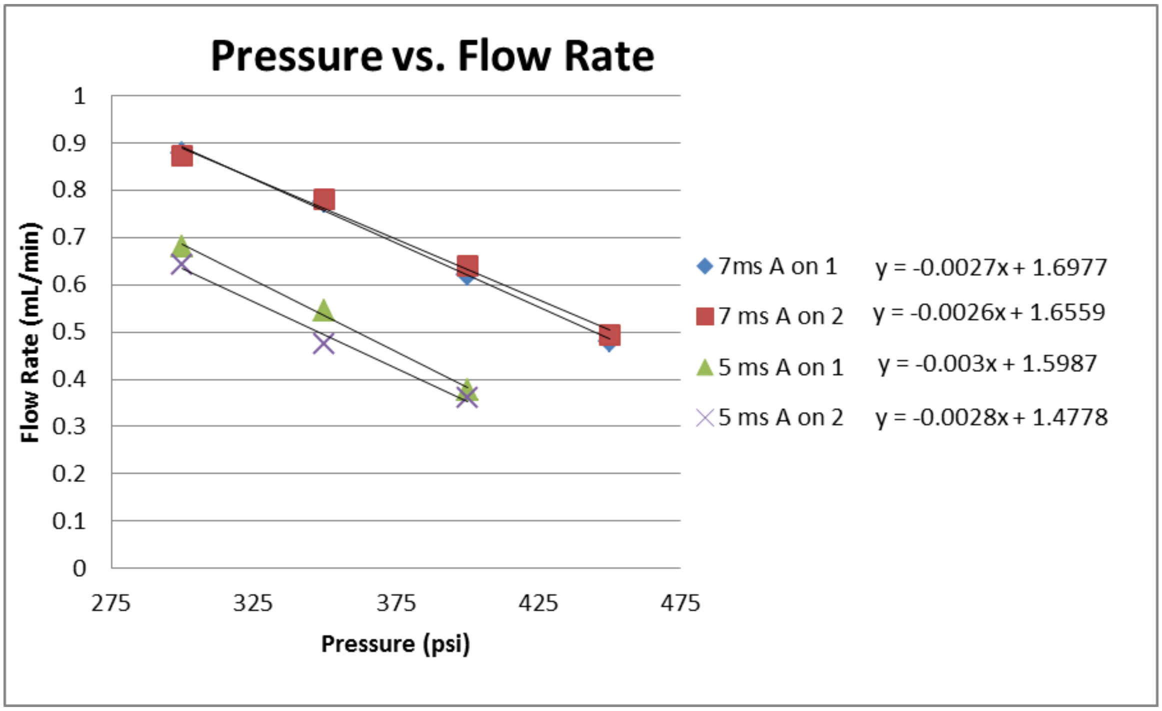

c) Effects of hold voltage on flow rate

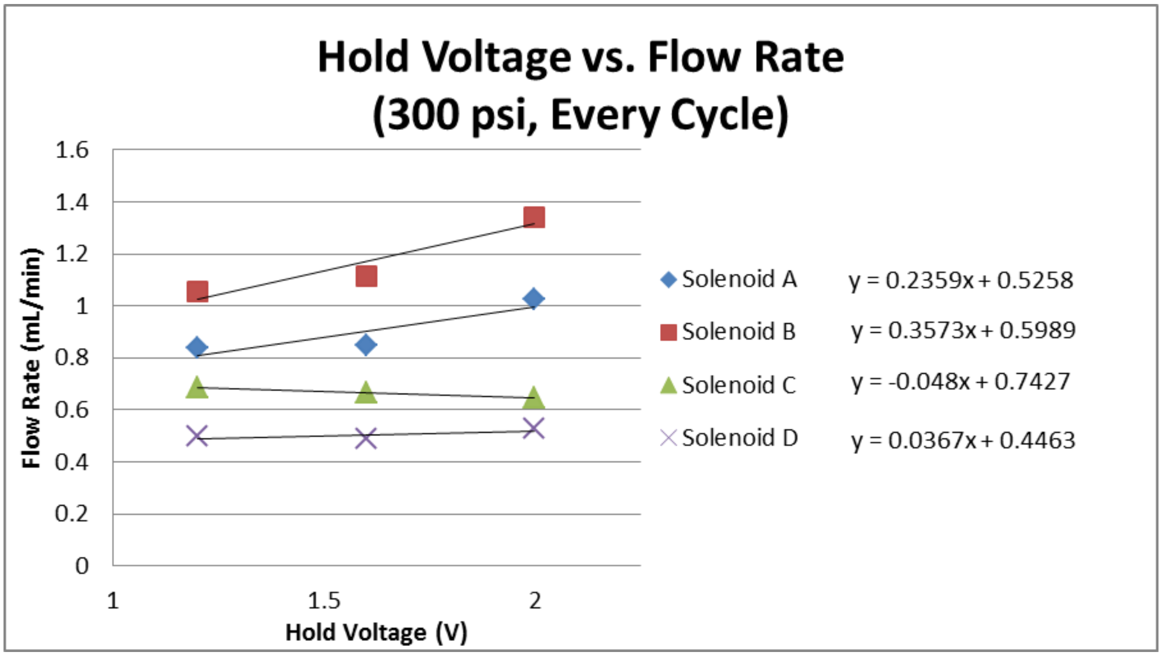


d) Effect of open duration on flow rate

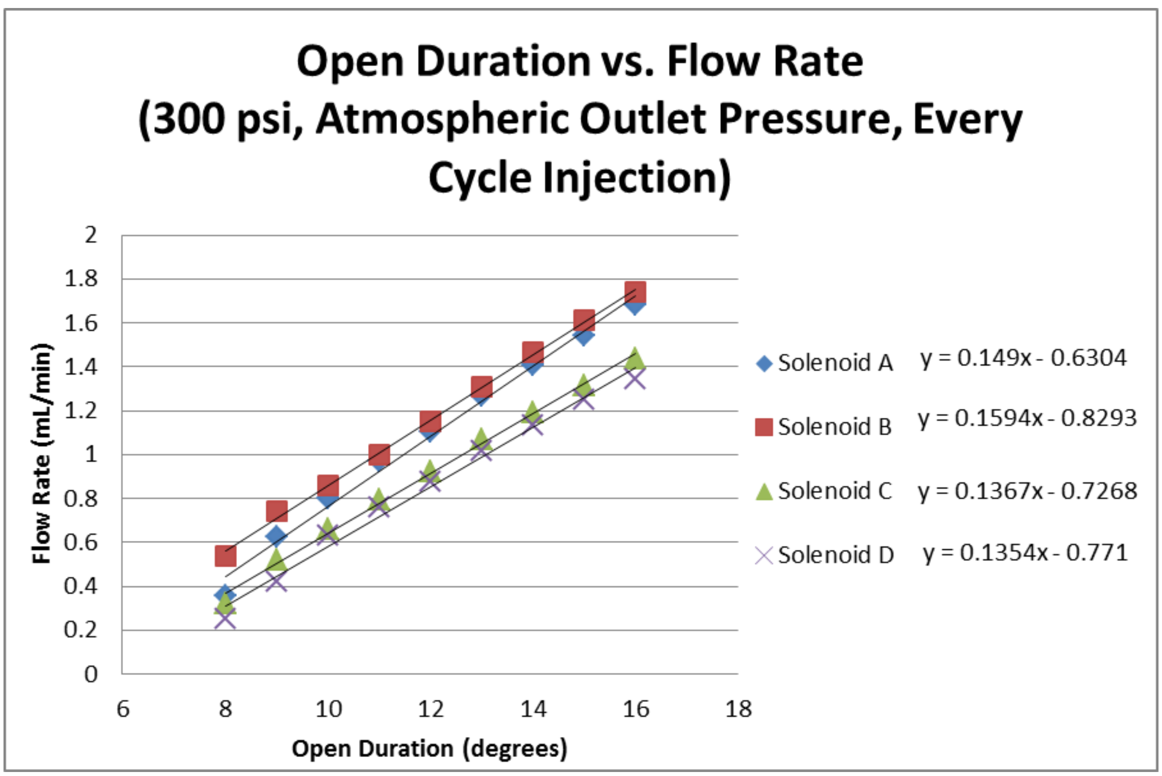

e) Effect of open duration on flow rate when oil injection of every other cycle (150 injections/min).

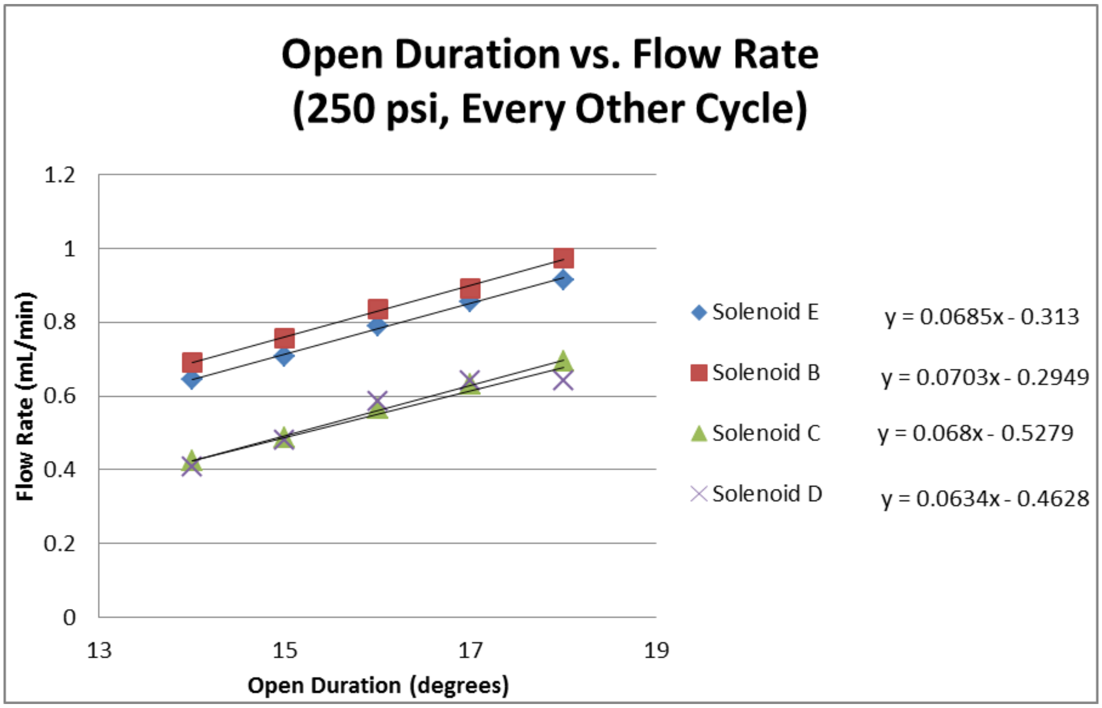


f) Effect of Backpressure on flow rate.

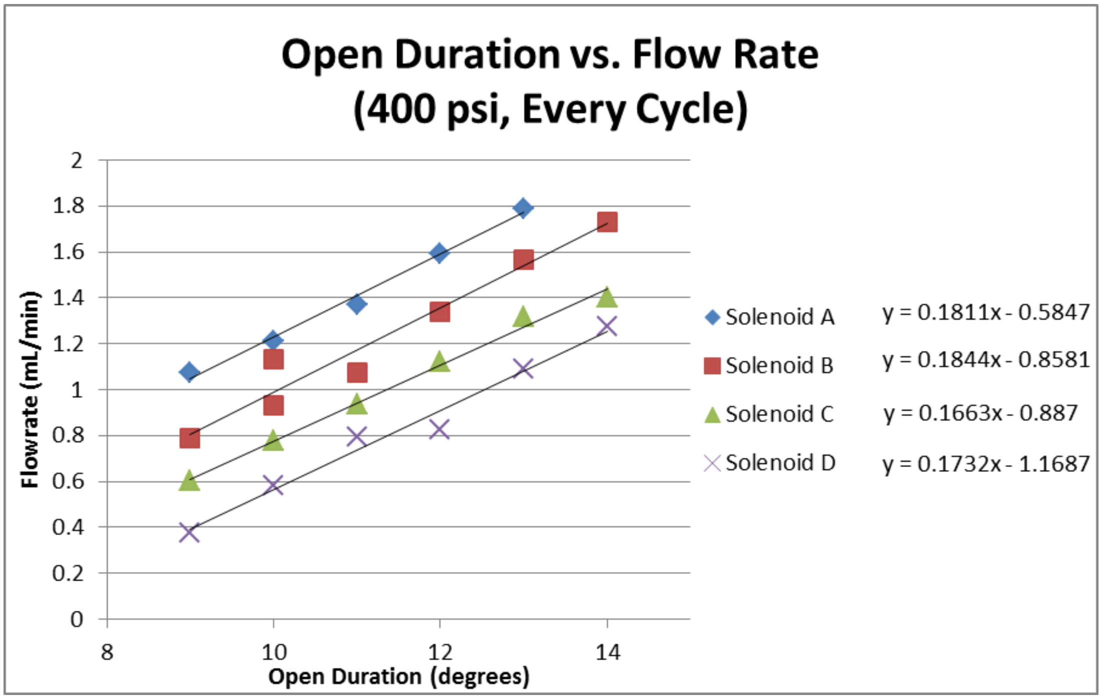

g) Effect of pressure on flow rate

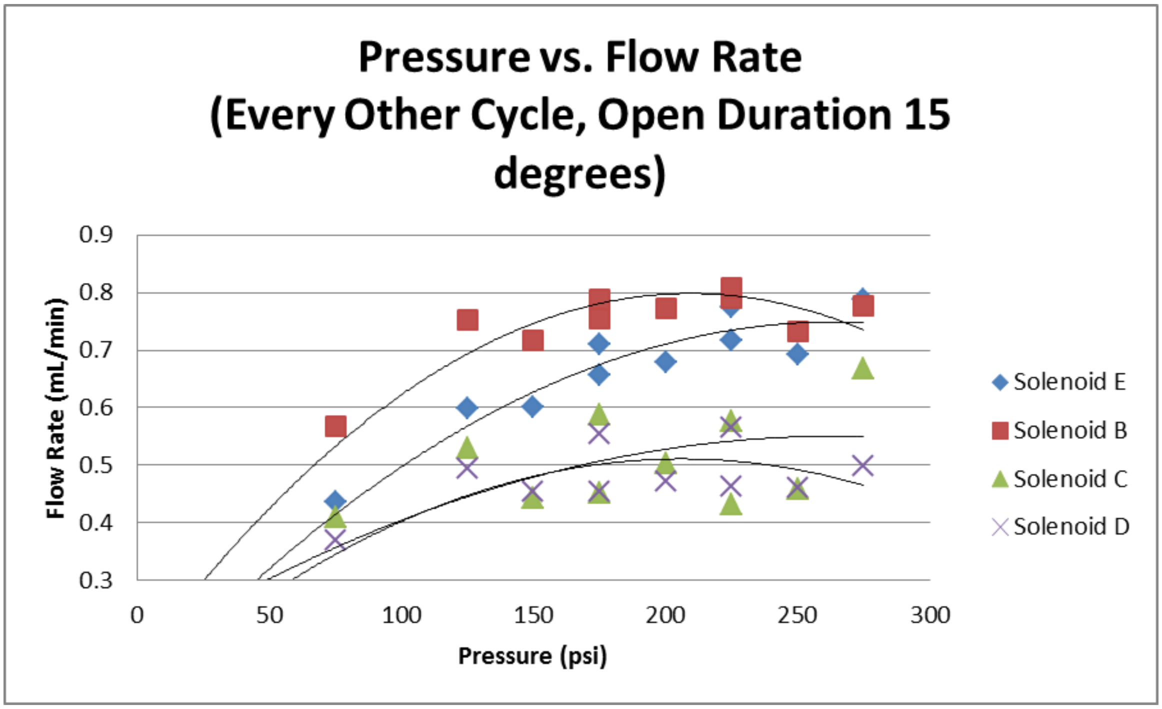


h) Nominal lube rate (8 pints/day, .67 mL/min) testing on engine.

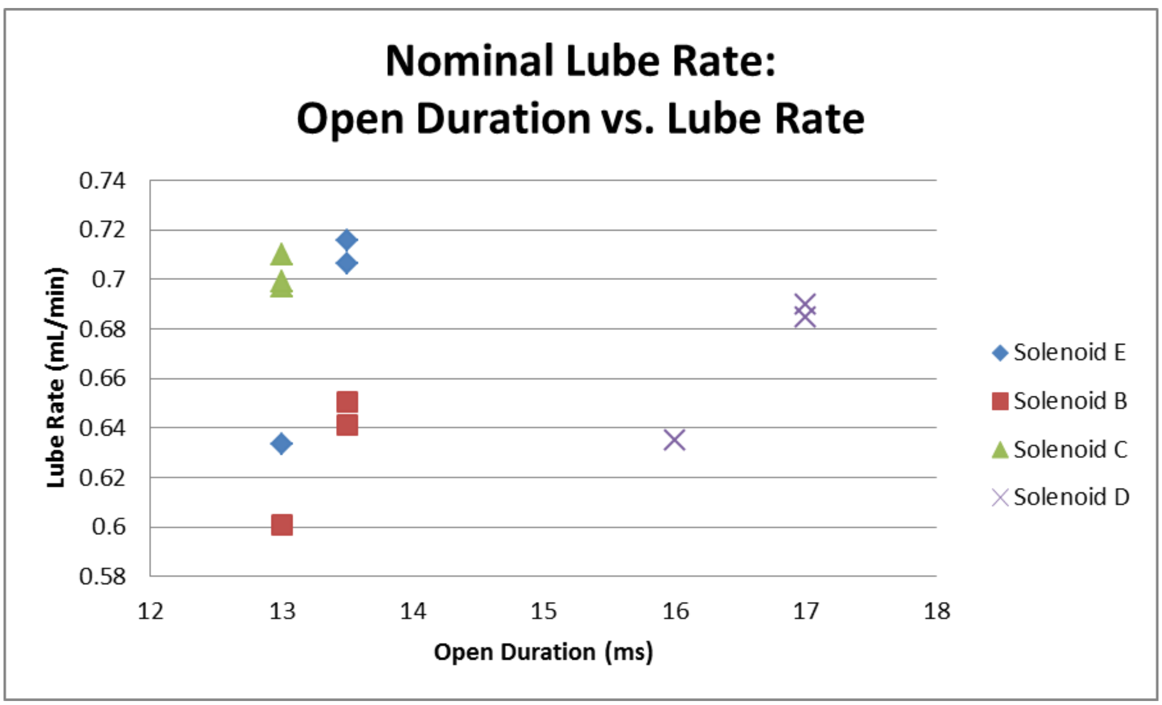

# APPENDIX III - ENGINE TESTING DATA TABLES

# MECHANICAL LUBRICATOR DATA TABLES

| Data Point Name<br><br>Engine Data | TLO-01<br>8/8/2012<br>100% Load | TLO-02<br>8/8/2012<br>100% Load | TLO-03<br>8/8/2012<br>100% Load | TLO-04<br>8/8/2012<br>100% Load | TLO-05<br>8/8/2012<br>100% Load | TLO-06<br>8/8/2012<br>100% Load |
|---|---|---|---|---|---|---|
| Speed [rpm] | 3.00E+02 | 3.00E+02 | 3.00E+02 | 3.00E+02 | 3.00E+02 | 3.00E+02 |
| Torque [lb-ft] | 7.74E+03 | 7.74E+03 | 7.72E+03 | 7.74E+03 | 7.74E+03 | 7.73E+03 |
| Power [bhp] | 4.42E+02 | 4.42E+02 | 4.41E+02 | 4.42E+02 | 4.42E+02 | 4.42E+02 |
| Load [%] | 1.00E+02 | 1.00E+02 | 9.99E+01 | 1.00E+02 | 1.00E+02 | 1.00E+02 |
| Ambient Press [psia] | 1.24E+01 | 1.24E+01 | 1.24E+01 | 1.24E+01 | 1.24E+01 | 1.24E+01 |
| Ambient Temp [F] | 1.52E+02 | 1.52E+02 | 1.53E+02 | 1.53E+02 | 1.54E+02 | 1.54E+02 |
| Ambient Humidity [%] | -6.54E+00 | -6.74E+00 | -7.62E+00 | -7.07E+00 | -7.72E+00 | -8.23E+00 |
| Inlet Air Pres [in Hg] | 7.50E+00 | 7.50E+00 | 7.49E+00 | 7.50E+00 | 7.50E+00 | 7.50E+00 |
| Inlet Air Temp [F] | 1.10E+02 | 1.10E+02 | 1.11E+02 | 1.11E+02 | 1.11E+02 | 1.11E+02 |
| Inlet Air Humidity [%] | 9.67E+00 | 9.30E+00 | 8.77E+00 | 9.12E+00 | 8.84E+00 | 8.62E+00 |
| Inlet Air Flow [scfm] | 1.70E+03 | 1.69E+03 | 1.69E+03 | 1.70E+03 | 1.70E+03 | 1.71E+03 |
| IC Water Temp [F] | 1.02E+02 | 1.02E+02 | 1.03E+02 | 1.03E+02 | 1.01E+02 | 1.02E+02 |
| Exh Back Pres [in Hg] | 5.00E+00 | 5.00E+00 | 5.00E+00 | 5.00E+00 | 5.00E+00 | 5.00E+00 |
| Exh Cyl 1 Temp [F] | 6.38E+02 | 6.39E+02 | 6.40E+02 | 6.41E+02 | 6.40E+02 | 6.46E+02 |
| Exh Cyl 2 Temp [F] | 7.22E+02 | 7.22E+02 | 7.21E+02 | 7.21E+02 | 7.19E+02 | 7.48E+02 |
| Exh Cyl 3 Temp [F] | 6.95E+02 | 6.95E+02 | 6.96E+02 | 6.92E+02 | 6.90E+02 | 6.81E+02 |
| Exh Cyl 4 Temp [F] | 8.68E+02 | 8.72E+02 | 8.70E+02 | 8.53E+02 | 8.22E+02 | 7.77E+02 |
| Avg Exh Temp [F] | 0.00E+00 | 0.00E+00 | 0.00E+00 | 0.00E+00 | 0.00E+00 | 0.00E+00 |
| Stack Temp [F] | 95.1 | 96.05 | 96.27 | 101.9 | 101.7 | 102.2 |
| Fuel Flow [lb/hr] | 184 | 184.2 | 184.1 | 183.5 | 182.2 | 181.6 |
| Orifice Stat Pres [psia] | 45.74 | 45.75 | 45.57 | 45.78 | 45.81 | 46.36 |
| Orifice Diff Pres [in H2O] | 0.000514 | 0.000514 | 0.000514 | 0.000514 | 0.000514 | 0.000514 |
| Orifice Temp [F] | 86.22 | 86.92 | 88.09 | 89.05 | 89.31 | 89.6 |
| Eng Fuel Pres [psig] | 20.83 | 20.92 | 20.91 | 20.94 | 20.87 | 20.85 |
| Eng Fuel Temp [F] | 138.7 | 139.9 | 140.6 | 140.9 | 139.6 | 136.1 |
| JW Out Temp [F] | 165 | 165.1 | 165 | 164.9 | 165.1 | 164.9 |
| JW In Temp [F] | 159.7 | 159.8 | 159.6 | 159.2 | 159 | 158.7 |
| JW Flow [gpm] | 378.7 | 375.3 | 368.9 | 368.7 | 369.6 | 369.4 |
| Lube Press [psig] | 38.34 | 38.08 | 38.64 | 38.27 | 38.01 | 38.67 |
| Lube In Temp [F] | 141.7 | 144 | 142.3 | 142.1 | 144.3 | 141.8 |
| Lube Out Temp [F] | 155.4 | 158 | 155.1 | 156.8 | 157.1 | 155.4 |
| Thrust 1 Temp [F] | 153.9 | 155.7 | 153.8 | 155.2 | 154.3 | 153.7 |
| Thrust 2 Temp [F] | 155.7 | 157.5 | 155.4 | 156.9 | 155.8 | 155.7 |
| Main 2A Temp [F] | 154 | 156.2 | 153.5 | 155.3 | 154.3 | 153.7 |
| Main 2B Temp [F] | 152.9 | 154.9 | 152.8 | 154.3 | 153.2 | 152.4 |
| Main 3A Temp [F] | 154.8 | 156.5 | 154.6 | 156.1 | 155.1 | 154.5 |
| Main 3B Temp [F] | 155.2 | 156.8 | 155 | 156.5 | 155.7 | 154.8 |
| Main 4A Temp [F] | 154.4 | 155.8 | 154 | 155.4 | 154.2 | 154 |
| Main 4B Temp [F] | 151.4 | 153.2 | 151.1 | 152.7 | 151.7 | 151 |
| | | | | | | |
| **Emissions Data** | | | | | | |
| THC [ppmd] | 782.8 | 783.1 | 793.7 | 797.9 | 798.2 | 822.2 |
| NOx [ppmd] | 998.8 | 1004 | 1002 | 1031 | 1061 | 1165 |
| NO [ppmd] | 0 | 0 | 0 | 0 | 0 | 0 |
| NO2 [ppmd] | 0 | 0 | 0 | 0 | 0 | 0 |
| O2 [%d] | 18.04 | 18.05 | 18.05 | 18.05 | 18.04 | 18.05 |
| CO2 [%d] | 4.291 | 4.288 | 4.29 | 4.265 | 4.23 | 4.194 |
| CO [ppmd] | 128.1 | 126.8 | 126.9 | 114.9 | 99.95 | 83.15 |
| AFR Left | 0 | 0 | 0 | 0 | 0 | 0 |
| AFR Right | 0 | 0 | 0 | 0 | 0 | 0 |
| PCC N2 Flow | 0 | 0 | 0 | 0 | 0 | 0 |
| Time[sec] | 3427000000 | 3427000000 | 3427000000 | 3427000000 | 3427000000 | 3427000000 |

| Data Point Name<br><br>Engine Data | TLO-01<br>8/8/2012<br>100% Load | TLO-02<br>8/8/2012<br>100% Load | TLO-03<br>8/8/2012<br>100% Load | TLO-04<br>8/8/2012<br>100% Load | TLO-05<br>8/8/2012<br>100% Load | TLO-06<br>8/8/2012<br>100% Load |
|---|---|---|---|---|---|---|
| **FTIR Data** | | | | | | |
| Carbon Dioxide | 42690 | 42680 | 42740 | 42550 | 42630 | 42370 |
| Nitric oxide | 1048 | 1054 | 1053 | 1086 | 1113 | 1235 |
| Nitrogen dioxide | 0 | 0 | 0 | 0 | 0 | 0 |
| Methane | 585.2 | 589.6 | 602 | 609.7 | 611.7 | 626.5 |
| Ethylene | 16.38 | 15.9 | 15.8 | 14.49 | 12.45 | 10.31 |
| Ethane | 60.11 | 60.11 | 60.6 | 60.77 | 61.65 | 67.12 |
| Propylene | 1.771 | 1.589 | 1.555 | 1.436 | 1.313 | 1.099 |
| Formaldehyde | 19.19 | 18.94 | 19.11 | 18.26 | 16.64 | 14.57 |
| Water | 115500 | 115100 | 114700 | 115100 | 114900 | 114100 |
| Propane | 18.99 | 18.86 | 18.95 | 18.86 | 18.79 | 19.96 |
| Hydrogen cyanide | 0.7176 | 0.6429 | 0.6192 | 0.5621 | 0.4442 | 0.3503 |
| Ammonia | 0 | 0 | 0 | 0 | 0 | 0 |
| Carbon Monoxide | 130.8 | 129.2 | 129.5 | 115.9 | 99.1 | 80.54 |
| NOx | 1048 | 1054 | 1053 | 1086 | 1113 | 1235 |
| Total Hydrocarbons | 777.9 | 781.1 | 794.5 | 799.8 | 799.5 | 823.7 |
| Non Methane Hydrocarb | 192.8 | 191.5 | 192.5 | 190.2 | 187.8 | 197.2 |
| VOC's | 82.76 | 81.51 | 81.6 | 78.95 | 75 | 74.35 |
| | | | | | | |
| **Calculated Data** | | | | | | |
| Fuel Flow [SCFH] | 1550 | 1560 | 1550 | 1550 | 1540 | 1530 |
| Fuel Flow [LB/HR] | 184 | 184 | 184 | 183 | 182 | 182 |
| BSFC [BTU/bhp-hr] | 8530 | 8540 | 8560 | 8510 | 8440 | 8420 |
| Stoich. A/F | 15.6 | 15.6 | 15.6 | 15.6 | 15.6 | 15.6 |
| U & S A/F | 54.5 | 54.5 | 54.5 | 54.7 | 55 | 55.4 |
| Trapped A/F | 26.1 | 26.1 | 26.1 | 26.1 | 26.3 | 26.4 |
| Mass Flow A/F | 46.6 | 46.6 | 46.6 | 46.9 | 47.2 | 47.6 |
| Air Flow [scfm] | 8580 | 8590 | 8580 | 8600 | 8610 | 8650 |
| BMEP [psi] | 67.7 | 67.7 | 67.5 | 67.7 | 67.7 | 67.6 |
| Thermal Eff. | 29.8 | 29.8 | 29.7 | 29.9 | 30.1 | 30.2 |
| Wobbe Index | 1950 | 1950 | 1950 | 1950 | 1950 | 1950 |
| Methane [%] | 0.00166 | 0.00165 | 0 | 0.0033 | 0.00167 | 0.00166 |
| LHV [BTU/cf] | 2430 | 2430 | 2430 | 2430 | 2420 | 2430 |
| Gas Density [lb/Mcf] | 125 | 125 | 125 | 125 | 125 | 125 |
| Water [%] | 11.5 | 11.5 | 11.5 | 11.5 | 11.5 | 11.4 |
| Abs. Humidity | 0.00486 | 0.00466 | 0.00446 | 0.0047 | 0.0045 | 0.00443 |
| NOx @ 15% O2 [ppmd] | 2060 | 2080 | 2070 | 2130 | 2190 | 2410 |
| BS THC [g/bhp-hr] | 10.5 | 10.6 | 10.7 | 10.8 | 10.8 | 11.2 |
| BS NOx Actual [g/bhp-hr] | 13.6 | 13.6 | 13.6 | 14 | 14.5 | 16 |
| BS NOx EPA Meth. 20 [g/bhp-hr] | 8.84 | 8.9 | 8.9 | 9.15 | 9.43 | 10.4 |
| BS NOx FTIR [g/bhp-hr] | 0 | 0 | 0 | 0 | 0 | 0 |
| BS NO FTIR [g/bhp-hr] | 0 | 0 | 0 | 0 | 0 | 0 |
| BS NO2 FTIR [g/bhp-hr] | 0 | 0 | 0 | 0 | 0 | 0 |
| BS CO [g/bhp-hr] | 1.06 | 1.05 | 1.05 | 0.952 | 0.829 | 0.694 |
| BS CH2O [g/bhp-hr] | 0.192 | 0.19 | 0.192 | 0.183 | 0.167 | 0.147 |
| BS CO2 [g/bhp-hr] | 557 | 557 | 559 | 555 | 551 | 550 |
| Phi Trapped | 0.599 | 0.6 | 0.6 | 0.598 | 0.595 | 0.593 |
| H2O MF [scfm] | 333 | 332 | 330 | 331 | 327 | 326 |
| Exh MF [scfm] | 8760 | 8770 | 8760 | 8780 | 8790 | 8830 |
| BS O2 [g/bhp-hr] | 1700 | 1710 | 1710 | 1710 | 1710 | 1720 |
| BS NMHC [g/bhp-hr] | 1.25 | 1.24 | 1.25 | 1.23 | 1.2 | 1.24 |
| BS VOC [g/bhp-hr] | 0.649 | 0.639 | 0.641 | 0.618 | 0.58 | 0.556 |
| U&S AF Total | 0 | 0 | 0 | 0 | 0 | 0 |
| Delivery Ratio | 1.77 | 1.77 | 1.77 | 1.78 | 1.78 | 1.78 |
| Trapping Efficiency | 0.477 | 0.477 | 0.477 | 0.476 | 0.476 | 0.475 |
| Scavenging Efficiency | 0.844 | 0.844 | 0.844 | 0.846 | 0.846 | 0.848 |

| Data Point Name<br><br>Engine Data | TLO-01<br>8/8/2012<br>100% Load | TLO-02<br>8/8/2012<br>100% Load | TLO-03<br>8/8/2012<br>100% Load | TLO-04<br>8/8/2012<br>100% Load | TLO-05<br>8/8/2012<br>100% Load | TLO-06<br>8/8/2012<br>100% Load |
|---|---|---|---|---|---|---|
| **Dillution Tunnel Data** | | | | | | |
| Sample Flow (aLPM) | 72.81 | 72.59 | 72.4 | 73.26 | 73.66 | 70.75 |
| Verturi Pressure (inH2O) | 16.91 | 16.86 | 16.82 | 17.02 | 17.11 | 16.43 |
| Air Flow (aLPM) | 740.16 | 726.66 | 723.13 | 735.85 | 756.3 | 726.65 |
| Residence Time (s) | 113.21 | 112.98 | 113.06 | 112.83 | 112.77 | 112.77 |
| aLPM Dilution Ratio (air/exhaust) | 10.14 | 10.01 | 723.13 | 10.04 | 10.26 | 10.29 |
| Mixture Temp (C) | 74.31 | 74.35 | 74.21 | 74.95 | 75.15 | 71.32 |
| Air Out Temp (C) | 83.98 | 84.48 | 84.28 | 85.77 | 86.17 | 82.95 |
| Residence Temp (C) | 38.69 | 39.52 | 39.11 | 40.01 | 40.18 | 40.1 |
| Measurement Humidity (%) | 150.59 | 150.56 | 150.56 | 150.57 | 150.54 | 150.54 |
| Ambient Pressure (kPa) | 85.29 | 85.26 | 85.24 | 85.22 | 85.19 | 85.18 |
| Ambient Humidity (%) | 29.2 | 29.2 | 29.2 | 29.2 | 29.2 | 29.2 |
| Ambient Temp (C) | 15.4 | 15.4 | 15.4 | 15.4 | 15.4 | 15.4 |
| Excess Flow (aLPM) | 170.3 | 170.64 | 170.52 | 170.87 | 170.97 | 170.96 |
| Sample Line Temp (F) | 230 | 230 | 230 | 230 | 230 | 230 |
| Sample Flow (SLM) | 64.09 | 63.89 | 63.71 | 64.47 | 64.81 | 62.25 |
| Air Flow (SLM) | 685.76 | 673.13 | 669.78 | 681.48 | 700.30 | 672.80 |
| Corrected Dillution Ratio (Air/Sample) | 10.70 | 10.54 | 10.51 | 10.57 | 10.81 | 10.81 |
| | | | | | | |
| **PM Calculation Data** | | | | | | |
| Lube Rate (pints/day) | 18.4 | 13.9 | 11.5 | 9.3 | 7.5 | 5.67 |
| Lube Rate (g/bhp-hr) | 0.727355621 | 0.549469735 | 0.456041411 | 0.367797217 | 0.296543552 | 0.224440818 |
| Sample Time (min) | 15 | 15 | 15 | 15 | 15 | 15 |
| Particulate Matter Sample (µg) | 777 | 608 | 547 | 474 | 418 | 319 |
| Particulate Matter Rate (µg/min) | 51.8 | 40.5 | 36.5 | 31.6 | 27.9 | 21.3 |
| Mass Flow Fuel (kg/sec) | 0.0245 | 0.0245 | 0.0245 | 0.0244 | 0.0243 | 0.0241 |
| Mass Flow Exhaust (kg/sec) | 1.359 | 1.361 | 1.360 | 1.360 | 1.362 | 1.362 |
| Mass Flow PM on Filter (kg/sec) | 8.63E-10 | 6.76E-10 | 6.08E-10 | 5.27E-10 | 4.64E-10 | 3.54E-10 |
| Mass Flow Sample through Filter (kg/sec) | 0.000764 | 0.000764 | 0.000764 | 0.000764 | 0.000764 | 0.000764 |
| Mass Flow PM in Total Exhaust (kg/sec) | 1.79624E-05 | 1.3875E-05 | 1.2448E-05 | 1.08463E-05 | 9.77255E-06 | 7.45649E-06 |
| Brake Specific PM (g/bhp-hr) | 0.146 | 0.113 | 0.102 | 0.088 | 0.080 | 0.061 |

# ECL I DATA TABLES

| Data Point Name<br><br>Engine Data | TLO-01<br>10/4/2012<br>100% Load | TLO-02<br>10/4/2012<br>100% Load | TLO-03<br>10/4/2012<br>100% Load | TLO-01<br>10/8/2012<br>100% Load | TLO-02<br>10/8/2012<br>100% Load | TLO-03<br>10/8/2012<br>100% Load | TLO-04<br>10/8/2012<br>100% Load | TLO-05<br>10/8/2012<br>100% Load | TLO-06<br>10/8/2012<br>100% Load | TLO-07<br>10/8/2012<br>100% Load | TLO-08<br>10/8/2012<br>100% Load | TLO-09<br>10/8/2012<br>100% Load | TLO-10<br>10/8/2012<br>100% Load | TLO-11<br>10/8/2012<br>100% Load | TLO-12<br>10/8/2012<br>100% Load |
|---|---|---|---|---|---|---|---|---|---|---|---|---|---|---|---|
| Speed [rpm] | 3.00E+02 | 3.00E+02 | 3.00E+02 | 3.00E+02 | 3.00E+02 | 3.00E+02 | 3.00E+02 | 3.00E+02 | 3.00E+02 | 3.00E+02 | 3.00E+02 | 3.00E+02 | 3.00E+02 | 3.00E+02 | 3.00E+02 |
| Torque [lb-ft] | 7.73E+03 | 7.72E+03 | 7.73E+03 | 7.73E+03 | 7.72E+03 | 7.72E+03 | 7.72E+03 | 7.72E+03 | 7.72E+03 | 7.73E+03 | 7.72E+03 | 7.73E+03 | 7.73E+03 | 7.73E+03 | 7.73E+03 |
| Power [bhp] | 4.41E+02 | 4.41E+02 | 4.41E+02 | 4.41E+02 | 4.41E+02 | 4.41E+02 | 4.41E+02 | 4.41E+02 | 4.41E+02 | 4.41E+02 | 4.41E+02 | 4.41E+02 | 4.42E+02 | 4.41E+02 | 4.42E+02 |
| Load [%] | 1.00E+02 | 9.99E+01 | 1.00E+02 | 1.00E+02 | 9.99E+01 | 1.00E+02 | 9.99E+01 | 9.99E+01 | 9.99E+01 | 1.00E+02 | 9.99E+01 | 1.00E+02 | 1.00E+02 | 1.00E+02 | 1.00E+02 |
| Ambient Press [psia] | 1.24E+01 | 1.24E+01 | 1.24E+01 | 1.23E+01 | 1.23E+01 | 1.22E+01 | 1.22E+01 | 1.22E+01 | 1.22E+01 | 1.22E+01 | 1.22E+01 | 1.22E+01 | 1.22E+01 | 1.22E+01 | 1.22E+01 |
| Ambient Temp [F] | 8.93E+01 | 8.89E+01 | 8.95E+01 | 1.12E+02 | 1.15E+02 | 1.16E+02 | 1.17E+02 | 1.18E+02 | 1.19E+02 | 1.22E+02 | 1.22E+02 | 1.20E+02 | 1.21E+02 | 1.22E+02 | 1.22E+02 |
| Ambient Humidity [%] | 1.61E+01 | 1.68E+01 | 1.73E+01 | -6.20E+00 | -6.26E+00 | -6.88E+00 | -7.13E+00 | -7.70E+00 | -8.36E+00 | -8.14E+00 | -8.26E+00 | -7.63E+00 | -7.59E+00 | -8.98E+00 | -8.47E+00 |
| Inlet Air Pres [in Hg] | 7.50E+00 | 7.50E+00 | 7.50E+00 | 7.50E+00 | 7.48E+00 | 7.50E+00 | 7.50E+00 | 7.50E+00 | 7.50E+00 | 7.50E+00 | 7.50E+00 | 7.50E+00 | 7.50E+00 | 7.50E+00 | 7.50E+00 |
| Inlet Air Temp [F] | 1.07E+02 | 1.02E+02 | 1.03E+02 | 1.10E+02 | 1.20E+02 | 1.14E+02 | 1.10E+02 | 1.13E+02 | 1.10E+02 | 1.17E+02 | 1.14E+02 | 1.09E+02 | 1.11E+02 | 1.09E+02 | 1.11E+02 |
| Inlet Air Humidity [%] | 3.65E+00 | 3.93E+00 | 4.69E+00 | 2.97E+00 | 3.21E+00 | 3.17E+00 | 3.08E+00 | 2.66E+00 | 2.87E+00 | 2.55E+00 | 3.06E+00 | 2.72E+00 | 3.06E+00 | 2.59E+00 | 3.01E+00 |
| Inlet Air Flow [scfm] | 1.70E+03 | 1.69E+03 | 1.69E+03 | 1.68E+03 | 1.68E+03 | 1.68E+03 | 1.68E+03 | 1.69E+03 | 1.68E+03 | 1.69E+03 | 1.68E+03 | 1.68E+03 | 1.68E+03 | 1.68E+03 | 1.69E+03 |
| IC Water Temp [F] | 1.29E+02 | 1.09E+02 | 1.09E+02 | 2.32E+03 | 2.32E+03 | 2.32E+03 | 2.32E+03 | 2.32E+03 | 2.32E+03 | 2.32E+03 | 2.32E+03 | 2.32E+03 | 2.32E+03 | 2.32E+03 | 2.32E+03 |
| Exh Back Pres [in Hg] | 5.00E+00 | 5.00E+00 | 5.00E+00 | 5.00E+00 | 5.01E+00 | 5.01E+00 | 5.01E+00 | 5.00E+00 | 5.00E+00 | 5.00E+00 | 5.00E+00 | 5.00E+00 | 5.00E+00 | 5.01E+00 | 5.00E+00 |
| Exh Cyl 1 Temp [F] | 6.81E+02 | 6.79E+02 | 6.80E+02 | 6.85E+02 | 6.96E+02 | 6.89E+02 | 6.80E+02 | 6.86E+02 | 6.86E+02 | 6.90E+02 | 6.88E+02 | 6.86E+02 | 6.86E+02 | 6.84E+02 | 6.84E+02 |
| Exh Cyl 2 Temp [F] | 7.57E+02 | 7.54E+02 | 7.56E+02 | 7.74E+02 | 7.89E+02 | 7.84E+02 | 7.83E+02 | 7.79E+02 | 7.81E+02 | 7.86E+02 | 7.86E+02 | 7.83E+02 | 7.84E+02 | 7.80E+02 | 7.82E+02 |
| Exh Cyl 3 Temp [F] | 6.21E+02 | 6.25E+02 | 6.27E+02 | 5.88E+02 | 6.00E+02 | 5.95E+02 | 5.79E+02 | 5.91E+02 | 5.91E+02 | 5.95E+02 | 5.94E+02 | 5.91E+02 | 5.92E+02 | 5.90E+02 | 5.90E+02 |
| Exh Cyl 4 Temp [F] | 7.90E+02 | 8.07E+02 | 8.12E+02 | 8.43E+02 | 8.57E+02 | 8.52E+02 | 8.25E+02 | 8.42E+02 | 8.43E+02 | 8.47E+02 | 8.47E+02 | 8.42E+02 | 8.44E+02 | 8.44E+02 | 8.43E+02 |
| Avg Exh Temp [F] | 7.12E+02 | 7.16E+02 | 7.19E+02 | 7.23E+02 | 7.35E+02 | 7.30E+02 | 7.17E+02 | 7.24E+02 | 7.25E+02 | 7.29E+02 | 7.29E+02 | 7.25E+02 | 7.26E+02 | 7.24E+02 | 7.25E+02 |
| Stack Temp [F] | 7.06E+01 | 7.56E+01 | 7.76E+01 | 7.73E+01 | 7.85E+01 | 8.00E+01 | 8.06E+01 | 8.17E+01 | 8.22E+01 | 8.33E+01 | 8.38E+01 | 8.42E+01 | 8.53E+01 | 8.55E+01 | 8.62E+01 |
| Fuel Flow [lb/hr] | 1.80E+02 | 1.81E+02 | 1.81E+02 | 1.74E+02 | 1.76E+02 | 1.76E+02 | 1.77E+02 | 1.76E+02 | 1.76E+02 | 1.77E+02 | 1.76E+02 | 1.75E+02 | 1.76E+02 | 1.76E+02 | 1.76E+02 |
| Orifice Stat Pres [psia] | 4.59E+01 | 4.57E+01 | 4.48E+01 | 4.55E+01 | 4.57E+01 | 4.56E+01 | 4.55E+01 | 4.57E+01 | 4.58E+01 | 4.54E+01 | 4.56E+01 | 4.58E+01 | 4.58E+01 | 4.62E+01 | 4.63E+01 |
| Orifice Diff Pres [in H2O] | 5.14E-04 | 5.18E-04 | 5.14E-04 | 5.18E-04 | 5.14E-04 | 5.14E-04 | 5.14E-04 | 5.14E-04 | 5.14E-04 | 5.14E-04 | 5.14E-04 | 5.14E-04 | 5.14E-04 | 5.14E-04 | 5.14E-04 |
| Orifice Temp [F] | 6.41E+01 | 6.48E+01 | 6.61E+01 | 7.10E+01 | 7.12E+01 | 7.16E+01 | 7.17E+01 | 7.24E+01 | 7.30E+01 | 7.32E+01 | 7.41E+01 | 7.45E+01 | 7.47E+01 | 7.49E+01 | 7.57E+01 |
| Eng Fuel Pres [psig] | 2.26E+01 | 2.28E+01 | 2.31E+01 | 2.48E+01 | 2.48E+01 | 2.48E+01 | 2.42E+01 | 2.48E+01 | 2.48E+01 | 2.51E+01 | 2.49E+01 | 2.49E+01 | 2.49E+01 | 2.48E+01 | 2.47E+01 |
| Eng Fuel Temp [F] | 1.07E+02 | 1.09E+02 | 1.10E+02 | 1.14E+02 | 1.15E+02 | 1.15E+02 | 1.13E+02 | 1.16E+02 | 1.17E+02 | 1.18E+02 | 1.18E+02 | 1.18E+02 | 1.18E+02 | 1.19E+02 | 1.19E+02 |
| JW Out Temp [F] | 1.65E+02 | 1.65E+02 | 1.65E+02 | 1.65E+02 | 1.66E+02 | 1.67E+02 | 1.42E+02 | 1.65E+02 | 1.65E+02 | 1.65E+02 | 1.65E+02 | 1.65E+02 | 1.65E+02 | 1.65E+02 | 1.65E+02 |
| JW In Temp [F] | 1.61E+02 | 1.61E+02 | 1.61E+02 | 1.60E+02 | 1.61E+02 | 1.63E+02 | 1.40E+02 | 1.60E+02 | 1.60E+02 | 1.60E+02 | 1.60E+02 | 1.61E+02 | 1.60E+02 | 1.60E+02 | 1.60E+02 |
| JW Flow [gpm] | 3.97E+02 | 3.97E+02 | 3.97E+02 | 3.91E+02 | 3.90E+02 | 3.92E+02 | 3.90E+02 | 3.90E+02 | 3.88E+02 | 3.88E+02 | 3.88E+02 | 3.88E+02 | 3.87E+02 | 3.88E+02 | 3.88E+02 |
| Lube Press [psig] | 3.83E+01 | 3.84E+01 | 3.83E+01 | 3.85E+01 | 3.85E+01 | 3.83E+01 | 3.85E+01 | 3.82E+01 | 3.82E+01 | 3.82E+01 | 3.87E+01 | 3.90E+01 | 3.83E+01 | 3.83E+01 | 3.84E+01 |
| Lube In Temp [F] | 1.43E+02 | 1.43E+02 | 1.42E+02 | 1.43E+02 | 1.43E+02 | 1.43E+02 | 1.42E+02 | 1.43E+02 | 1.42E+02 | 1.43E+02 | 1.43E+02 | 1.42E+02 | 1.42E+02 | 1.42E+02 | 1.42E+02 |
| Lube Out Temp [F] | 1.55E+02 | 1.55E+02 | 1.55E+02 | 1.55E+02 | 1.56E+02 | 1.55E+02 | 1.54E+02 | 1.55E+02 | 1.55E+02 | 1.56E+02 | 1.56E+02 | 1.55E+02 | 1.55E+02 | 1.55E+02 | 1.55E+02 |
| Thrust 1 Temp [F] | 1.53E+02 | 1.53E+02 | 1.54E+02 | 1.53E+02 | 1.54E+02 | 1.54E+02 | 1.53E+02 | 1.53E+02 | 1.54E+02 | 1.54E+02 | 1.54E+02 | 1.54E+02 | 1.54E+02 | 1.53E+02 | 1.53E+02 |
| Thrust 2 Temp [F] | 1.55E+02 | 1.55E+02 | 1.55E+02 | 1.54E+02 | 1.54E+02 | 1.55E+02 | 1.55E+02 | 1.55E+02 | 1.55E+02 | 1.55E+02 | 1.55E+02 | 1.55E+02 | 1.55E+02 | 1.55E+02 | 1.55E+02 |
| Main 2A Temp [F] | 1.54E+02 | 1.54E+02 | 1.54E+02 | 1.54E+02 | 1.54E+02 | 1.54E+02 | 1.54E+02 | 1.54E+02 | 1.54E+02 | 1.54E+02 | 1.54E+02 | 1.54E+02 | 1.54E+02 | 1.53E+02 | 1.53E+02 |
| Main 2B Temp [F] | 1.53E+02 | 1.53E+02 | 1.53E+02 | 1.53E+02 | 1.53E+02 | 1.53E+02 | 1.53E+02 | 1.53E+02 | 1.53E+02 | 1.53E+02 | 1.53E+02 | 1.53E+02 | 1.53E+02 | 1.53E+02 | 1.53E+02 |
| Main 3A Temp [F] | 1.54E+02 | 1.54E+02 | 1.54E+02 | 1.54E+02 | 1.55E+02 | 1.55E+02 | 1.54E+02 | 1.54E+02 | 1.54E+02 | 1.55E+02 | 1.55E+02 | 1.55E+02 | 1.54E+02 | 1.54E+02 | 1.54E+02 |
| Main 3B Temp [F] | 1.54E+02 | 1.54E+02 | 1.55E+02 | 1.54E+02 | 1.55E+02 | 1.55E+02 | 1.55E+02 | 1.55E+02 | 1.55E+02 | 1.55E+02 | 1.55E+02 | 1.55E+02 | 1.54E+02 | 1.54E+02 | 1.54E+02 |
| Main 4A Temp [F] | 1.54E+02 | 1.54E+02 | 1.54E+02 | 1.54E+02 | 1.54E+02 | 1.54E+02 | 1.54E+02 | 1.54E+02 | 1.54E+02 | 1.54E+02 | 1.54E+02 | 1.54E+02 | 1.53E+02 | 1.54E+02 | 1.53E+02 |
| Main 4B Temp [F] | 1.51E+02 | 1.51E+02 | 1.51E+02 | 1.51E+02 | 1.51E+02 | 1.51E+02 | 1.51E+02 | 1.51E+02 | 1.51E+02 | 1.51E+02 | 1.51E+02 | 1.51E+02 | 1.51E+02 | 1.51E+02 | 1.51E+02 |

| Data Point Name | TLO-01 | TLO-02 | TLO-03 | TLO-01 | TLO-02 | TLO-03 | TLO-04 | TLO-05 | TLO-06 | TLO-07 | TLO-08 | TLO-09 | TLO-10 | TLO-11 | TLO-12 |
|---|---|---|---|---|---|---|---|---|---|---|---|---|---|---|---|
| | 10/4/2012 | 10/4/2012 | 10/4/2012 | 10/8/2012 | 10/8/2012 | 10/8/2012 | 10/8/2012 | 10/8/2012 | 10/8/2012 | 10/8/2012 | 10/8/2012 | 10/8/2012 | 10/8/2012 | 10/8/2012 | 10/8/2012 |
| **Engine Data** | 100% Load | 100% Load | 100% Load | 100% Load | 100% Load | 100% Load | 100% Load | 100% Load | 100% Load | 100% Load | 100% Load | 100% Load | 100% Load | 100% Load | 100% Load |
| **Emissions Data** | | | | | | | | | | | | | | | |
| THC [ppmd] | 1.02E+03 | 1.03E+03 | 1.03E+03 | 1.12E+03 | 1.13E+03 | 1.12E+03 | 1.14E+03 | 1.12E+03 | 1.13E+03 | 1.11E+03 | 1.11E+03 | 1.11E+03 | 1.11E+03 | 1.11E+03 | 1.11E+03 |
| NOx [ppmd] | 1.07E+03 | 9.77E+02 | 9.92E+02 | 1.35E+03 | 1.43E+03 | 1.39E+03 | 1.32E+03 | 1.36E+03 | 1.35E+03 | 1.40E+03 | 1.37E+03 | 1.33E+03 | 1.33E+03 | 1.32E+03 | 1.34E+03 |
| NO [ppmd] | 9.28E+02 | 8.53E+02 | 8.61E+02 | 0.00E+00 | 0.00E+00 | 0.00E+00 | 0.00E+00 | 0.00E+00 | 0.00E+00 | 0.00E+00 | 0.00E+00 | 0.00E+00 | 0.00E+00 | 0.00E+00 | 0.00E+00 |
| NO2 [ppmd] | 1.43E+02 | 1.25E+02 | 1.32E+02 | 0.00E+00 | 0.00E+00 | 0.00E+00 | 0.00E+00 | 0.00E+00 | 0.00E+00 | 0.00E+00 | 0.00E+00 | 0.00E+00 | 0.00E+00 | 0.00E+00 | 0.00E+00 |
| O2 [%d] | 1.81E+01 | 1.81E+01 | 1.81E+01 | 1.81E+01 | 1.81E+01 | 1.81E+01 | 1.81E+01 | 1.81E+01 | 1.81E+01 | 1.81E+01 | 1.81E+01 | 1.81E+01 | 1.81E+01 | 1.81E+01 | 1.81E+01 |
| CO2 [%d] | 4.15E+00 | 4.17E+00 | 4.16E+00 | 4.18E+00 | 4.28E+00 | 4.24E+00 | 4.21E+00 | 4.22E+00 | 4.21E+00 | 4.25E+00 | 4.23E+00 | 4.20E+00 | 4.21E+00 | 4.20E+00 | 4.21E+00 |
| CO [ppmd] | 1.10E+02 | 1.13E+02 | 1.14E+02 | 1.71E+02 | 1.91E+02 | 1.81E+02 | 1.66E+02 | 1.74E+02 | 1.73E+02 | 1.79E+02 | 1.77E+02 | 1.73E+02 | 1.76E+02 | 1.74E+02 | 1.76E+02 |
| AFR Left | 0.00E+00 | 0.00E+00 | 0.00E+00 | 0.00E+00 | 0.00E+00 | 0.00E+00 | 0.00E+00 | 0.00E+00 | 0.00E+00 | 0.00E+00 | 0.00E+00 | 0.00E+00 | 0.00E+00 | 0.00E+00 | 0.00E+00 |
| AFR Right | 0.00E+00 | 0.00E+00 | 0.00E+00 | 0.00E+00 | 0.00E+00 | 0.00E+00 | 0.00E+00 | 0.00E+00 | 0.00E+00 | 0.00E+00 | 0.00E+00 | 0.00E+00 | 0.00E+00 | 0.00E+00 | 0.00E+00 |
| PCC N2 Flow | 0.00E+00 | 0.00E+00 | 0.00E+00 | 0.00E+00 | 0.00E+00 | 0.00E+00 | 0.00E+00 | 0.00E+00 | 0.00E+00 | 0.00E+00 | 0.00E+00 | 0.00E+00 | 0.00E+00 | 0.00E+00 | 0.00E+00 |
| Time[sec] | 3.43E+09 | 3.43E+09 | 3.43E+09 | 3.43E+09 | 3.43E+09 | 3.43E+09 | 3.43E+09 | 3.43E+09 | 3.43E+09 | 3.43E+09 | 3.43E+09 | 3.43E+09 | 3.43E+09 | 3.43E+09 | 3.43E+09 |
| | | | | | | | | | | | | | | | |
| **FTIR Data** | | | | | | | | | | | | | | | |
| Carbon Dioxide | 3.92E+04 | 4.38E+04 | 3.95E+04 | 4.02E+04 | 4.13E+04 | 4.09E+04 | 4.05E+04 | 4.05E+04 | 4.06E+04 | 4.10E+04 | 4.10E+04 | 4.08E+04 | 4.10E+04 | 4.09E+04 | 4.06E+04 |
| Nitric oxide | 1.11E+03 | 1.48E+03 | 1.01E+03 | 1.43E+03 | 1.51E+03 | 1.47E+03 | 1.40E+03 | 1.45E+03 | 1.43E+03 | 1.49E+03 | 1.45E+03 | 1.41E+03 | 1.42E+03 | 1.40E+03 | 1.43E+03 |
| Nitrogen dioxide | 0.00E+00 | 0.00E+00 | 0.00E+00 | 0.00E+00 | 0.00E+00 | 0.00E+00 | 0.00E+00 | 0.00E+00 | 0.00E+00 | 0.00E+00 | 0.00E+00 | 0.00E+00 | 0.00E+00 | 0.00E+00 | 0.00E+00 |
| Methane | 7.99E+02 | 8.40E+02 | 8.37E+02 | 8.57E+02 | 8.51E+02 | 8.44E+02 | 8.58E+02 | 8.49E+02 | 8.52E+02 | 8.41E+02 | 8.39E+02 | 8.37E+02 | 8.39E+02 | 8.27E+02 | 8.30E+02 |
| Ethylene | 1.07E+01 | 1.25E+01 | 1.15E+01 | 1.81E+01 | 1.96E+01 | 1.92E+01 | 1.86E+01 | 1.91E+01 | 1.90E+01 | 1.92E+01 | 1.91E+01 | 1.89E+01 | 1.87E+01 | 1.92E+01 | 1.96E+01 |
| Ethane | 6.18E+01 | 6.24E+01 | 4.73E+01 | 8.14E+01 | 8.17E+01 | 8.17E+01 | 8.35E+01 | 8.13E+01 | 8.19E+01 | 7.78E+01 | 7.79E+01 | 7.84E+01 | 7.68E+01 | 7.96E+01 | 7.99E+01 |
| Propylene | 1.01E+00 | 3.77E+00 | 1.28E+00 | 1.14E+00 | 1.29E+00 | 1.33E+00 | 1.33E+00 | 1.47E+00 | 1.40E+00 | 1.44E+00 | 1.41E+00 | 1.39E+00 | 1.39E+00 | 1.57E+00 | 1.75E+00 |
| Formaldehyde | 1.79E+01 | 1.93E+01 | 2.06E+01 | 2.32E+01 | 2.43E+01 | 2.37E+01 | 2.38E+01 | 2.37E+01 | 2.37E+01 | 2.40E+01 | 2.38E+01 | 2.36E+01 | 2.36E+01 | 2.36E+01 | 2.39E+01 |
| Water | 1.07E+05 | 5.59E+04 | 1.10E+05 | 1.05E+05 | 1.08E+05 | 1.07E+05 | 1.06E+05 | 1.06E+05 | 1.06E+05 | 1.07E+05 | 1.07E+05 | 1.07E+05 | 1.08E+05 | 1.07E+05 | 1.06E+05 |
| Propane | 1.84E+01 | 1.58E+01 | 1.63E+01 | 1.37E+01 | 1.54E+01 | 1.59E+01 | 1.62E+01 | 1.66E+01 | 1.63E+01 | 1.67E+01 | 1.62E+01 | 1.62E+01 | 1.60E+01 | 1.91E+01 | 2.05E+01 |
| Hydrogen cyanide | 0.00E+00 | 6.85E+00 | 0.00E+00 | 6.75E-01 | 9.56E-01 | 9.29E-01 | 8.85E-01 | 8.49E-01 | 7.89E-01 | 9.08E-01 | 9.04E-01 | 9.16E-01 | 9.38E-01 | 8.54E-01 | 8.23E-01 |
| Ammonia | 0.00E+00 | 0.00E+00 | 0.00E+00 | 0.00E+00 | 0.00E+00 | 0.00E+00 | 0.00E+00 | 0.00E+00 | 0.00E+00 | 0.00E+00 | 0.00E+00 | 0.00E+00 | 0.00E+00 | 0.00E+00 | 0.00E+00 |
| Carbon Monoxide | 1.12E+02 | 1.11E+02 | 1.16E+02 | 1.78E+02 | 1.96E+02 | 1.88E+02 | 1.72E+02 | 1.81E+02 | 1.79E+02 | 1.85E+02 | 1.83E+02 | 1.80E+02 | 1.82E+02 | 1.80E+02 | 1.83E+02 |
| NOx | 1.11E+03 | 1.48E+03 | 1.01E+03 | 1.43E+03 | 1.51E+03 | 1.47E+03 | 1.40E+03 | 1.45E+03 | 1.43E+03 | 1.49E+03 | 1.45E+03 | 1.41E+03 | 1.42E+03 | 1.40E+03 | 1.43E+03 |
| Total Hydrocarbons | 9.83E+02 | 1.02E+03 | 9.89E+02 | 1.08E+03 | 1.08E+03 | 1.07E+03 | 1.09E+03 | 1.08E+03 | 1.08E+03 | 1.07E+03 | 1.06E+03 | 1.06E+03 | 1.06E+03 | 1.06E+03 | 1.07E+03 |
| Non Methane Hydrocarb | 1.84E+02 | 1.81E+02 | 1.53E+02 | 2.20E+02 | 2.28E+02 | 2.29E+02 | 2.32E+02 | 2.30E+02 | 2.30E+02 | 2.24E+02 | 2.22E+02 | 2.23E+02 | 2.19E+02 | 2.34E+02 | 2.39E+02 |
| VOC's | 7.07E+01 | 6.67E+01 | 6.63E+01 | 7.12E+01 | 7.88E+01 | 7.92E+01 | 7.89E+01 | 8.09E+01 | 8.01E+01 | 8.16E+01 | 7.98E+01 | 7.95E+01 | 7.87E+01 | 8.83E+01 | 9.27E+01 |

| Data Point Name<br>Engine Data | TLO-01<br>10/4/2012<br>100% Load | TLO-02<br>10/4/2012<br>100% Load | TLO-03<br>10/4/2012<br>100% Load | TLO-01<br>10/8/2012<br>100% Load | TLO-02<br>10/8/2012<br>100% Load | TLO-03<br>10/8/2012<br>100% Load | TLO-04<br>10/8/2012<br>100% Load | TLO-05<br>10/8/2012<br>100% Load | TLO-06<br>10/8/2012<br>100% Load | TLO-07<br>10/8/2012<br>100% Load | TLO-08<br>10/8/2012<br>100% Load | TLO-09<br>10/8/2012<br>100% Load | TLO-10<br>10/8/2012<br>100% Load | TLO-11<br>10/8/2012<br>100% Load | TLO-12<br>10/8/2012<br>100% Load |
|---|---|---|---|---|---|---|---|---|---|---|---|---|---|---|---|
| **Calculated Data** | | | | | | | | | | | | | | | |
| Fuel Flow [SCFH] | 1.54E+03 | 1.54E+03 | 1.56E+03 | 1.47E+03 | 1.48E+03 | 1.49E+03 | 1.49E+03 | 1.49E+03 | 1.48E+03 | 1.50E+03 | 1.49E+03 | 1.48E+03 | 1.49E+03 | 1.48E+03 | 1.48E+03 |
| Fuel Flow [LB/HR] | 1.80E+02 | 1.81E+02 | 1.81E+02 | 1.74E+02 | 1.76E+02 | 1.76E+02 | 1.77E+02 | 1.76E+02 | 1.75E+02 | 1.77E+02 | 1.76E+02 | 1.75E+02 | 1.76E+02 | 1.76E+02 | 1.76E+02 |
| BSFC [BTU/bhp-hr] | 8.33E+03 | 8.37E+03 | 8.35E+03 | 8.10E+03 | 8.18E+03 | 8.18E+03 | 8.21E+03 | 8.16E+03 | 8.15E+03 | 8.21E+03 | 8.17E+03 | 8.14E+03 | 8.17E+03 | 8.16E+03 | 8.16E+03 |
| Stoich. A/F | 1.55E+01 | 1.55E+01 | 1.55E+01 | 1.56E+01 | 1.56E+01 | 1.56E+01 | 1.56E+01 | 1.56E+01 | 1.56E+01 | 1.56E+01 | 1.56E+01 | 1.56E+01 | 1.56E+01 | 1.56E+01 | 1.56E+01 |
| U & S A/F | 5.54E+01 | 5.52E+01 | 5.52E+01 | 5.51E+01 | 5.42E+01 | 5.46E+01 | 5.48E+01 | 5.47E+01 | 5.48E+01 | 5.44E+01 | 5.47E+01 | 5.49E+01 | 5.48E+01 | 5.49E+01 | 5.48E+01 |
| Trapped A/F | 2.68E+01 | 2.71E+01 | 2.68E+01 | 2.70E+01 | 2.64E+01 | 2.66E+01 | 2.67E+01 | 2.67E+01 | 2.68E+01 | 2.65E+01 | 2.66E+01 | 2.68E+01 | 2.67E+01 | 2.68E+01 | 2.67E+01 |
| Mass Flow A/F | 4.77E+01 | 4.75E+01 | 4.75E+01 | 4.72E+01 | 4.61E+01 | 4.66E+01 | 4.68E+01 | 4.68E+01 | 4.68E+01 | 4.64E+01 | 4.67E+01 | 4.69E+01 | 4.69E+01 | 4.70E+01 | 4.69E+01 |
| Air Flow [scfm] | 8.59E+03 | 8.58E+03 | 8.60E+03 | 8.23E+03 | 8.11E+03 | 8.21E+03 | 8.28E+03 | 8.22E+03 | 8.22E+03 | 8.22E+03 | 8.22E+03 | 8.23E+03 | 8.25E+03 | 8.26E+03 | 8.24E+03 |
| BMEP [psi] | 6.76E+01 | 6.75E+01 | 6.76E+01 | 6.76E+01 | 6.75E+01 | 6.76E+01 | 6.75E+01 | 6.75E+01 | 6.75E+01 | 6.76E+01 | 6.76E+01 | 6.76E+01 | 6.76E+01 | 6.76E+01 | 6.76E+01 |
| Thermal Eff. | 3.05E+01 | 3.04E+01 | 3.05E+01 | 3.14E+01 | 3.11E+01 | 3.11E+01 | 3.10E+01 | 3.12E+01 | 3.12E+01 | 3.10E+01 | 3.12E+01 | 3.13E+01 | 3.12E+01 | 3.12E+01 | 3.12E+01 |
| Wobbe Index | 1.93E+03 | 1.93E+03 | 1.92E+03 | 1.95E+03 | 1.95E+03 | 1.95E+03 | 1.95E+03 | 1.95E+03 | 1.95E+03 | 1.95E+03 | 1.95E+03 | 1.95E+03 | 1.95E+03 | 1.95E+03 | 1.95E+03 |
| Methane [%] | 0.00E+00 | 3.36E-03 | 1.67E-03 | 1.66E-03 | 1.65E-03 | 0.00E+00 | 3.30E-03 | 1.67E-03 | 1.66E-03 | 3.33E-03 | 1.67E-03 | 3.32E-03 | 3.30E-03 | 1.66E-03 | 3.31E-03 |
| LHV [BTU/cf] | 2.39E+03 | 2.39E+03 | 2.37E+03 | 2.43E+03 | 2.43E+03 | 2.43E+03 | 2.43E+03 | 2.42E+03 | 2.43E+03 | 2.42E+03 | 2.42E+03 | 2.42E+03 | 2.42E+03 | 2.43E+03 | 2.43E+03 |
| Gas Density [lb/Mcf] | 1.24E+02 | 1.24E+02 | 1.23E+02 | 1.25E+02 | 1.25E+02 | 1.25E+02 | 1.25E+02 | 1.25E+02 | 1.25E+02 | 1.25E+02 | 1.25E+02 | 1.25E+02 | 1.25E+02 | 1.25E+02 | 1.26E+02 |
| Water [%] | 1.07E+01 | 5.59E+00 | 1.10E+01 | 1.05E+01 | 1.08E+01 | 1.07E+01 | 1.06E+01 | 1.06E+01 | 1.06E+01 | 1.07E+01 | 1.07E+01 | 1.07E+01 | 1.08E+01 | 1.06E+01 | 1.06E+01 |
| Abs. Humidity | 1.67E-03 | 1.55E-03 | 1.90E-03 | 1.47E-03 | 2.13E-03 | 1.80E-03 | 1.53E-03 | 1.47E-03 | 1.42E-03 | 1.53E-03 | 1.72E-03 | 1.31E-03 | 1.57E-03 | 1.26E-03 | 1.55E-03 |
| NOx @ 15% O2 [ppmd] | 2.22E+03 | 2.03E+03 | 2.06E+03 | 2.80E+03 | 2.97E+03 | 2.89E+03 | 2.73E+03 | 2.81E+03 | 2.80E+03 | 2.91E+03 | 2.84E+03 | 2.75E+03 | 2.77E+03 | 2.73E+03 | 2.78E+03 |
| BS THC [g/bhp-hr] | 1.36E+01 | 1.37E+01 | 1.37E+01 | 1.45E+01 | 1.45E+01 | 1.45E+01 | 1.49E+01 | 1.46E+01 | 1.46E+01 | 1.44E+01 | 1.43E+01 | 1.44E+01 | 1.44E+01 | 1.45E+01 | 1.45E+01 |
| BS NOx Actual [g/bhp-hr] | 1.46E+01 | 1.33E+01 | 1.36E+01 | 1.77E+01 | 1.85E+01 | 1.82E+01 | 1.74E+01 | 1.78E+01 | 1.77E+01 | 1.83E+01 | 1.79E+01 | 1.74E+01 | 1.75E+01 | 1.73E+01 | 1.76E+01 |
| BS NOx EPA Meth. 20 [g/bhp-hr] | 9.53E+00 | 8.70E+00 | 8.84E+00 | 1.15E+01 | 1.21E+01 | 1.19E+01 | 1.13E+01 | 1.16E+01 | 1.15E+01 | 1.19E+01 | 1.17E+01 | 1.13E+01 | 1.14E+01 | 1.13E+01 | 1.15E+01 |
| BS NOx FTIR [g/bhp-hr] | 0.00E+00 | 0.00E+00 | 0.00E+00 | 0.00E+00 | 0.00E+00 | 0.00E+00 | 0.00E+00 | 0.00E+00 | 0.00E+00 | 0.00E+00 | 0.00E+00 | 0.00E+00 | 0.00E+00 | 0.00E+00 | 0.00E+00 |
| BS NO FTIR [g/bhp-hr] | 8.26E+00 | 7.59E+00 | 7.67E+00 | 0.00E+00 | 0.00E+00 | 0.00E+00 | 0.00E+00 | 0.00E+00 | 0.00E+00 | 0.00E+00 | 0.00E+00 | 0.00E+00 | 0.00E+00 | 0.00E+00 | 0.00E+00 |
| BS NO2 FTIR [g/bhp-hr] | 1.95E+00 | 1.70E+00 | 1.80E+00 | 0.00E+00 | 0.00E+00 | 0.00E+00 | 0.00E+00 | 0.00E+00 | 0.00E+00 | 0.00E+00 | 0.00E+00 | 0.00E+00 | 0.00E+00 | 0.00E+00 | 0.00E+00 |
| BS CO [g/bhp-hr] | 9.14E-01 | 9.38E-01 | 9.49E-01 | 1.36E+00 | 1.50E+00 | 1.44E+00 | 1.34E+00 | 1.39E+00 | 1.38E+00 | 1.43E+00 | 1.41E+00 | 1.38E+00 | 1.41E+00 | 1.39E+00 | 1.41E+00 |
| BS CH2O [g/bhp-hr] | 1.78E-01 | 1.83E-01 | 2.06E-01 | 2.22E-01 | 2.29E-01 | 2.26E-01 | 2.29E-01 | 2.27E-01 | 2.27E-01 | 2.30E-01 | 2.28E-01 | 2.26E-01 | 2.27E-01 | 2.27E-01 | 2.29E-01 |
| BS CO2 [g/bhp-hr] | 5.42E+02 | 5.44E+02 | 5.43E+02 | 5.24E+02 | 5.29E+02 | 5.29E+02 | 5.31E+02 | 5.28E+02 | 5.27E+02 | 5.32E+02 | 5.29E+02 | 5.27E+02 | 5.29E+02 | 5.28E+02 | 5.28E+02 |
| Phi Trapped | 5.85E-01 | 5.78E-01 | 5.85E-01 | 5.80E-01 | 5.92E-01 | 5.88E-01 | 5.86E-01 | 5.86E-01 | 5.84E-01 | 5.92E-01 | 5.88E-01 | 5.83E-01 | 5.86E-01 | 5.84E-01 | 5.85E-01 |
| H2O MF [scfm] | 2.98E+02 | 2.98E+02 | 3.01E+02 | 2.86E+02 | 2.94E+02 | 2.92E+02 | 2.90E+02 | 2.88E+02 | 2.88E+02 | 2.91E+02 | 2.91E+02 | 2.86E+02 | 2.90E+02 | 2.87E+02 | 2.89E+02 |
| Exh MF [scfm] | 8.77E+03 | 8.76E+03 | 8.78E+03 | 8.41E+03 | 8.29E+03 | 8.38E+03 | 8.45E+03 | 8.40E+03 | 8.39E+03 | 8.40E+03 | 8.40E+03 | 8.40E+03 | 8.43E+03 | 8.43E+03 | 8.42E+03 |
| BS O2 [g/bhp-hr] | 1.71E+03 | 1.71E+03 | 1.72E+03 | 1.65E+03 | 1.62E+03 | 1.64E+03 | 1.66E+03 | 1.64E+03 | 1.64E+03 | 1.64E+03 | 1.64E+03 | 1.64E+03 | 1.65E+03 | 1.65E+03 | 1.65E+03 |
| BS NMHC [g/bhp-hr] | 1.18E+00 | 1.15E+00 | 1.05E+00 | 1.37E+00 | 1.41E+00 | 1.42E+00 | 1.45E+00 | 1.43E+00 | 1.43E+00 | 1.40E+00 | 1.39E+00 | 1.39E+00 | 1.38E+00 | 1.46E+00 | 1.48E+00 |
| BS VOC [g/bhp-hr] | 5.61E-01 | 5.61E-01 | 5.71E-01 | 5.91E-01 | 6.34E-01 | 6.38E-01 | 6.42E-01 | 6.49E-01 | 6.44E-01 | 6.55E-01 | 6.44E-01 | 6.41E-01 | 6.39E-01 | 6.90E-01 | 7.15E-01 |
| U&S AF Total | 0.00E+00 | 0.00E+00 | 0.00E+00 | 0.00E+00 | 0.00E+00 | 0.00E+00 | 0.00E+00 | 0.00E+00 | 0.00E+00 | 0.00E+00 | 0.00E+00 | 0.00E+00 | 0.00E+00 | 0.00E+00 | 0.00E+00 |
| Delivery Ratio | 1.75E+00 | 1.70E+00 | 1.74E+00 | 1.70E+00 | 1.71E+00 | 1.71E+00 | 1.71E+00 | 1.71E+00 | 1.70E+00 | 1.72E+00 | 1.72E+00 | 1.70E+00 | 1.72E+00 | 1.71E+00 | 1.71E+00 |
| Trapping Efficiency | 4.80E-01 | 4.87E-01 | 4.81E-01 | 4.88E-01 | 4.86E-01 | 4.86E-01 | 4.86E-01 | 4.86E-01 | 4.88E-01 | 4.84E-01 | 4.85E-01 | 4.87E-01 | 4.85E-01 | 4.86E-01 | 4.86E-01 |
| Scavenging Efficiency | 8.40E-01 | 8.30E-01 | 8.39E-01 | 8.30E-01 | 8.31E-01 | 8.32E-01 | 8.32E-01 | 8.32E-01 | 8.30E-01 | 8.35E-01 | 8.33E-01 | 8.30E-01 | 8.33E-01 | 8.31E-01 | 8.32E-01 |

| Data Point Name | TLO-01 | TLO-02 | TLO-03 | TLO-01 | TLO-02 | TLO-03 | TLO-04 | TLO-05 | TLO-06 | TLO-07 | TLO-08 | TLO-09 | TLO-10 | TLO-11 | TLO-12 |
|---|---|---|---|---|---|---|---|---|---|---|---|---|---|---|---|
| | 10/4/2012 | 10/4/2012 | 10/4/2012 | 10/8/2012 | 10/8/2012 | 10/8/2012 | 10/8/2012 | 10/8/2012 | 10/8/2012 | 10/8/2012 | 10/8/2012 | 10/8/2012 | 10/8/2012 | 10/8/2012 | 10/8/2012 |
| **Engine Data** | 100% Load | 100% Load | 100% Load | 100% Load | 100% Load | 100% Load | 100% Load | 100% Load | 100% Load | 100% Load | 100% Load | 100% Load | 100% Load | 100% Load | 100% Load |
| **Combustion Data** | | | | | | | | | | | | | | | |
| Engine Avg Peak Pressure[psi] | 5.17E+02 | 5.08E+02 | 5.04E+02 | 5.30E+02 | 5.30E+02 | 5.31E+02 | 5.29E+02 | 5.38E+02 | 5.37E+02 | 5.37E+02 | 5.37E+02 | 5.33E+02 | 5.34E+02 | 5.36E+02 | 5.33E+02 |
| Engine Avg Peak Pres Std Dev[psi] | 3.36E+01 | 3.06E+01 | 2.93E+01 | 3.51E+01 | 3.48E+01 | 3.42E+01 | 3.51E+01 | 3.57E+01 | 3.53E+01 | 3.56E+01 | 3.60E+01 | 3.65E+01 | 3.60E+01 | 3.56E+01 | 3.71E+01 |
| Engine Avg Peak Pres COV[%] | 6.46E+00 | 6.02E+00 | 5.82E+00 | 6.63E+00 | 6.59E+00 | 6.45E+00 | 6.62E+00 | 6.63E+00 | 6.58E+00 | 6.64E+00 | 6.70E+00 | 6.86E+00 | 6.75E+00 | 6.64E+00 | 6.96E+00 |
| Engine Max Peak Pres COV Ch. #4[%] | 8.01E+00 | 7.55E+00 | 7.34E+00 | 8.88E+00 | 8.63E+00 | 8.52E+00 | 8.45E+00 | 8.61E+00 | 8.37E+00 | 8.35E+00 | 8.54E+00 | 9.07E+00 | 8.90E+00 | 8.41E+00 | 8.92E+00 |
| Engine Min Peak Pres COV Ch. #3[%] | 4.30E+00 | 4.25E+00 | 4.10E+00 | 3.55E+00 | 3.52E+00 | 3.45E+00 | 3.85E+00 | 3.76E+00 | 3.69E+00 | 3.67E+00 | 3.62E+00 | 3.73E+00 | 3.72E+00 | 3.64E+00 | 3.72E+00 |
| Engine Avg Peak Loc[*ATDC] | 1.99E+01 | 2.05E+01 | 2.07E+01 | 1.91E+01 | 1.92E+01 | 1.92E+01 | 1.92E+01 | 1.87E+01 | 1.87E+01 | 1.89E+01 | 1.88E+01 | 1.89E+01 | 1.89E+01 | 1.88E+01 | 1.90E+01 |
| Engine Avg IMEP[psi] | 9.54E+01 | 9.33E+01 | 9.45E+01 | 9.54E+01 | 9.52E+01 | 9.50E+01 | 9.44E+01 | 9.44E+01 | 9.37E+01 | 9.37E+01 | 9.44E+01 | 9.42E+01 | 9.39E+01 | 9.37E+01 | 9.37E+01 |
| Engine Avg IMEP COV[%] | 2.64E+00 | 2.51E+00 | 2.22E+00 | 2.68E+00 | 2.65E+00 | 2.79E+00 | 2.54E+00 | 3.01E+00 | 2.54E+00 | 2.66E+00 | 2.95E+00 | 2.99E+00 | 3.02E+00 | 2.66E+00 | 3.10E+00 |
| Engine Max IMEP COV Ch. #4[%] | 4.42E+00 | 4.37E+00 | 3.30E+00 | 4.15E+00 | 3.97E+00 | 4.75E+00 | 3.58E+00 | 4.14E+00 | 3.72E+00 | 4.33E+00 | 5.27E+00 | 4.22E+00 | 5.07E+00 | 4.14E+00 | 5.92E+00 |
| Engine Min IMEP COV Ch. #3[%] | 1.15E+00 | 1.13E+00 | 1.17E+00 | 1.39E+00 | 1.43E+00 | 1.39E+00 | 1.46E+00 | 1.39E+00 | 1.35E+00 | 1.34E+00 | 1.30E+00 | 1.40E+00 | 1.43E+00 | 1.42E+00 | 1.44E+00 |
| | | | | | | | | | | | | | | | |
| **Dilution Tunnel Data** | | | | | | | | | | | | | | | |
| Sample Flow (aLPM) | 72.81 | 74.65 | 75.67 | 75.9 | 75.42 | 75.96 | 75.29 | 75.05 | 74.96 | 75.43 | 75.52 | 75.72 | 75.7 | 75.58 | 75.48 |
| Verturi Pressure (inH2O) | 16.91 | 17.34 | 17.58 | 17.63 | 17.52 | 17.64 | 17.49 | 17.43 | 17.41 | 17.52 | 17.54 | 17.59 | 17.58 | 17.56 | 17.53 |
| Air Flow (aLPM) | 740.16 | 763.76 | 771.3 | 769.22 | 769.92 | 759.62 | 757.7 | 761.25 | 763.02 | 747.44 | 747.63 | 749.59 | 751.07 | 750.67 | 751.64 |
| Residence Time (s) | 113.21 | 115.53 | 115.1 | 113.88 | 113.66 | 113.5 | 113.36 | 113.23 | 113.14 | 112.93 | 112.79 | 112.71 | 112.63 | 112.5 | 112.39 |
| aLPM Dilution Ratio (air/exhaust) | 10.14 | 10.26 | 10.2 | 10.13 | 10.21 | 10 | 10.06 | 10.14 | 10.18 | 9.91 | 9.9 | 9.9 | 9.92 | 9.93 | 9.96 |
| Mixture Temp (C) | 74.31 | 65.19 | 67.67 | 70.35 | 70.91 | 71.9 | 71.95 | 72 | 72.29 | 73.61 | 73.99 | 74.1 | 74.42 | 74.64 | 74.77 |
| Air Out Temp (C) | 83.98 | 72.84 | 75.63 | 79.1 | 79.96 | 80.86 | 81.1 | 81.21 | 81.48 | 83.1 | 83.63 | 83.98 | 84.37 | 84.8 | 85.03 |
| Residence Temp (C) | 38.69 | 24.34 | 26.03 | 27.39 | 28.2 | 28.79 | 29.17 | 29.54 | 29.85 | 30.56 | 31.03 | 31.32 | 31.67 | 32.17 | 32.47 |
| Measurement Humidity (%) | 150.59 | 150.88 | 150.8 | 150.79 | 150.78 | 150.76 | 150.75 | 150.74 | 150.72 | 150.74 | 150.72 | 150.71 | 150.72 | 150.69 | 150.67 |
| Ambient Pressure (kPa) | 85.29 | 85.49 | 85.48 | 84.46 | 84.44 | 84.41 | 84.36 | 84.31 | 84.3 | 84.26 | 84.22 | 84.21 | 84.21 | 84.21 | 84.17 |
| Ambient Humidity (%) | 29.2 | 29.2 | 29.2 | 29.2 | 29.2 | 29.2 | 29.2 | 29.2 | 29.2 | 29.2 | 29.2 | 29.2 | 29.2 | 29.2 | 29.2 |
| Ambient Temp (C) | 15.4 | 15.4 | 15.4 | 15.4 | 15.4 | 15.4 | 15.4 | 15.4 | 15.4 | 15.4 | 15.4 | 15.4 | 15.4 | 15.4 | 15.4 |
| Excess Flow (aLPM) | 170.3 | 2.59 | 167.51 | 169.3 | 169.62 | 169.88 | 170.07 | 170.27 | 170.4 | 170.71 | 170.94 | 171.05 | 171.18 | 171.37 | 171.53 |
| Sample Line Temp (F) | 165 | 165 | 165 | 165 | 165 | 165 | 165 | 165 | 165 | 165 | 165 | 165 | 165 | 165 | 165 |
| Sample Flow (SLM) | 67.35 | 69.11 | 70.05 | 69.92 | 69.44 | 69.95 | 69.32 | 69.08 | 68.99 | 69.41 | 69.48 | 69.67 | 69.65 | 69.54 | 69.43 |
| Air Flow (SLM) | 685.76 | 708.45 | 715.40 | 709.20 | 709.77 | 700.15 | 698.17 | 701.23 | 702.82 | 688.31 | 688.32 | 690.08 | 691.44 | 691.08 | 691.80 |
| Corrected Dillution Ratio (Air/Sample) | 10.18 | 10.25 | 10.21 | 10.14 | 10.22 | 10.01 | 10.07 | 10.15 | 10.19 | 9.92 | 9.91 | 9.91 | 9.93 | 9.94 | 9.96 |

| Data Point Name<br>Engine Data | TLO-01<br>10/4/2012<br>100% Load | TLO-02<br>10/4/2012<br>100% Load | TLO-03<br>10/4/2012<br>100% Load | TLO-01<br>10/8/2012<br>100% Load | TLO-02<br>10/8/2012<br>100% Load | TLO-03<br>10/8/2012<br>100% Load | TLO-04<br>10/8/2012<br>100% Load | TLO-05<br>10/8/2012<br>100% Load | TLO-06<br>10/8/2012<br>100% Load | TLO-07<br>10/8/2012<br>100% Load | TLO-08<br>10/8/2012<br>100% Load | TLO-09<br>10/8/2012<br>100% Load | TLO-10<br>10/8/2012<br>100% Load | TLO-11<br>10/8/2012<br>100% Load | TLO-12<br>10/8/2012<br>100% Load |
|---|---|---|---|---|---|---|---|---|---|---|---|---|---|---|---|
| **PM Calculation Data** | | | | | | | | | | | | | | | |
| Lube Rate (pints/day) | 1.83 | 2.75 | 7.79 | 9.6 | 10.1 | 10.5 | 11 | 11 | 11.5 | 11.9 | 12.8 | 12.8 | 12.8 | 13.3 | 13.3 |
| Lube Rate (g/bhp-hr) | 0.0724714 | 0.108954489 | 0.308498475 | 0.3801778 | 0.4005233 | 0.416008 | 0.43601565 | 0.43591678 | 0.4557312 | 0.4711553 | 0.506904 | 0.5070187 | 0.5065594 | 0.5269435 | 0.5264661 |
| Sample Time (min) | 15 | 15 | 15 | 16 | 17 | 18 | 19 | 20 | 21 | 22 | 23 | 24 | 25 | 26 | 27 |
| Particulate Matter Sample (µg) | 313 | 283 | 470 | 557 | 605 | 609 | 641 | 608 | 637 | 662 | 650 | 661 | 663 | 679 | 671 |
| Particulate Matter Rate (µg/min) | 20.9 | 18.9 | 31.3 | 34.8 | 35.6 | 33.8 | 33.7 | 30.4 | 30.3 | 30.1 | 28.3 | 27.5 | 26.5 | 26.1 | 24.9 |
| Mass Flow Fuel (kg/sec) | 0.0241 | 0.0242 | 0.0241 | 0.0232 | 0.0234 | 0.0234 | 0.0235 | 0.0235 | 0.0233 | 0.0236 | 0.0235 | 0.0234 | 0.0235 | 0.0234 | 0.0236 |
| Mass Flow Exhaust (kg/sec) | 1.358 | 1.359 | 1.357 | 1.302 | 1.292 | 1.303 | 1.312 | 1.307 | 1.303 | 1.309 | 1.310 | 1.309 | 1.313 | 1.307 | 1.316 |
| Mass Flow PM on Filter (kg/sec) | 3.48E-10 | 3.14E-10 | 5.22E-10 | 5.80E-10 | 5.93E-10 | 5.64E-10 | 5.62E-10 | 5.07E-10 | 5.06E-10 | 5.02E-10 | 4.71E-10 | 4.59E-10 | 4.42E-10 | 4.35E-10 | 4.14E-10 |
| Mass Flow Sample through Filter (kg/sec) | 0.000764 | 0.000764 | 0.000764 | 0.000764 | 0.000764 | 0.000764 | 0.000764 | 0.000764 | 0.000764 | 0.000764 | 0.000764 | 0.000764 | 0.000764 | 0.000764 | 0.000764 |
| Mass Flow PM in Total Exhaust (kg/sec) | 7.22918E-06 | 6.58128E-06 | 1.08748E-05 | 1.153E-05 | 1.177E-05 | 1.107E-05 | 1.1178E-05 | 1.0108E-05 | 1.008E-05 | 9.809E-06 | 9.21E-06 | 8.969E-06 | 8.679E-06 | 8.514E-06 | 8.179E-06 |
| Brake Specific PM (g/bhp-hr) | 0.059 | 0.054 | 0.089 | 0.094 | 0.096 | 0.090 | 0.091 | 0.083 | 0.082 | 0.080 | 0.075 | 0.073 | 0.071 | 0.069 | 0.067 |
| | | | | | | | | | | | | | | | |
| **Injection Data** | | | | | | | | | | | | | | | |
| Injection Interval (cycles/injection) | 2 | 2 | 1 | 1 | 1 | 1 | 1 | 1 | 1 | 1 | 1 | 1 | 1 | 1 | 1 |
| Cylinder 1 Injection Start time (degrees) | 114 | 45 | 204 | 204 | 249 | 294 | 339 | 24 | 69 | 114 | 159 | 204 | 294 | 24 | 69 |
| Cylinder 1 Injection Duration (ms) | 14 | 14 | 14 | 14 | 14 | 14 | 14 | 14 | 14 | 14 | 14 | 14 | 14 | 14 | 14 |
| Cylinder 2 Injection Start time (degrees) | 173 | 29 | 263 | 263 | 308 | 353 | 38 | 83 | 128 | 173 | 218 | 263 | 353 | 83 | 128 |
| Cylinder 2 Injection Duration (ms) | 14 | 14 | 14 | 14 | 14 | 14 | 14 | 14 | 14 | 14 | 14 | 14 | 14 | 14 | 14 |
| Cylinder 3 Injection Start time (degrees) | 294 | 45 | 24 | 24 | 69 | 114 | 159 | 204 | 249 | 294 | 339 | 24 | 114 | 204 | 249 |
| Cylinder 3 Injection Duration (ms) | 13 | 13 | 13 | 16 | 16 | 16 | 16 | 16 | 16 | 16 | 16 | 16 | 16 | 16 | 16 |
| Cylinder 4 Injection Start time (degrees) | 353 | 45 | 84 | 84 | 129 | 174 | 219 | 264 | 309 | 354 | 39 | 84 | 174 | 264 | 309 |
| Cylinder 4 Injection Duration (ms) | 17 | 14 | 17 | 16 | 16 | 16 | 16 | 16 | 16 | 16 | 16 | 16 | 16 | 16 | 16 |